2019

Structural Controls and Depositional Environments of the Glen Rose Subgroup in Pelahatchie Field in Rankin County, Mississippi

Chesney Petkovsek
University of Mississippi

STRUCTURAL CONTROLS AND DEPOSITIONAL ENVIRONMENTS OF THE GLEN ROSE SUBGROUP IN PELAHATCHIE FIELD IN RANKIN COUNTY, MISSISSIPPI

A thesis
presented in partial fulfillment of requirements
for the degree of Master in Engineering Science
in the Department of Geology and Geological Engineering
The University of Mississippi

By

CHESNEY PETKOVSEK

December 2018

ABSTRACT

Following Lion Oil's drilling of the Sowell #1, Lower Cretaceous step-out drilling in Pelahatchie Field has led to the establishment of Mooringsport, Paluxy, Rodessa, Sligo, and Hosston oil and gas condensate production along the flanks and crest of a salt feature within Rankin County, Mississippi. Exploration of salt features has been intermittent throughout Mississippi, but has shifted from targeting pay zones along the crests of domal and piercement salt features in the 1940s, to targeting reserves along the flanks of these features in the 1970s. The dominant structural feature in Pelahatchie Field is an elongate north-south-trending salt ridge. Results of this study suggest that combination traps predominate. The Glen Rose Subgroup in southern Rankin County transitions from upper shoreface to the south of the study area, to estuarine tidal flats in a more restrictive environment within Pelahatchie Field. The discovery of a channel within the lower Rodessa Formation records a short period of fluvial deposition. A more clear definition of paleo-depositional environments in association with structural and stratigraphic controls on production are important to the continued oil and gas exploration of salt dome plays in the Mississippi Interior Salt Basin.

DEDICATION

This thesis is dedicated to my family, who has supported me throughout this process. I would also like to dedicate this thesis to my encouraging team and bosses at Callon, especially Josh, Jamaine, and John.

LIST OF ABBREVIATIONS

MCF	Thousand cubic feet
MISB	Mississippi Interior Salt Basin
MSOGB	Mississippi Oil and Gas Board
GoM	Gulf of Mexico
GGX	GeoGraphix
PeF	Photoelectric factor
AOI	Area of interest
TVT	Total vertical thickness
TST	Total stratigraphic thickness
LWD	Logging while drilling
GC	Gas Chromatograph

ACKNOWLEDGEMENTS

I would like to thank my advisor, Dr. Greg Easson, and my committee members Dr. Louis Zachos, and Dr. Brian Platt for their guidance, as well as the Department of Geology and Geological Engineering and the MMRI for providing the necessary data for the completion of this project. I would like to thank Larry Baria for his insight to the field and communication on this project.

I would like to also express my gratitude to Callon Petroleum for providing me with access to the AAPG datapages archives, as well as the company's geological resources. The encouragement of my asset team and the willingness of my advisors to provide feedback has been astounding.

TABLE OF CONTENTS

LIST OF FIGURES

INTRODUCTION

Pelahatchie Field (Fig. 1) in Rankin County Mississippi has produced 1,442,633

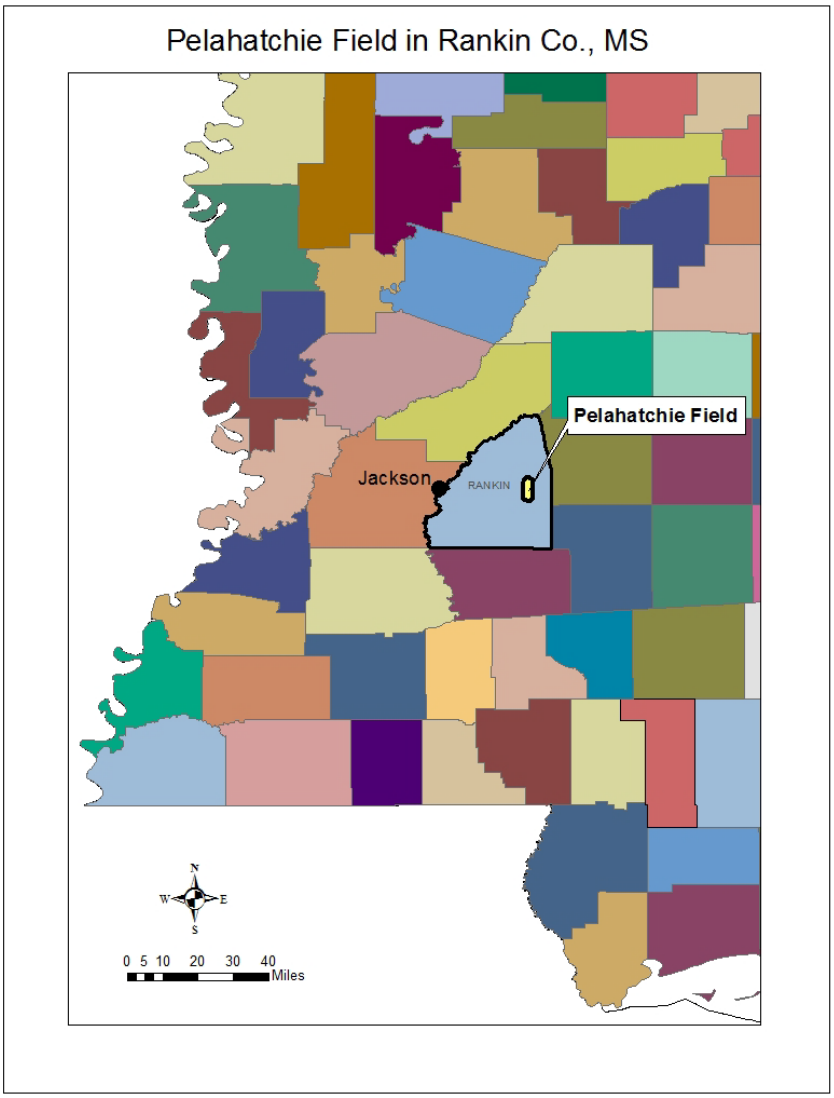

Figure 1. Pelahatchie Field location shaded in yellow showing proximity to state capital, Jackson.

cumulative barrels of oil, 6,250 MCF of natural gas, and 7,759,244 cumulative barrels of water (DrillingInfo, 2018) since its discovery in 1956 and could still hold potential as an important energy resource. Outside of private prospectors and proprietary data, the field is largely unstudied and nearly absent from energy literature. The field is located near the up-dip limit of Lower Cretaceous oil production and the down-dip limit of Smackover production (Karges, 1968). Hydrocarbon potential was first discovered in 1956 with Lion Oil's Leon No. 1, which encountered oil shows in the sands of the Rodessa Formation (Fig. 2).

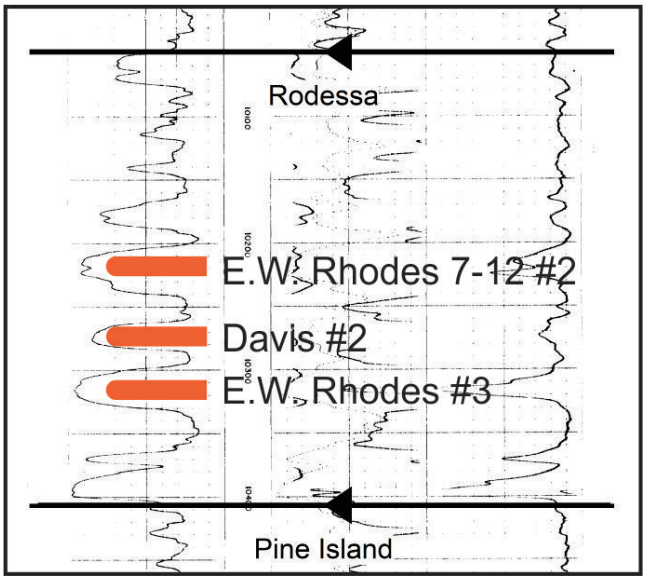

Figure 2. Producing sand intervals in Rodessa Formation as indicated by perforating records in labelled wells. Well log shown is Davis #2.

Beginning in 1957, C.F. Martin and American Petrofina step outs encountered oil shows in the Rodessa, as well as the Hosston Formation sands. Following discoveries in the Rodessa

and Hosston, expansion of the field was pursued by American Petrofina and Love Petroleum. This led to the establishment of production in the Hosston, Sligo, Rodessa, Mooringsport, and Paluxy Formations (Karges, 1968). Results from this attempted expansion resulted in identification of the eastern extent of the field when American Petrofina drilled the L. E. Knight, a dry hole one half mile east of the Rhodes Sowell #1 in section 18 (Karges, 1968). Later attempts to explore deeper horizons, such as the Smackover and Norphlet Formations, resulted in high produced volumes of CO_2 and H_2S gas. Large volumes of high purity CO_2 accumulations within Jurassic formations are common in central Mississippi where salt-cored anticlines occur in close proximity to the intrusive Jackson Volcano, located 21 miles to the west of Pelahatchie Field (Studlick et al., 1990). Another early target, the basal Smackover sand, is supersaturated in brine formation water. Wells producing out of this sand experienced considerable production complications in the late 1960's, such as tubing and flow line plugging by salt crystals when brought to the surface (Karges, 1968). The discovery of sour gas in conjunction with production difficulties discouraged deep testing in the area. In response to the difficulties in Jurassic formations, multiple Upper and Lower Cretaceous horizons have been discovered and proven to be productive, though many previously targeted Upper Cretaceous reservoirs have been abandoned due to non-commercial production values. Current zones of interest yielding economic quantities of oil are the Mooringsport, Rodessa, Sligo, and Hosston Formations (Odyssey, 2005). Historically, Pelahatchie Field produced little natural gas from these and other reservoirs although they are known natural gas producers in nearby fields.

In addition to anomalous gas production, hydrocarbon development, specifically within the Glen Rose Subgroup, has provided highly inconsistent production data, suggesting the

existence of a complex interaction of geologic controls. This study will focus on horizons within the Glen Rose Subgroup (Fig. 3) and use structural characteristics from the underlying Sligo

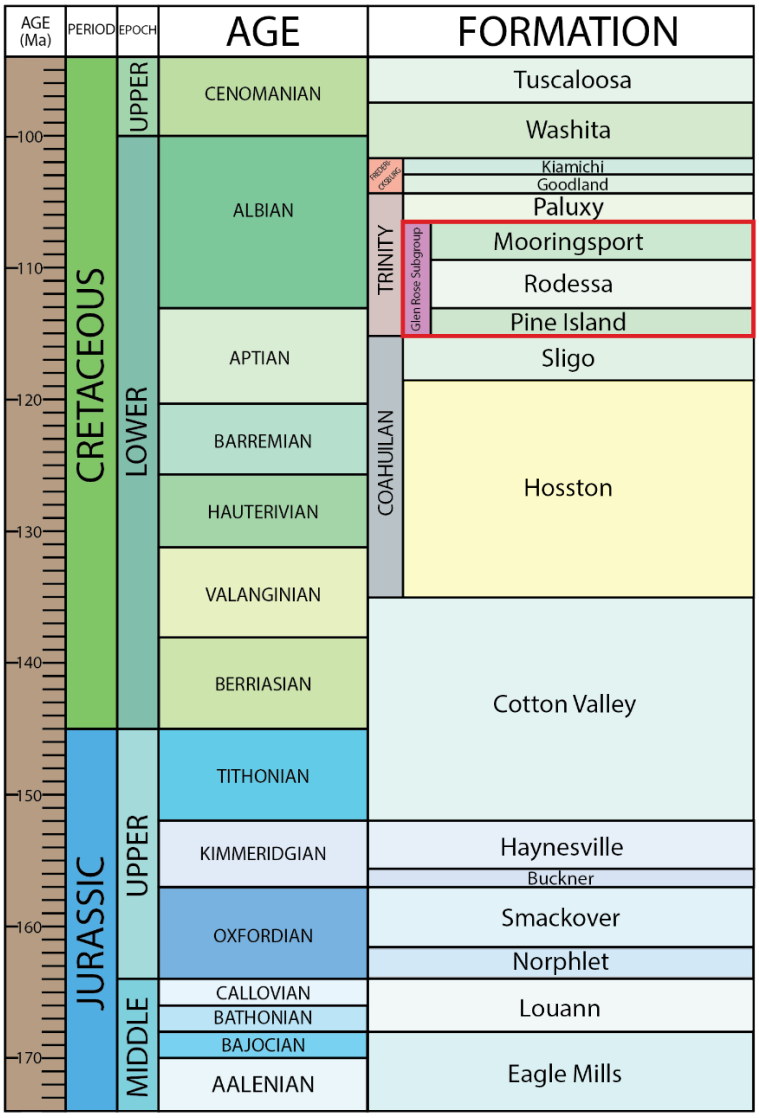

Figure 3. Stratigraphic column of Central Mississippi with Glen Rose Subgroup highlighted in red (modified from Fails, 1990).

and Hosston Formations, as well as the overlying Paluxy Formation to aid in the reconstruction of the Glen Rose Subgroup environments of deposition.

FIELD STRUCTURE

The prominent structure of Pelahatchie Field is an elongate, north-south trending salt-cored anticline, which dips steeply on the east and west flanks, demonstrating closure on Late Jurassic horizons, but little on Lower Cretaceous horizons. Lack of significant structural closure on Lower Cretaceous horizons suggests stratigraphic trapping mechanisms predominate. Seismic and gravity studies indicate the presence of a generally north-south trending salt ridge, which veers slightly southwest in the southern extent of the field (Karges, 1968). Although salt movement is known to have occurred, previous studies state that the structure has little or no fault complications, but reference a possible west-east normal fault separating two structural highs in section 7 (Karges, 1968). Spatial anomalies in production may indicate that faulting has a greater impact on production than previously observed (L. Baria, personal communication, September 2016). Although production and downhole data can be used for chemical analyses in relation to Smackover sour gas, sedimentary accumulation rates, and reservoir calculations, there exist too little public data to effectively evaluate these parameters. Therefore, this study will focus on the sequence stratigraphy, lithostratigraphy, structural influences, and qualitative timing of such events. Deposition in this area differs from surrounding depocenters in central Mississippi, Louisiana, and Alabama in that there is increased clastic deposition in Lower Cretaceous formations known along the northern and northwestern rims of the GoM basin to be predominantly shallow marine carbonates (McFarlan, 1991). The increase in clastic deposition is

interpreted as representing the sediment load of major rivers draining the Ouachita and Appalachian uplands along the northern extents of the basin (McFarlan, 1991). Channel sands and sand lenses have been suggested to exist throughout the field on the basis of differing water levels identified through oil-water contacts in downhole data (Karges, 1968). No distinct channels have been proven in this field to date.

This complex geologic history has made stratigraphic analysis and correlation challenging. Because of the field's location along previously delineated production limit margins and being within one of the interior salt basins along the Lower Cretaceous Gulf of Mexico (GoM) margin, this field could serve as a possible analog to aid in interpretation of locally similar fields in the salt anticline play of central Mississippi. This research will investigate the depositional environments of the Glen Rose Subgroup in Pelahatchie Field, which will provide new insight into previous regional studies and future hydrocarbon development.

DEVELOPMENTAL HISTORY

Early wells drilled by Lion Oil such as the Sowell No. 1, and the Leon No. 1, encountered oil and gas shows in the Eutaw, Tuscaloosa, and Rodessa Formations in 1947 and 1956 (Karges, 1968). In 1957, C. F. Martin's Ragsdale No. 1, two miles south of the Leon No.1, extended exploration to the deeper Hosston Formation, where good oil shows were encountered as well as oil shows in the previously established Rodessa sands. In 1962, production in the Mooringsport Formation sand was discovered by American Petrofina. Expansion of the field was accomplished through American Petrofina and Love Petroleum's northern step-outs which encountered oil shows in the Paluxy, Rodessa, Sligo, and Hosston sands. Love Petroleum's Church No. 1 and Purina No. 1 extended the field, initially centered around sections 7 and 18 of east-central Rankin Co., one mile south and one mile north, respectively (Fig. 4).

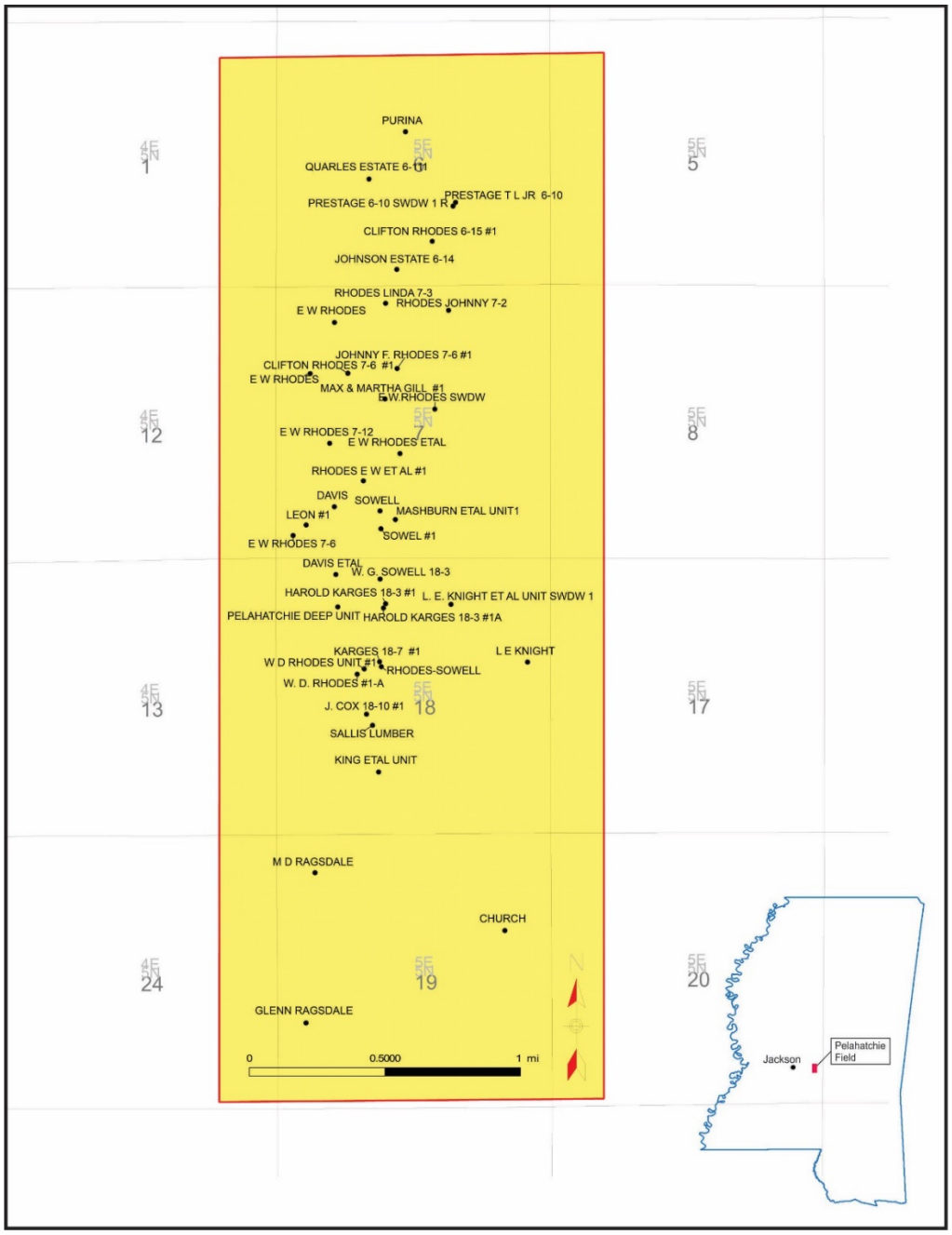

Figure 4. Pelahatchie Field AOI with well names and numbers.

American Petrofina attempted to extend the field one half mile east of section 18 with their L.E. Knight No. 1 in 1963. The well was dry and currently serves as the eastern bound of the field (Mississippi Oil and Gas Board, 2017). The Church No. 1 well encountered a Mooringsport and a Paluxy oil show in non-commercial quantities (Karges, 1968).

In 1965, two deep Smackover zones were tested for CO_2, and a middle Smackover zone was tested for H_2S at a concentration of 21 tons per mcf (Karges, 1968) in the Gooch No. 1 with a total depth reaching 17,501 feet. This was the first Smackover well in the area, but was considered to be non-commercial and abandoned (Mississippi Oil and Gas Board, 2017). The Shell-Love, W. D. Rhodes No. 1 was the first deep pay discovery well, but was plugged and abandoned in 1994. This well was converted into an injection well in 2016 (Mississippi Oil and Gas Board, 2017). The Buckner and Norphlet Formations contain CO_2 which has less than 10 ppm H_2S and considered a "sweet" gas. The Smackover, however, contains higher volumes of H_2S, which require treatment before transportation or use (Studlick et al., 1990). Although Jurassic formations are outside of the scope of this research, it is important to acknowledge the possibility of CO_2 floods being transported up-dip. This process is recorded in the Pisgah anticline by Studlick et al. (1990). The Pisgah anticline is the largest of the salt-cored anticlinal structures north-east of the intrusive Jackson Volcano within the Mississippi Interior Salt Basin (Fig. 5).

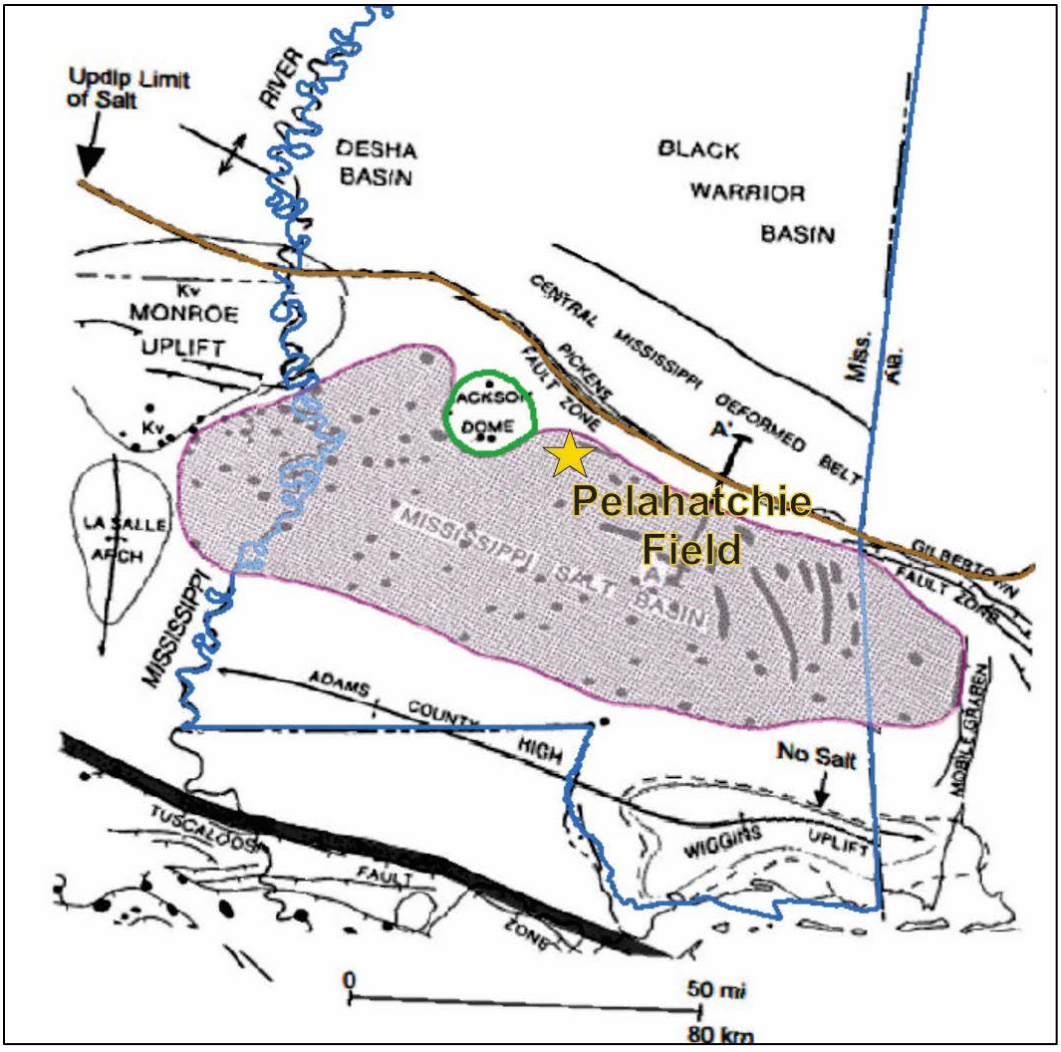

Figure 5. Regional tectonic map of salt structures within the Mississippi Interior Salt Basin (Montgomery and Ericksen, 1997).

CO_2 reserves in this feature surpass 4 TCFG and have been located in mid-dip Cretaceous formations (Studlick et al., 1990). Recent advanced in CO_2 recovery methods, as well as the log realization of CO_2 as a production enhancement for liquid hydrocarbon recovery, has led to renewed interest in the extraction of gas in Pelahatchie Field (Studlick et al., 1990).

GEOLOGIC SETTING

A complete understanding of the stratigraphy of Pelahatchie Field requires knowledge of the complex developmental history of the GoM Basin. Reconstructions of the GoM Basin state that the North American and South American plates were joined during the late Paleozoic and earliest Mesozoic as a part of the supercontinent Pangea, which existed over what is now the GoM (Salvador, 1991). The current GoM is considered a divergent basin characterized by a period of crustal extension and thinning in the form of extensional rift tectonics and wrench faulting (Pilger, 1981; Miller, 1982; Klitgord, et al., 1984; Van Siclen, 1984; Pindell, 1985; Salvador, 1987; Winker and Buffler, 1988; Buffler, 1991) in the Late Triassic to Middle Jurassic, followed by a period of thermal subsidence (Nunn, 1984) during the Late Jurassic and into the Cretaceous (Salvador, 1991). The paleotopographic highs are interpreted to be relicts of rifting in the form of unrotated continental blocks that have experienced little internal deformation (Sawyer et al., 1991). Paleotopographic lows are depressions formed in response to crustal extension (Sawyer et al., 1991) related to the opening of the GoM (Montgomery and Erickson, 1997). The Wiggins Arch would be an example of a paleotopographic high, and the Mississippi Interior Salt Basin (MISB) would be an example of a paleotopographic low allowing for the deposition of thick salt deposits, non-marine clastic sediments, and volcanics as it was actively subsiding throughout the Mesozoic and into the Cenozoic (Mancini et al., 2012). The MISB is the largest of several salt-diapir provinces along the northern margin of the GoM (Montgomery and Ericksen, 1997). The MISB is important to this research because Pelahatchie Field is

considered a salt dome play. The MISB is a tectonic depression covering over 6,000 square miles in area with well-defined structural margins (Montgomery and Ericksen, 1997). Pelahatchie Field lies within the northernmost extent of the MISB.

i. Late Triassic to late Middle Jurassic

The Late Triassic to the late Middle Jurassic was characterized by a period of active rifting associated with the breakup of Pangea, crustal attenuation, and the evolution of alternating basement highs and lows. As previously stated, this period of rifting initiated the formation of the Gulf of Mexico (Salvador, 1991; Mancini et al., 2012). Sedimentation during the early part of this period was dominated by thick accumulations of nonmarine clastics, continental red beds, lacustrine deposits and associated volcanics deposited in rapidly subsiding grabens and rift basins (Mancini et al., 2012; Salvador 1991).

ii. Late Middle Jurassic to late Upper Jurassic

During the late Middle Jurassic, extensive and thick evaporite deposits accumulated over most of the Gulf of Mexico and were most likely formed in extensive, shallow bodies of hyper saline water in limited communication with the present day Pacific Ocean across central Mexico. At the time of deposition, evaporation exceeded the inflow of marine water and large volumes of halite were able to accumulate in the arid-semiarid climate (Salvador, 1991) contemporaneously with continued basin subsidence. Although the exact age of salt deposition remains unknown, it has been largely agreed upon that deposition of the Louann Salt began during this late Middle Jurassic and continued into the earliest part of the Late Jurassic (Salvador, 1991). Salt movement occurred mainly during the Late Jurassic and continued into the Early Cretaceous, with limited

movement in the Late Cretaceous (Kupfer et al., 1976 and Lobao and Pilger (1985) though piercement features have been recorded as late as the Cenozoic (Montgomery and Ericksen, 1997). Within the northern region of salt distribution, Salvador (1991) recognized four distinct belts of salt occurrence. The MISB lies within the northernmost area of salt occurrence and is characterized by a series of interior salt basins separated by structural highs.

Following the period of substantial salt formation during the late Middle Jurassic, an extensive marine transgression covered most of the present-day GoM as a result of sea-floor spreading and oceanic crust formation in the Late Jurassic (Mancini et al., 2012). This transgression was active throughout the duration of the Late Jurassic, peaking during the Tithonian or early Cretaceous, with only smaller regressive episodes throughout. As subsidence continued into the Early Cretaceous, a carbonate shelf margin developed along the tectonic hinge zone between thick and thin transitional crusts (Salvador, 1991; Mancini et al., 2012). This pattern of deposition was broken by the mid-Cenomanian unconformity that will be discussed in later sections. Despite existing within a period of sea-level rise, the northern flank of the Gulf of Mexico experienced an influx of terrigenous clastics from major streams draining the Appalachians, Ouachitas, and other areas of previous tectonic uplift experiencing erosion (Salvador, 1991). This influx of sediment along the northern and northeastern flank of the GoM resulted in a thick, prograding wedge of clastics not necessarily connected with a regression (Salvador, 1991).

iii. Early Lower Cretaceous to Upper Cretaceous

Throughout the Early Cretaceous, the GoM basin continued to experience continental and marine deposition. It was tectonically stable with the exception of gradual subsidence taking

place in the central area, growth faulting, and small-scale deformation due to halokinesis (McFarlan, 1991). Shallow-marine water covered the peripheral shelves, and deepened basinward. Shelf deposits of the Lower Cretaceous GoM are characterized predominantly by carbonates and evaporates (Fig. 6).

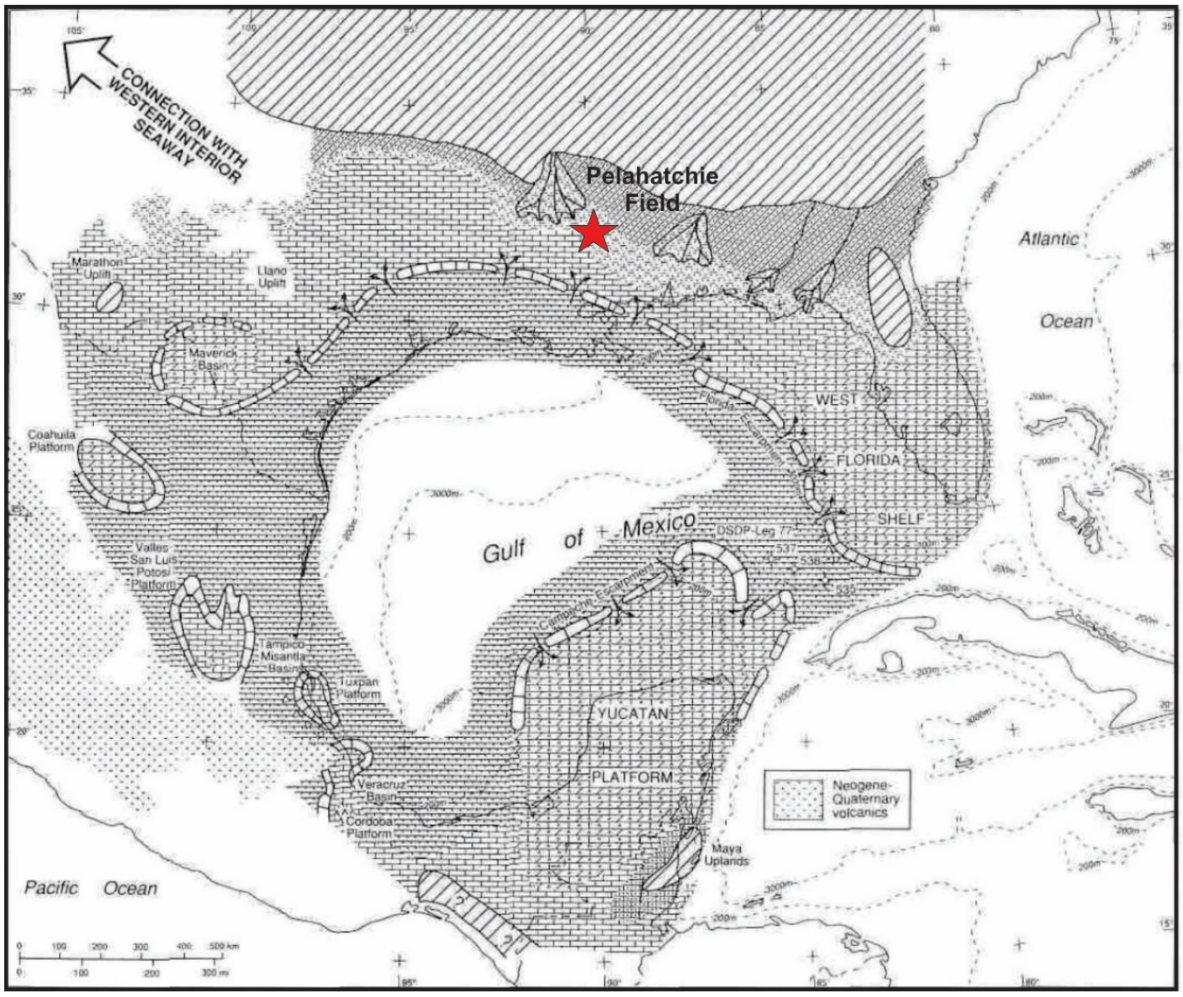

Figure 6. Lithofacies paleogeographic map of shallow-marine carbonate and evaporite distribution, Albian (McFarlan and Menes, 1991).

The continental slope at this time was dominated by carbonate deposition. The northern flanks of the basin were characterized by continental and shallow-marine terrigenous clastic sediments (McFarlan, 1991). Widespread carbonate deposition ceased in the mid-Cenomanian and another depositional cycle, dominated by terrigenous clastics, began. The shift from carbonate deposition to clastic deposition is marked by a mid-Cenomanian unconformity. The unconformity is a result of a period of global sea-level fall which resulted in the exposure of the shallow platform margin that rimmed the Gulf during the Lower Cretaceous (Salvador, 1991). It is generally concluded that two cycles of progradation are recorded in the Early Cretaceous: the Cohuilan (Hosston/Sligo) and the Comanchean (Pine Island to Washita) (Mancini et al., 2012).

REGIONAL CHRONOSTRATIGRAPHY

The Upper Triassic-Lower and Middle Jurassic nonmarine sequence is called the Eagle Mills Formation. The Eagle Mills Formation has more recently been divided, in ascending order, into the Eagle Mills, Werner, Louann, and Norphlet Formations (Mancini, 2005; Salvador, 1991). The Louann and Norphlet Formations are more widely considered to be Middle and Late Jurassic in age, respectively (Salvador, 1991). After deposition, the Louann Salt was later subject to deformation by the overburden of younger strata. Common deformation types that have been either encountered by drilling or by seismic reflection are domal features, pillows, massifs, and salt-supported anticlines (Mancini et al., 2012), similar to that of Pelahatchie Field.

Because of the expansive transgression during the Late Jurassic, the Upper Jurassic is a predominantly marine section showing no evidence of substantial tectonic influence. The lower Upper Jurassic is represented by non-marine or littoral coarse-clastic units. These units grade into nearshore and shallow-shelf sequences basinward. These non-marine and coarse-clastic units are predominantly composed of carbonates, calcareous shales, and evaporates (Salvador, 1991). Lower Upper Jurassic formations are, in ascending order, the Norphlet, Smackover, and Haynesville. In northern Louisiana, across northern Mississippi, and into Alabama, The Norphlet is a coarse-clastic unit composed mainly of sandstones and conglomeratic sandstones deposited in coalescing alluvial fans by erosion of the southern Appalachians (Mancini et al., 1985).

However, in central Mississippi, the Norphlet is a finer-grained, mature sandstone. The difference in grain size is attributed to the paleogeography of central Mississippi at the time, which was considered to be a desert plain bound to the north and east by the Appalachians, and to the south by an emerging shallow sea (Mancini et al., 1985). Norphlet deposits in central Mississippi have been interpreted as eolian sands (Hartman, 1968; Badon, 1975; McBride, 1981; Pepper, 1982; Mancini et al., 1985; Marzano et al., 1988). The Smackover is a carbonate-shale unit, and along certain paleohighs, a local shoal complex. The Smackover was deposited on a ramp surface during the major Jurassic marine transgression in the GoM (Mancini et al., 2005).

The upper Upper Jurassic is composed of a finer-grained clastic section than the underlying coarse-clastics of the lower Upper Jurassic. This section is called the Cotton Valley Group. Units in the lower and upper Upper Jurassic become increasingly shaley basinward, indicating deep-water deposition. Terrigenous sediments in central Mississippi from this time are indicative of an ancestral Mississippi River and its associated deltal lobes contributing coarse clastics to the GoM (Salvador, 1991). According to Salvador (1991), the Upper Jurassic of the GoM basin can be divided into three intervals that approximately correspond to global chronostratigraphic, and recognized lithostratigraphic units. They are, from youngest to oldest: Tithonian, Kimmeridgian, and Oxfordian.

The Lower Cretaceous has been divided into three chronostratigraphic units. They are, in ascending order, The (1) Berriasian and Valanginian; (2) Hauterivian, Barremain, and Aptian; and (3) Albian and lower Cenomanian (McFarlan, 1991). The sedimentary units deposited within these chronostratigraphic units are, in ascending order, the Hosston, Sligo, and Trinity Group (Pine Island, James Limestone, Rodessa, Ferry Lake Anhydrite, Mooringsport, and Paluxy).

Because this research focuses on Lower Cretaceous strata, these chronostratigraphic units will be discussed in further detail, followed by a brief discussion of lithostratigraphy.

The Berriasian and Valanginian units record a period of clastic sedimentation along the northern and northeastern coast of the Gulf of Mexico, and of carbonate deposition along continental shelves. The clastic sediments were deposited in alluvial valley, deltaic, and inter deltaic environments (McFarlan, 1991).

The Hauterivian-Barremian-Aptian succession records an episode of sea-level rise, followed by progradation of sediments with the regression of sea-level. This was followed by a period of aggradation of shelfal and platform carbonates, which are capped by a widespread marine-shale unit in the late Aptian. This aggradational period is associated with sea-level rise. In the late Hauterivian and early Barremian, eustatic sea-level rise accompanied by regional subsidence continued. As accommodation increased and the shoreline was covered by transgressing marine waters, coastal plains were inundated, causing a decrease in clastic deposition in nearshore areas (McFarlan, 1991). The Hauterivian, Barremain, and lower Aptian are recorded by the terrigenous clastics of the Hosston Formation. In Mississippi, the Hosston/Sligo beds increase in thickness within the MISB and other subbasins (Devery, 1981) and generally dip to the southwest throughout the state. In Mississippi, the Hosston is notably coarser than in adjacent depositional areas due to fluvial deposition by rivers draining the continental interior and Appalachian and Ouachita uplands (McFarlan, 1991). Throughout most of Mississippi, the Hosston is conformably overlain by the Sligo, but up-dip in central and north-central Mississippi along the northern flanks of the GoM, Hosston clastics interfinger gulfward with the massive, shelfal limestones of the Sligo Formation (Devery, 1981). The Hosston and

Sligo are significant to Pelahatchie Field because they are proven hydrocarbon reservoirs (Mancini et al., 2012).

The Albian-lower Cenomanian consists of a prograding and aggrading stratigraphic sequence of shelfal carbonates with marginal shelf sediments (McFarlan, 1991). Subsidence and a continuing rise in eustatic sea-level influenced deposition of Albian-lower Cenomanian sediments (McFarlan, 1991). An alluvial and deltaic plain was present during this time that extended from central Mississippi to southern Florida and consisted of multiple deltaic features. The most prominent of these features was the ancestral Mississippi delta. Basal Albian deposits are represented by the Glen Rose Subgroup, which is subdivided in Louisiana, Mississippi, and Alabama into three units. They are, in ascending order: the Rodessa Formation, a calcium cemented sandstone and shale unit, the Ferry Lake Anhydrite, and the Mooringsport Formation, also a predominantly sandstone interval. The Glen Rose Subgroup becomes increasingly calcareous basinward (McFarlan, 1991). The Glen Rose Subgroup is onlapped by shelfal limestones of the Fredericksburg Group. The Fredericksburg Group is divided, in ascending order, into the Paluxy, which is composed of sandstones and shales, the Goodland, and the Kiamichi. Of significance to the Pelahatchie Field study area are the Rodessa, Ferry Lake, Mooringsport, and Paluxy because they include productive sand intervals.

REGIONAL LOWER CRETACEOUS LITHOSTRATIGRAPHY

Hosston Formation: During the lower Lower and upper Lower Cretaceous, deposition included a wide range of lithologies from delta-plain to shallow-marine shelf environments (Mancini et al., 2012). In the northern GoM, the Hosston is interpreted to be a transgressive sequence consisting primarily of terrigenous clastics. The terrigenous clastics of the Hosston interfinger gulfward, and are overlain by the limestones and grey shales of the Sligo Formation. Blount et al., (1986) identified five major lithofacies characteristic of a fluvial-deltaic system in the Travis Peak Hosston equivalent in a study of Trawick Field in east Texas. Blount et al. (1986) also noted various braided stream and crevasse splay deposits and distribution differences between the upper and lower Hosston. The distribution differences are summarized as follows: in the lower Hosston, channel, crevasse splay, and interdistributary bay facies were most common, and in the upper Hosston, a marginal marine delta-fringe system was prevalent. This is consistent with more recent results from the USGS's (2006) assessment of the Hosston Formation, which extended the depositional study area across northern Louisiana and into southern Mississippi and found the Hosston in southern Mississippi to be a wedge of terrigenous clastics derived from deposition of an ancestral Mississippi River (Fig. 7) (Dyman and Condon, 2006). From east Texas, across northern Louisiana, and to Mississippi, the Hosston is a predominantly arenaceous siliciclastic section, which ranges from pink and white to gray sandstones, shales, and siltstones, to conglomerates (Beckman and Bloomer, 1953; Cullom et al., 1962; Gorrod, 1980; Saucier et

al., 1985; Garner et al., 1987). Locally, the Hosston is more coarse-grained and graveliferous due to the field's up-dip position and increased fluvial deposition draining uplands to the north and northeast (Dyman and Condon, 2006). As noted by Karges (1968), The Hosston sands are thick and generally a blanket type, with the producing horizon showing little change in thickness in Pelahatchie Field.

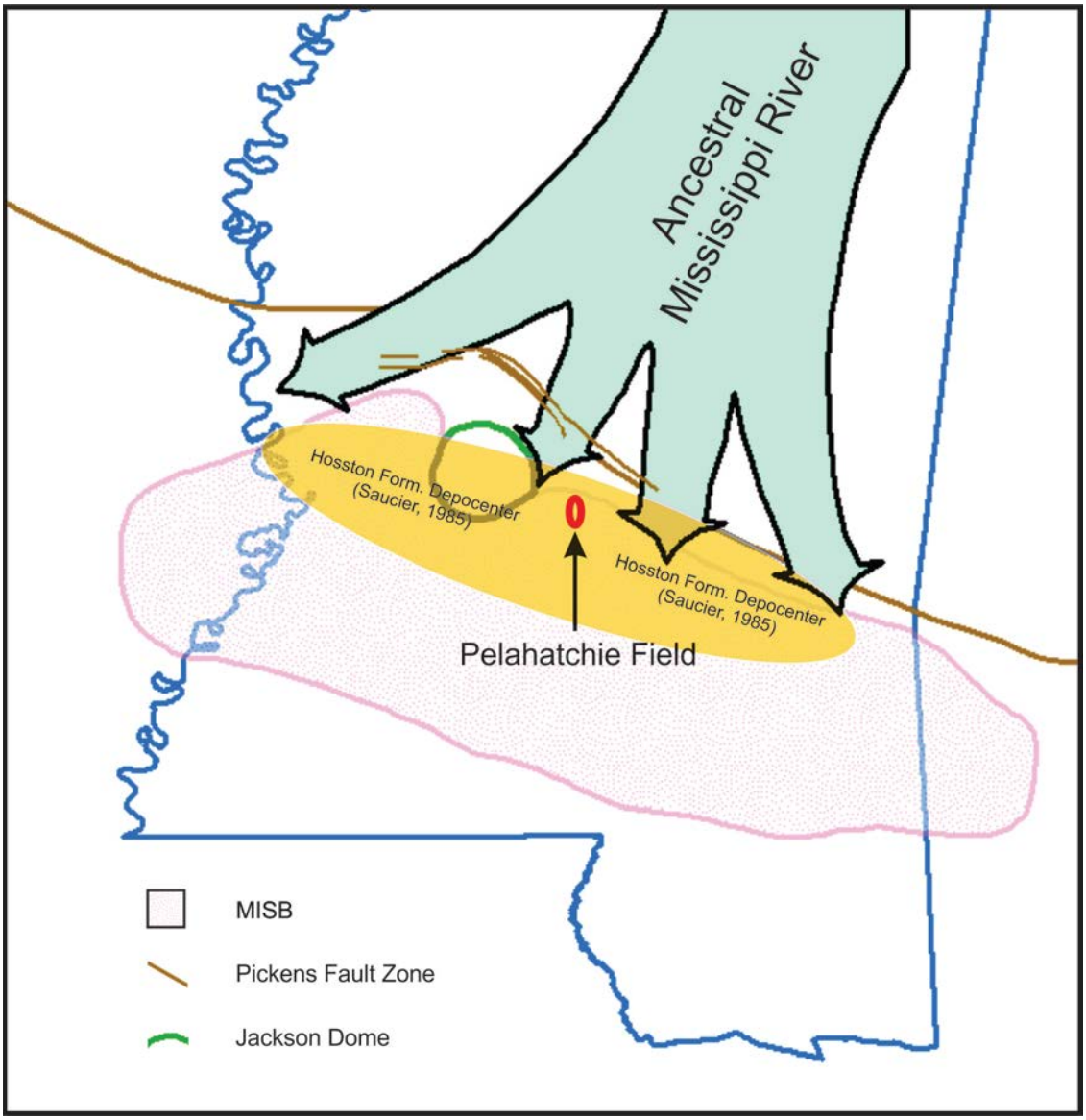

Figure 7. Pelahatchie Field in relation to Ancestral Mississippi River depocenter during the Lower Cretaceous. After Dyman (2006).

The highest consistent reservoir qualities come from the lower channel sands. In northern Louisiana and Mississippi, the reservoir sands have little permeability and require hydraulic fracturing for economic recovery (Dutton and Finley, 1988; Dutton et al., 1990, 1993; Davies et al., 1991). Hydrocarbons produced in the Hosston are typically 25° to 46° API gravity oil, condensate, and gas (Mancini et al., 2012). The Hosston interfingers gulfward, and is overlain by the Sligo Formation.

Sligo Formation: The Sligo Formation is generally thought to be a transgressive, shallow-marine carbonate shelf sequence (Forgotson and Forgotson, 1975). The Sligo is composed of gray to brown argillaceous and fossiliferous limestones that aggrade and prograde in the shelfal areas (Mancini et al., 2012). In southern and central Mississippi, the Sligo Formation is a massive fossiliferous shelfal limestone (McFarlan, 1977) and occurs stratigraphically higher than the Hosston. This carbonate deposition was succeeded by the predominantly clastic Pine Island Formation.

Pine Island Formation: Updip of the MISB, the Pine Island Formation is a terrigenous clastic section characterized by calcareous black shales interbedded with thin, dense, grey, and often crystalline, limestones, with interbedded fine-grained sandstones. The crystalline limestone layers are associated with lagoonal and nearshore marine environments (Mancini et al., 2012). Because the marine shales present in the Pine Island can be correlated throughout the basin, Yurewicz et al. (1993) have interpreted them to be regional transgressive deposits. In southern Mississippi, McFarlan (1991) described the Pine Island as more arenaceous and argillaceous than its up-dip equivalents. Pine Island hydrocarbons are typically 24° to 30° API gravity oil, gas, and condensate and are produced from a basal sand unit (Mancini et al., 2012).

The James Limestone: The James Limestone is an argillaceous miliolid lime mudstone, wackestone, and packstone deposited in a fairly low-energy open shelf environment (Yurewicz et al., 1993) which typically overlays the Pine Island Formation. The lithology of the James Limestone is inconsistent throughout the northern GoM, with descriptions spanning from a sandy, chalky, fossiliferous lime (Forgotson, 1957) to a reef-like deposit (Hermann, 1976) in north-central Louisiana. In contrast, a study by Mancini et al. (2012) determined the James Limestone to be non-reef in origin. Isopach maps show that the James Limestone is a detrital deposit accumulating in basin lows, not a reef complex like previously defined. Due to the widely varying lithology, The James Limestone will be included in the Rodessa Limestone sequence for the purpose of this study.

The James Limestone is a known producer in certain reef facies along structural highs related to salt deformation within the interior salt basins of east Texas, north Louisiana, and Mississippi (Hermann, 1976). Hydrocarbons produced in these plays are generally light oils and condensates. Gas is produced in porous limestone intervals (Mancini et al., 2012).

The Rodessa Formation: Overlying the Pine Island Formation is the Rodessa Limestone, which has been described in northwestern Louisiana to be a grey, arenaceous, argillaceous, oolitic, skeletal limestone interbedded with thin, often lenticular, sandstones and grey shale layers (Weeks, 1938; Forgotson, 1957). In east Texas, the Rodessa is described as a skeletal-peloid-oncoid packstone that grades into skeletal grainstones and packstones down-dip at the platform margin (Yurewicz et al., 1993). Anhydrite beds have also been known to occur throughout the formation in parts of Louisiana (Mancini et al., 2012). Siliciclastic input was derived from the craton to the north (Mancini et al., 2012). Within the MISB, the Rodessa more locally consists of stacked channel sands. The increase in siliciclastics has been attributed to the

possibility of an ancient stream or tributary of a precursory Mississippi River (Karges, 1968). These channel sands are interbedded with thin shales.

Hydrocarbons produced in the Rodessa are generally 34° to 41° API gravity oil, gas, and condensate (Mancini et al., 2012). Reservoir porosities range from 10-26%. Permeability ranges from 10-650 md (Mancini et al., 2012). The Rodessa Limestone is overlain by the Ferry Lake Anhydrite.

The Ferry Lake Anhydrite: The Ferry Lake Anhydrite is a massive, white to grey, finely crystalline anhydrite, interbedded with thin limestones, shales, and dolomites (Imlay, 1940a). The Ferry Lake Anhydrite is a distinctive, widespread sedimentary unit extending from east Texas, across southern Arkansas and northern Louisiana, central Mississippi, to southern Alabama and south Florida (Forgotson, 1957) deposited in an extensive lagoonal sea. Because the formation represents a regional episode, it is commonly used as a marker bed in this region (Petty, 1995; Montgomery et al., 2002). For correlation purposes, the Ferry Lake Anhydrite will be included in what is referred to as the Mooringsport Formation hereto forward in this paper. The Ferry Lake Anhydrite will serve as a marker bed to ensure consistency for structural and stratigraphic analysis.

The Mooringsport Formation: The Rodessa Formation is overlain by the Mooringsport Formation, which is composed of shallow-marine carbonates that are predominantly crystalline, fossiliferous, and oolitic limestones interbedded with shale, sandstone, red beds, anhydrite, and marl (Imlay, 1940a; Yurewicz et al., 1993). Adams (1985) described six depositional environments in the Mooringsport Formation. These include a basin, fore-reef, reef, bank margin, bank interior, and restricted shelf. Adams (1985) also reported that uncharacteristically thick Mooringsport reef complexes are the result of rapid subsidence/sea-level rise.

Hydrocarbons produced in the Mooringsport are primarily gas and condensate (Mancini et al., 2012). The Mooringsport Formation is uncomformably overlain by the Paluxy Formation.

The Paluxy Formation is composed of numerous bodies of nonfossiliferous red, brown, and gray sandstones (Hill, 1984), separated by shales. The time of deposition of the Paluxy is characterized as a time of uplift and erosion (Granata, 1963).

Following the deposition of the Fredericksburg Group, a major lowering of sea level in the region exposed the Lower Cretaceous platform margin. This event is represented by the mid Cenomanian unconformity (Salvador, 1991) and the removal of parts of the Trinity and Fredericksburg Group throughout the northern part of the basin (Mancini et al., 2012). Following this, the Lower Cretaceous formations were inundated with the advance of the Gulfian seas (Granata, 1963), marking the end of the Lower Cretaceous. The mid-Cenomanian unconformity marks the end of widespread carbonate deposition and the beginning of abundant terrigenous clastic deposition (McFarlan, 1991).

MATERIALS

i. Public well data

Data for Pelahatchie Field are a composite of public data found on the Mississippi Oil and Gas Board (MSOGB) website, IHS, Inc., and DrillingInfo, as well as donated collections within the Mississippi Mineral Resource Institute's (MMRI) database and website, and core from the Mississippi Department of Environmental Quality (MDEQ). Public data from the MSOGB, IHS, and DrillingInfo databases consist of well records and permits, well logs, scout cards, and scattered production data. The donated collections within the MMRI database typically include printed originals as well as scanned logs. In some collections, exclusive hand-drawn maps made by the donating geologist are also included. Proprietary seismic data exist for the field, however, the University of Mississippi was not able to obtain access to these data. There is much overlap in well records between the four online databases. The use of four unrelated databases ensured quality control and serves as a way to mitigate discrepancies.

In total, 48 wells were used for mapping in this study. Criteria for mapping includes having an XY coordinate as well as log data. Of the 48, 42 wells were within the field extents and 3 were step outs. Of the 42 wells within the field extents, 36 were logged over the entire Glen Rose Subgroup section.

The three step outs previously referenced are the C M Gooch #1, which is used as a northern step out for mapping purposes, the Earl Huffman #1, which is used as an eastern step out for mapping purposes, and the Loper #1-25, which is used as a core point.

ii. Well logs

The primary data type used in the analysis of Pelahatchie Field is downhole well logs. Logging is a process by which in situ reservoir characteristics can be measured and recorded along the length of a wellbore using an array of tools called sondes. This is typically accomplished by lowering a combination of several sondes in one toolstring into the borehole by a wireline, or by multiple logging runs for the same result (Andersen, 2011). An alternate approach to wireline logging is referred to as logging while drilling (LWD), in which case the logging tools are included as part of the drilling tool assembly (Andersen, 2011). Either of these tool assemblies can be employed within a casing (cased-hole logs), or in an open borehole (open-hole logs) before the hole has been cased. Although cased-hole logs can be beneficial in recording production parameters, the steel casing will interfere with many of the logging instruments, resulting in less robust data retrieval. The cement effect also leads to difficulties in separating resistivity contribution of the cement from that of the formation (Zhou, 2005). Caliper logs help to identify possible zones of interference in this case. The most common type of log suite within the field is the electric log. Curves included in the electric log are spontaneous potential and/or gamma ray, resistivity, and conductivity.

Spontaneous potential, or SP, logs indirectly record the electrical potential differences of fluids within the formation and can be used as an indicator of porosity and permeability. The

baseline of an SP curve usually corresponds to impervious strata, while kicks to the left are indicative of permeable strata (Doll, 1949; Varhaug, 2016).

Resistivity logs are a type of electric log which measures a formation's resistivity to an electric current. Hydrocarbon-rich zones will be more resistive than formation water in a given chemostratigaphic unit. Conductivity is the reciprocal of resistivity. The SP curve is generally displayed alongside the resistivity curve for ease of correlation (Varhaug, 2016; Andersen, 2011).

Another common log in the field is the neutron density log. These are used to help determine fluid type and lithology (Asquith, 2004). The neutron porosity tool is often run with a density porosity tool, and a tool measuring the photoelectric absorption properties of the formation. The resulting log is referred to as a lithodensity log. The photoelectric factor, neutron porosity, density porosity log is the most useful in lithologic identification where core is not present. This is especially helpful when correlating core studies to a gamma ray signature and determining an appropriate core shift, if any.

Gamma ray logs are common in the Pelahatchie database and are basic indicators of lithology. Gamma ray logs measure naturally occurring radioactive materials, or NORMs, within the formation. Typically, quartz and carbonates contain little or no intrinsic radioactivity (Andersen, 2011). This is in contrast to shales, which tend to have a high gamma response. When considered collectively, the lithodensity and gamma ray curves can aid in lithologic identification.

Other logs, and their number of occurrence in the field are: micro (8), sonic (12), dipmeter (3), production (8), cement bond (6), mud (3), sample (3), bulk density (1), GR spectralog (1), and caliper (1) PeF (1).

The well logs used in this investigation were raster images. Raster logs require depth registry before they can be used in accurate subsurface mapping by any geologic software. The depth registration process includes rigorously depth matching the image file to a given measured depth (MD) and straightening the file to minimize logs that may have been slightly askew when scanned. An overly askew log could introduce a false deviation of the well from vertical. Depth registering also includes adding appropriate ground and kelly busing elevations to the well database for the most accurate true vertical depth (TVD) and MD readings. Raster logs used in this study's analysis were depth registered in the PRIZM application of GeoGraphix, and stored in the program's database tool.

iii. Core

Core data is an effective supplement to downhole data. The MDEQ does not have record of any full core data within the study area in its warehouse. Cores used in the study are either short intervals of half core, cuttings, and in one case, what seems to be broken quarter core samples in discontinuous intervals. The one full core is located 4 miles to the southeast of the field in the Loper #1-25. Core descriptions were recorded using a template developed by Louis Zachos and modified from Boyles et al. (1986), for specific usage in describing Cotton Valley and Smackover core in the state of Mississippi appendix (a and b).

iv. Mud logs

As mentioned, this study uses 4 mud logs or sample logs. These are typically completed on the well site during the drilling process. The drilling fluid carries cuttings of the formation up through the wellbore to surface shakers on location. These cutting are then analyzed and

recorded on what is referred to as a mud log. The mud log gives a detailed record of the borehole as drilling proceeds. In some cases, mud logging is accompanied by gas chomatography. The gas chromatograph is an instrument that qualitatively measures total hydrocarbons in the drilling fluid. Gas chromatograph (GC) measurements are often unreliable unless accompanied by a daily calibration and use of a constant volume trap. Minor changes in drilling parameters, trap mechanisms, or weather, can have a negative effect on the accuracy of GC measurements.

v. Drilling, completion, and production data

In addition to well header information, production data is commonly associated with each well in online public databases. Although analysis of production data is beyond the scope of this research, the data can be helpful in quantifying the productivity of producing zones. Drilling records provide information on zones that were problematic during the drilling process. Completion records are especially helpful in depth control of information that may be recorded qualitatively elsewhere. For example, completion data can assist in assigning an absolute depth to a producing zone submitted by the operator. Of the 48 wells used for mapping, 35 have publically available production data. DrillingInfo records the total depth (TD) of the hydrocarbon source, however, many are misleading due to the order in which the site generates data for this depth. The depth is usually derived from the completion data. In the absence of completion data, the depth is derived from the deepest plugging. In the absence of plugging data, the number is derived from the deepest permit. In the absence of all previously stated data sources, the number is derived from scout card headers of well logs. Because only 35 of the 48 wells used for mapping have production data, this mean that at least 13 wells are gathering TD data solely from header information. This tends to be unreliable. Another source of error exists in discrepancies of

what is considered the top of a given formation. Public production data is sparse and contains many holes in data vital for data normalization. For these reasons, detailed analyses of production data are excluded in this work. Production data are only used in a qualitative sense to investigate the relationship between cumulative production and structural controls.

vi. Analytical software

Data interpretation for this research is performed using GeoGraphix version 2017.1, ArcGIS version 10.4, and MATLAB. GeoGraphix, or GGX, is an integrated geoscience software suite that includes stratigraphic workflows, subsurface data mapping and contouring, and 3D wellbore viewing capabilities. GGX is the primary software used in subsurface interpretation. All well information and associated logs are uploaded and stored in the geodatabase created in GGX. ArcGIS is used for most surface mapping. Quantitative analysis is achieved by use of MATLAB, a numerical computing software. Other visualization applications used are Corel and Adobe Illustrator.

METHODS

i. Data

GGX version 2017.1 was chosen as the primary interpretation software over ArcGIS 10.4 because of its advanced subsurface mapping capabilities. A new project and AOI were set up using a database coordinate system of NAD 27. The map display coordinate system used is SPCS27 – Mississippi West. Culture layers created in ArcGIS were then imported to help delineate the study area and confirm well locations. IHS well data were imported into GGX by exporting .297 well datasets and importing the data into WellBase, a database application within GGX. Additional data found through use of scout cards or production reports were then associated with their respective wells in the application. Additional data include, but are not limited to, well symbols, current status, current operator, well name, number, API, spud date, ground and kelly bushing elevations. Raster images were then imported into PRIZM, a petrophysical application within GGX. The rasters were then depth registered for accurate mapping. None of the 48 wells were horizontal, although many were deviated. To account for the discrepancy in measured depths between the wells, all formation tops were assigned using total vertical depth. Both structural and stratigraphic cross sections were created in XSection and SmartSection in order to understand the stratigraphic and depositional relationships within the field.

ii. Pelahatchie Field AOI

Pelahatchie Field extends north-south across sections 6, 7, and 18 of Township 5 North, Range 5 East with southern step outs in section 19, a northern step out in section 30, and an eastern step out in section 14. Of the 48 wells used for mapping, 4 are active, 13 are inactive, 23 are plugged and abandoned, 5 are expired permits, 1 is a dry hole, and the status of 2 is unknown. Of the 4 active wells, 2 are oil wells, and 2 are converted disposals. The field AOI will be represented by a yellow hatched rectangle in mapping. The AOI is cropped to exclude the northernmost well in the field located in section 30. Control points are sparse in sections 6 and nonexistent in sections 30. Therefore, the interpretations from section 6 to section 30 would be done with little confidence. The same is true for the three sections leading up to the easternmost well in section 14.

iii. Log analysis

Because inconsistencies exist in formation top picks gathered from mud logs and scout cards throughout Rankin County, the tops chosen for this study are a combination of tops published in the Mississippi Geological Society's Field Archives. Type log tops from Martinville and Merit Fields in Simpson County, and from Boykin Church and Traxler Fields in Smith County were integrated due to their proximity to Pelahatchie Field and distinct log signatures (Davis and Lambert, 1963). In general, mudlogger tops matched those chosen for this study. The main discrepancies were found in the Sligo top picks. These picks were inconsistent when mapped across the field.

The resulting type log used for this study area is shown in Figure 8.

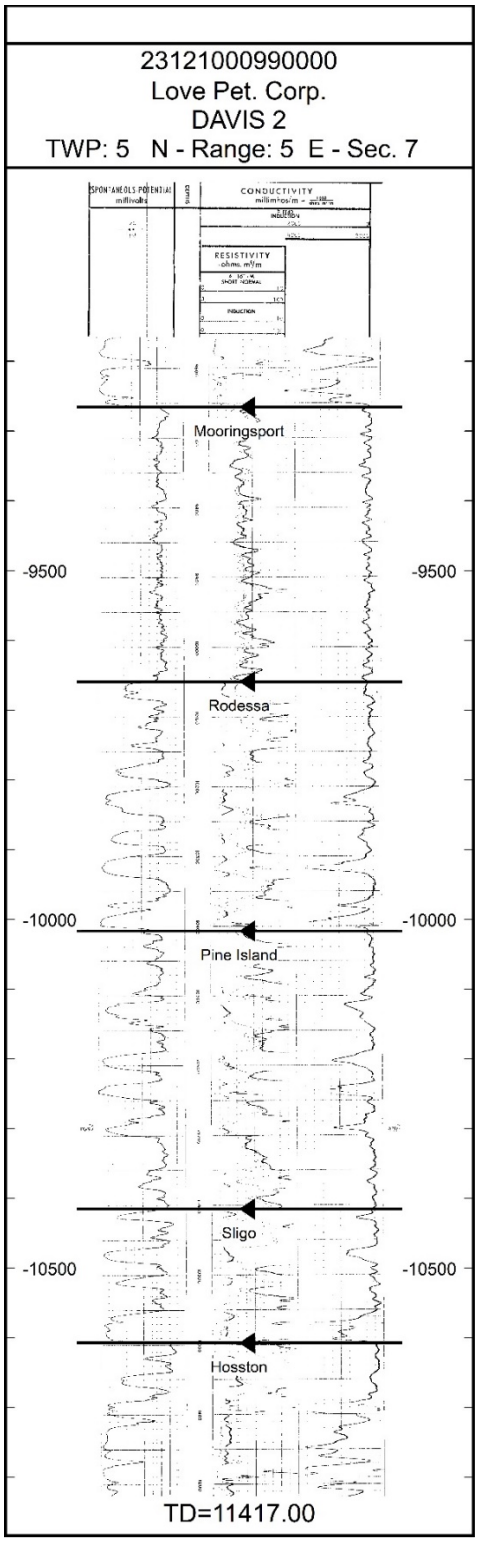

Figure 8. Davis #2 Type Log showing relevant Lower Cretaceous tops in the Glenrose Subgroup. API 23121000990000.

The type log, Love Petroleum's Davis #2, is located in the southwest quarter of section 7. This was chosen as the field's type well because the logged interval exhibits the complete stratigraphic section studied in this research. This well also penetrates the highest number of well-developed sands in each formation, with the most characteristic log signatures. The Davis #2 did not encounter any faulting.

One limitation in this study is the lack of core data within the field. Without core data, mud logs and drill cuttings are of increased value as they are considered to be direct field observations that can serve as constraints to associated wireline responses such as density and photoelectric factor. The one available PeF-density porosity-neutron porosity log in the field is found in the Clifton Rhodes #6-15. This litho-density log was then tied to the Davis #2 type log, as well as a mud log and cuttings from the Earl Huffman #1 to produce a synthetic lithology track based on the PeF-density porosity-neutron porosity log responses in the Clifton Rhodes. The lithologic interpretation in the Clifton Rhodes was analogous to mud log records and data in the Earl Huffman #1 and provided the confidence in the interpretation. The next step was to correlate the synthetic mud log created in the Clifton Rhodes to the Earl Huffman mud log, and the Loper #1's SP and resistivity curves and associated core description. In addition to the Earl Huffman, three other sample logs were donated to the MMRI library from a private collection. A map of wells with sample logs is shown in Figure 9.

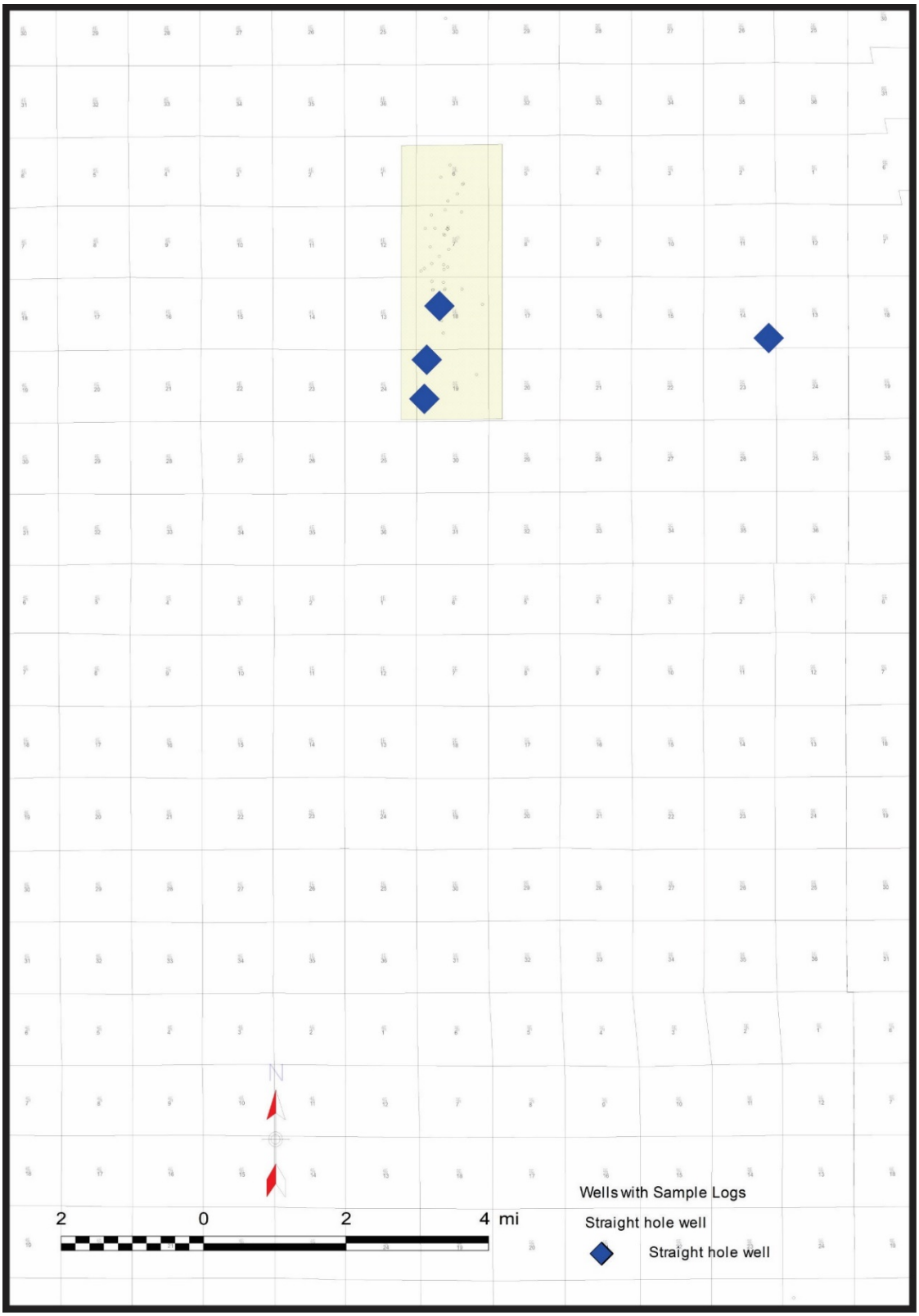

Figure 9. Map showing wells with sample logs throughout area of interest.

The orientation of available sample logs provides good data points for a N-S cross section over sections 18 and 19, but leaves a gap over section 7, which is where the highest density of wells are located. To gain a more complete view of the subsurface lithology, the Clifton Rhodes #6-15 synthetic lithology log was used in place of a sample log for section 7. The incorporation of a lithodensity log provided a more complete lithologic interpretation across the field. The resulting N-S cross section is shown in Figure 10.

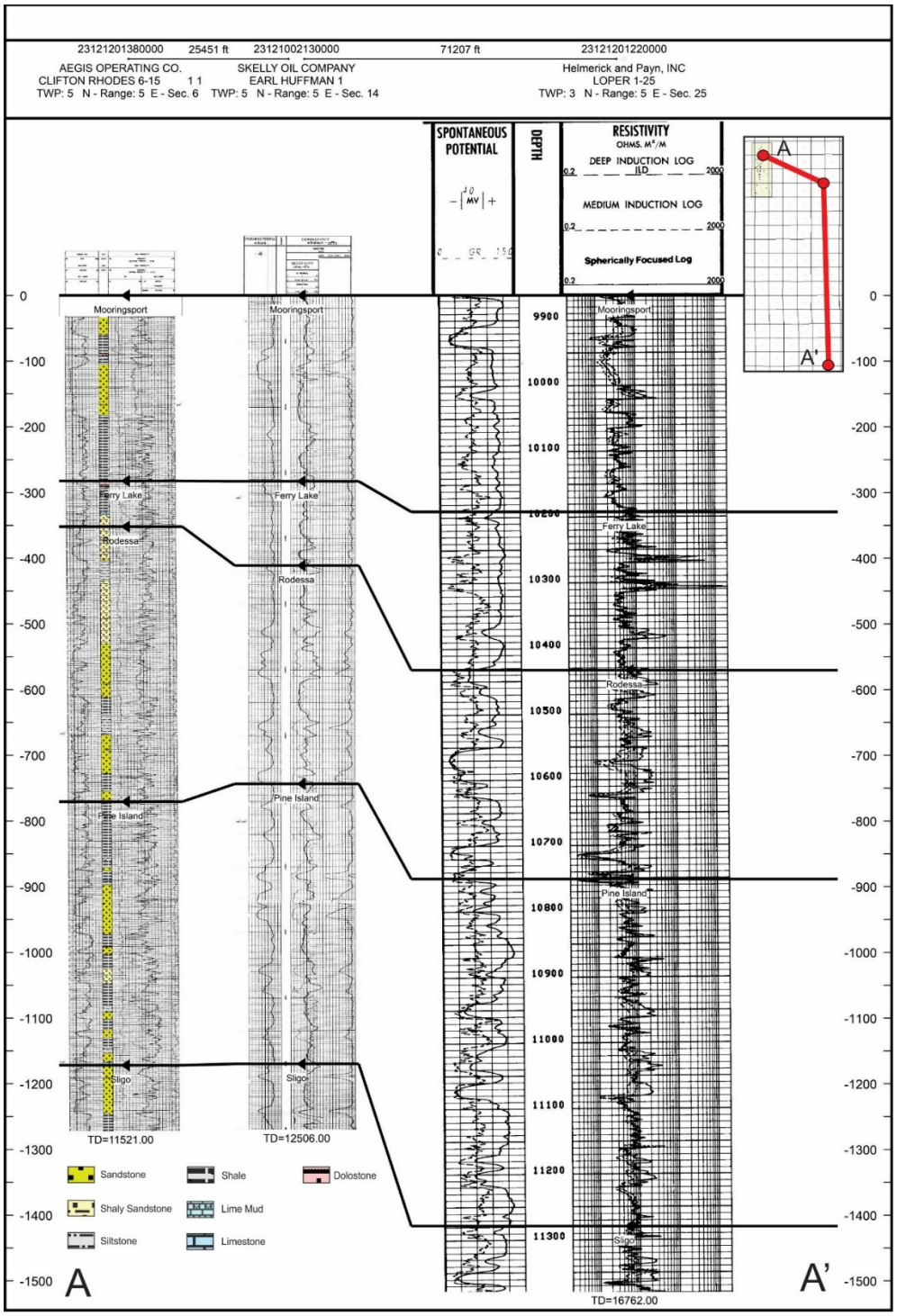

Figure 10. Stratigraphic cross section showing synthetic lithologic log based on Clifton Rhodes #6-15 PE-density porosity-neutron porosity log responses, correlated to the Earl Huffman #1 original mud log and the Loper #1-25. Datum is Mooringsport.

iv. Structure

Structure contour maps were created using GeoGraphix's IsoMap utility. The data set used for surface modeling in this field is constrained by previous drilling operations. As previously stated, data points are lacking to the east and west, and are more robust along the north-south axis. Irregularity in the spacing of data points affects the contour accuracy on the eastern and western flanks of the core data set. To minimize this effect, preliminary structure contour maps and isopach maps were created manually. Eighteen structure contour maps were then created testing sensitivities to different gridding algorithms, search methods, convergences and tolerances, and smoothing factors. The method that best fit the preliminary structure contoured surfaces was then employed during contouring of remaining maps. All maps were made using a minimum curvature gridding algorithm, natural neighbor search method, a convergence of 5%, a tolerance of 5%, 10 iterations of grid smoothing. Grid spacing was set to a smallest feature radius of 1,200 feet, with a corresponding radius of influence. This radius was chosen using the preliminary structure as a benchmark. The perimeters and diameters of closed features in the preliminary map were measured and the smallest used as the minimum feature radius. The initial boundary polygon was used for all structure and isopach maps for consistency. Structure maps were created by subtracting the depth of the horizon found in each electric log from the land surface datum. Isochore maps were produced by subtracting the depth of occurrence of the underlying formation from the overlying formation in order to get the true vertical thickness of the overlying formation at each well point. TVT values were then corrected for dip to yield TST values. All final structure maps and isopachs are the same scale and coverage. Color gradients for both sets of deliverables are also unchanged.

Four faults were identified in the field based on electric log correlation and the isolation of missing section to these locations. Two of the faults were identified first by their missing sections in wells to the south. The missing sections were then calculated in measured log thickness, and converted to true vertical thickness using the Setchell equation, a three dimensional correction factor. Resulting missing sections were then used for offset in the structure contour maps of the tops of formations of interest.

v. Correlation and interpretation of depositional environment(s)

Cross sections developed in this investigation are essential to the examination of subsurface structure and stratigraphy. Determination of fault data, such as missing section due to normal faulting, are derived from well log correlation and used in the construction of integrated subsurface structure maps. Final structural cross sections are used as compliments to structure contour maps. Other important interpretations derived from stratigraphic cross sections in this study are erosional surfaces and the assessment of possible infill sediment. Together, structure and stratigraphic cross sections can be used to validate interpretations of structure and original deposition. Stratigraphic cross sections use the top of the Ferry Lake Formation as a datum. All structural cross sections are displayed in TVD with a vertical and horizontal scaling of 1.00 and a vertical exaggeration of 1.00. The preferred raster image displayed is the 2-inch resistivity log. In cases where this does not exist, a resistivity log of a different scale or another type of log is displayed. A combination of structural, stratigraphic, well-to-well, and projected cross sections was compiled for field interpretation. In one case, a projected structural cross section was displayed in 3D space cutting through formation top surfaces. This view displays formation thickness in relation to field structure and will be used as a visual aid in later discussions.

RESULTS AND DISCUSSION

i. Structure and Stratigraphy

Previous literature has confirmed the presence of a salt dome underlying the field (Karges, 1968), to which the field lends its prominent structure. This salt dome is considered the principal structural control of the field and interpreted to be a narrow, elliptical north-south trending feature. The dome is generally symmetric with a north-south axial trace. Within the extent of the principal dome, structure contour maps show the existence of three structural highs within the Hosston and Sligo Formations, and two structural highs within the Pine Island, Rodessa, and Mooringsport Formations. A north-south structural cross section covering the entire AOI (Fig. 11) illustrates the structure of the field, as well as the overall dip direction of the formations to the south. Formations have been projected onto a north-south axis line and color filled in Figure 12 to further visualize well interaction with structural influences. Formations within the Glen Rose Subgroup dip locally to the south.

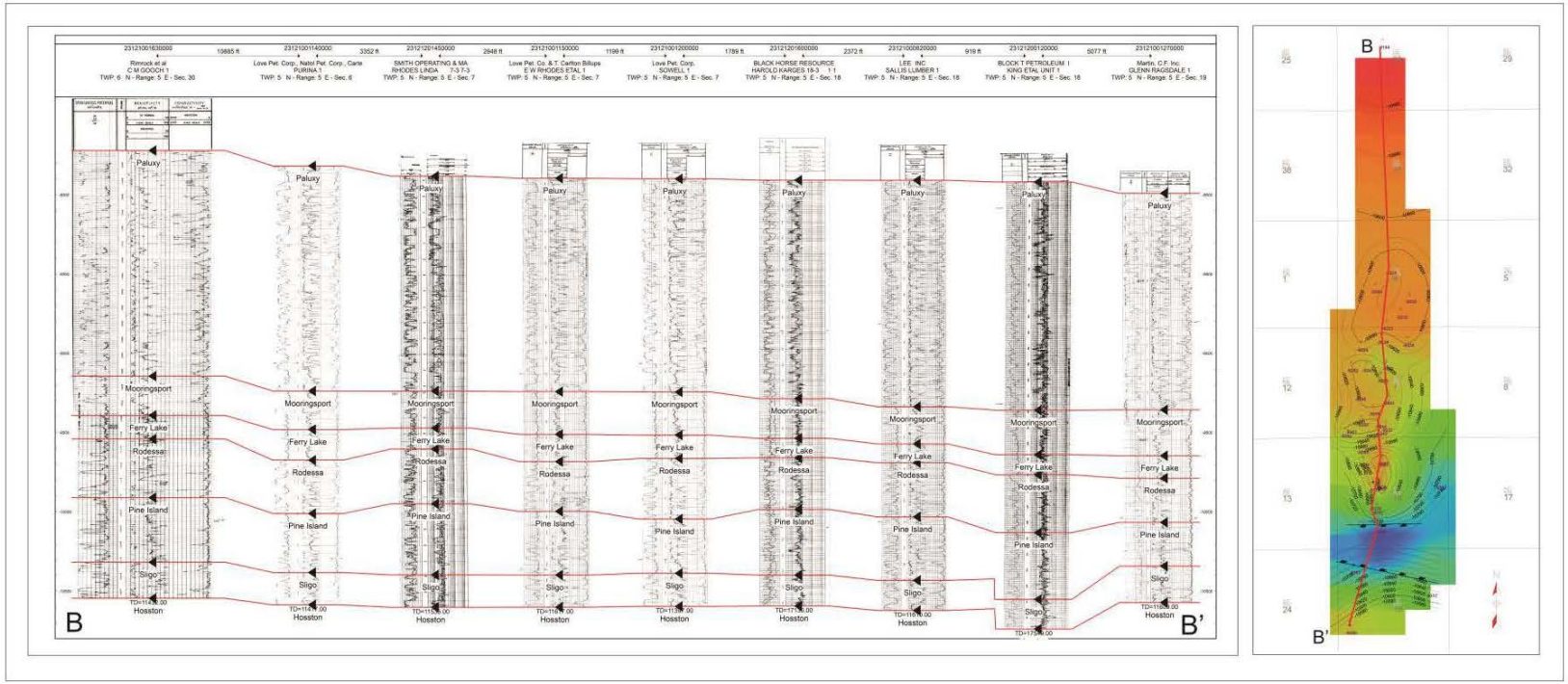

Figure 11. N-S structural cross section displayed over Top of Hosston Structure map.

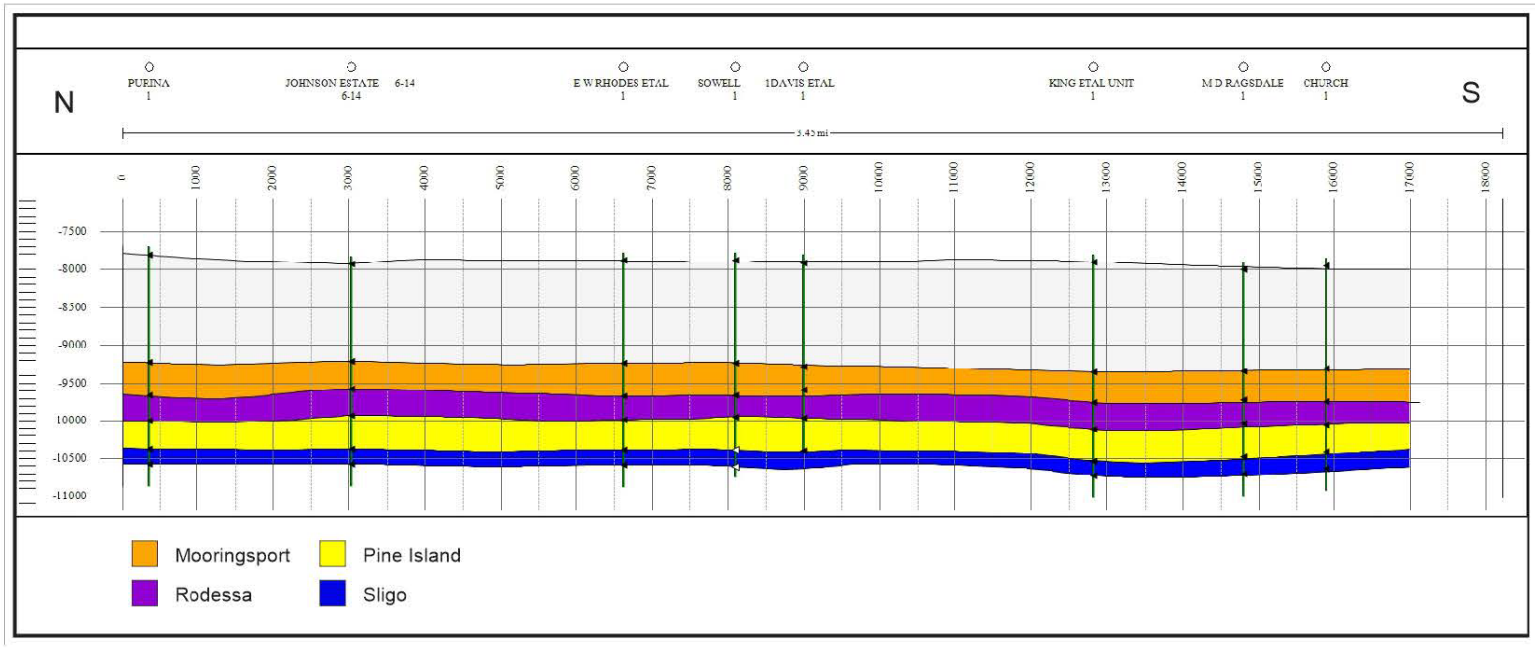

Figure 12. Projected N-S cross section showing structural surfaces along the N-S axis of the primary field structure.

Three faults were identified using electric log correlation in the field. Although the exact azimuth of fault planes cannot be confirmed due to a lack of number of wells encountering the same faults, anticipated fault traces have been delineated based on structural contours. The two fault traces cut by wells in section 18 and section 19 strike west-east. The two faults traces strike generally parallel to the strike of the southernmost edge of the principal feature. Wells in this area do not demonstrate significant deviation from vertical. Because the deviation effect is minimal in the area, no meaningful trigonometric corrections are required to measure the missing section of faults. Missing section values measured in TVD depths are equal to true vertical thickness values and can be used directly. The fault identified in the southern portion of section 18 is a normal fault, with the downthrown block to the south, and has a missing section of 130 feet. The fault is encountered in the King et al. Unit #1 at a depth of -10,868. The fault identified in the northern margin of section 19 is normal, with the downthrown block to the north, and has a missing section of 147 feet. The fault is encountered in the M.D. Ragsdale #1 at a depth of -10, 837. The downthrown blocks of both faults being toward one another, this paleographic low in between these wells is interpreted as a graben that is present in the Hosston, Sligo, and Pine Island Formations, and is partially infilled by younger strata beginning in the Rodessa. It could be argued that both faults propagate into the Rodessa. The faults were terminated at the Rodessa because the Rodessa displays thickening of as much as 42 feet within the graben, suggesting that displacement due to faulting was minimal and sedimentation in the downthrown block began to infill the paleotopographic low. The log signature in the King et al. Unit #1 within the Rodessa indicates a more fine-grained interval than wells on the north and south of the paleotopographic low, indicating enhanced deposition of mudstones and siltstones within topographic lows. Strata in the Mooringsport show little influence of this graben feature (Fig. 13) and are contoured to

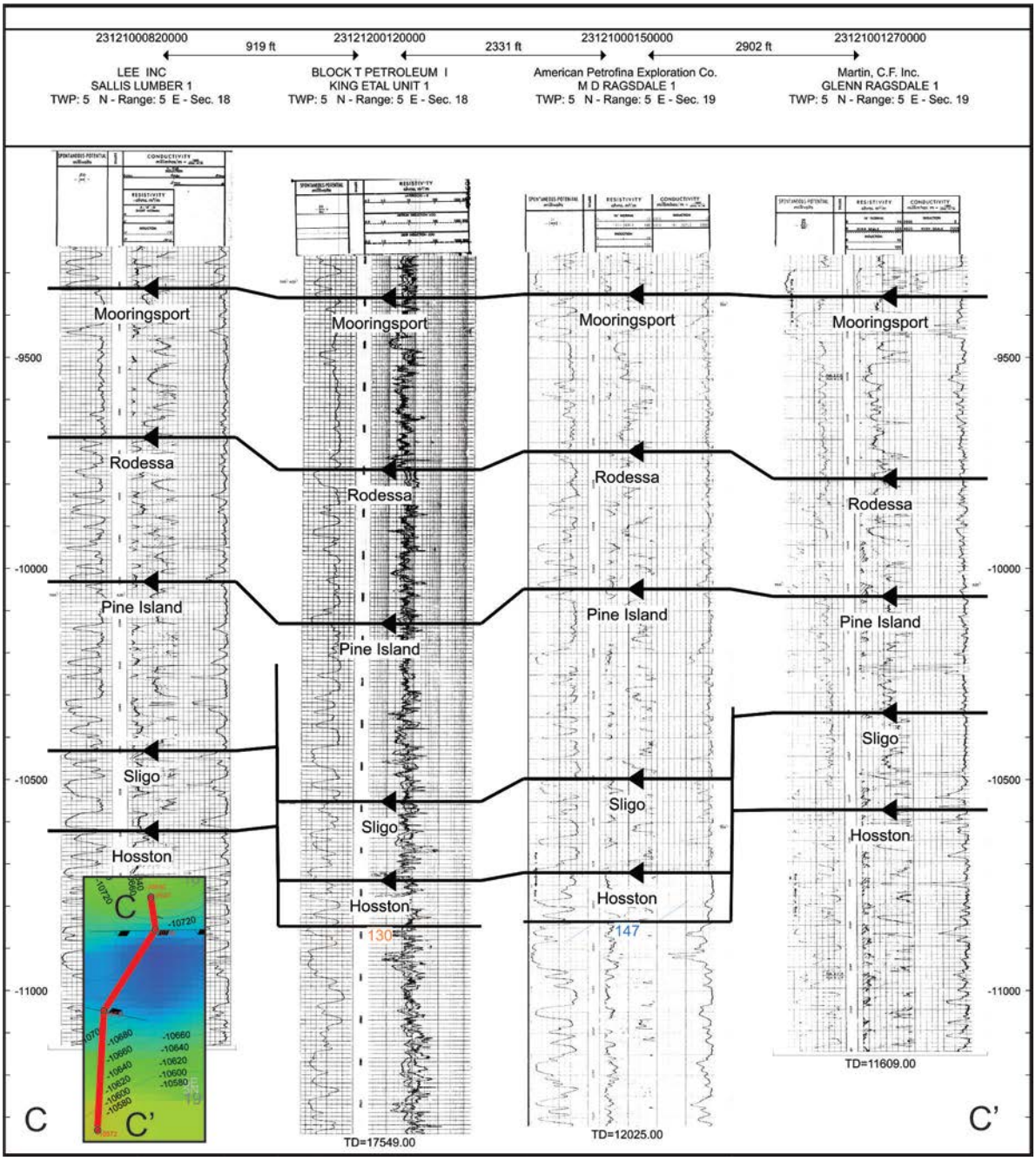

Figure 13. North to south structural cross section over sections 18 and 19 showing faulting in the King et al. Unit 1 and the M.D. Ragsdale #1. Missing section labeled at each fault depth. Formations are offset according to missing section. Cross section location is displayed over the Pine Island structure contour map.

reflect this. Structure maps include one fault on the southwest corner of section 7 (Fig. 14). This fault is not encountered by a well. Instead, this fault is identified based on a 50’ displacement between the E.W. Rhodes 7-6 #4 and the Leon #1, which are located only 320 feet from one another on surface. This fault surface is not formatted to show vertical offset in strata in cross sections because the fault does not penetrate wells. The two faults in section 18 are shown with vertical offset of strata in cross section because they are encountered within the Kind et al. Unit #1 and the M.D. Ragsdale #1.

The one area of contour pinching due to a 45’ formation top offset in the Sowell #1 in section 7 is not representative of a fault encountered by the well in this study, though a 50’ fault in the Rodessa at a depth of -9,940 was noted by the site geologist, Marvin Oxley in the nearby Rhodes E W et al. #1. This study did not identify a fault at this depth, however, this 50’ offset does match the missing section found in this study to be caused by a small stream in the base of the Rodessa Formation. This stream cuts into the upper Pine Island shale, causing the Rodessa Formation top picks within the channel to have offsets of about 40’ compared to top picks in surrounding wells. Based on the structure contour maps, the structural influence of the underlying salt feature is more prominent in the deeper horizons, and has increasingly less influence on younger horizons as faults terminate and paleotopographic lows are infilled by younger strata. The remainder of this section will report the structural results of each of the mapped formations in order from oldest to youngest.

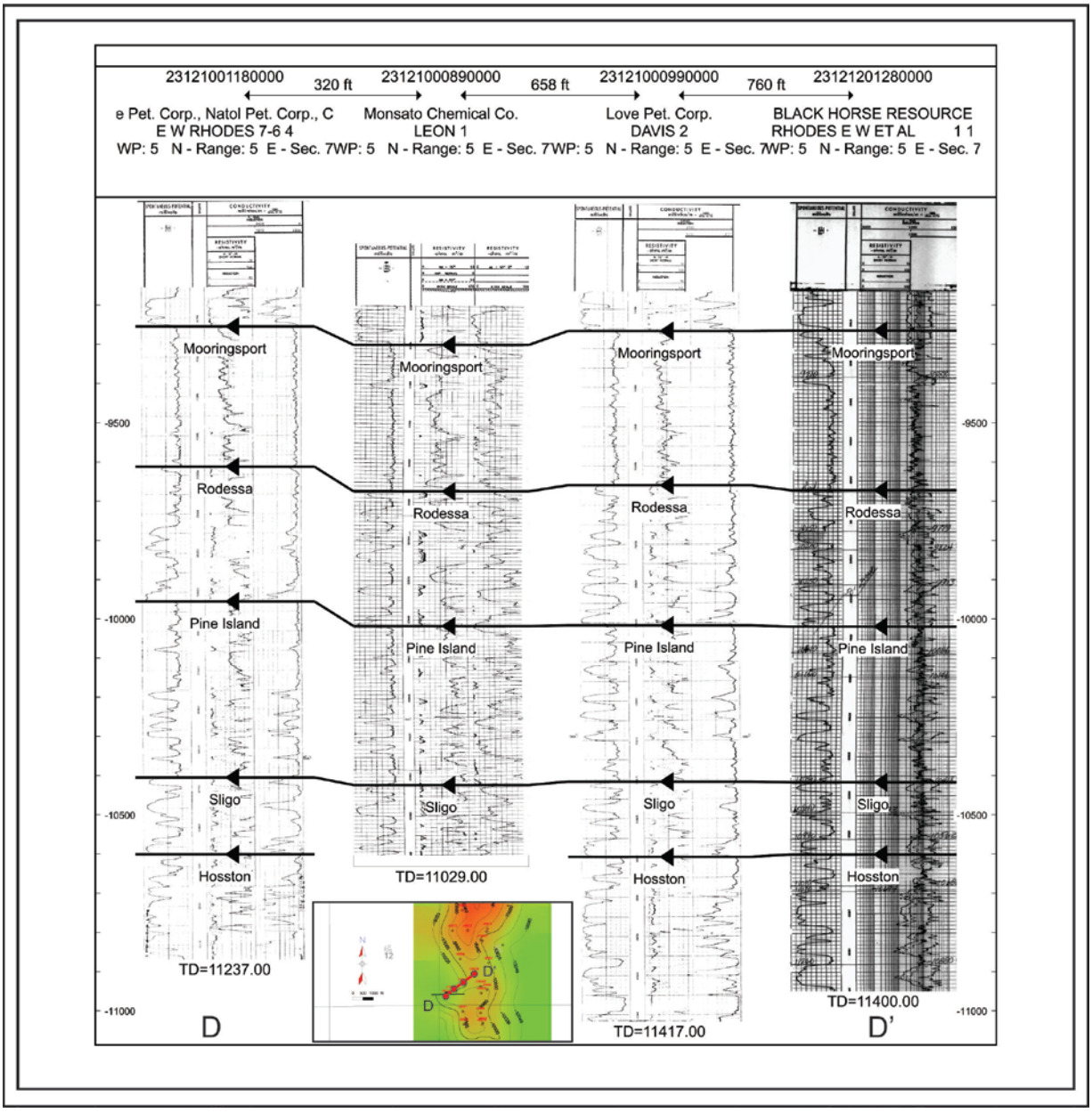

Figure 14. Southwest to northeast structural cross section over section 7 showing fault on western flank of section 7 paleohigh between the E. W. Rhodes 7-6 #4 and the Leon #1. Cross section location is displayed over the Pine Island structure contour map.

Hosston Formation: The Hosston Formation is characterized by three major north-south trending elongate paleohighs and a graben to the south. The minimum Z value in the Hosston subsea dataset is -10739. The maximum Z value is -10517. The Mean Z value is -10614. The three structural highs present in the Hosston Formation are located in sections 18, 7, and 6 (Fig. 15). The Hosston Formation does not have a TST map because the underlying formation top was not picked and many wells in the field have a total depth that does not penetrate deeper than the Hosston Formation.

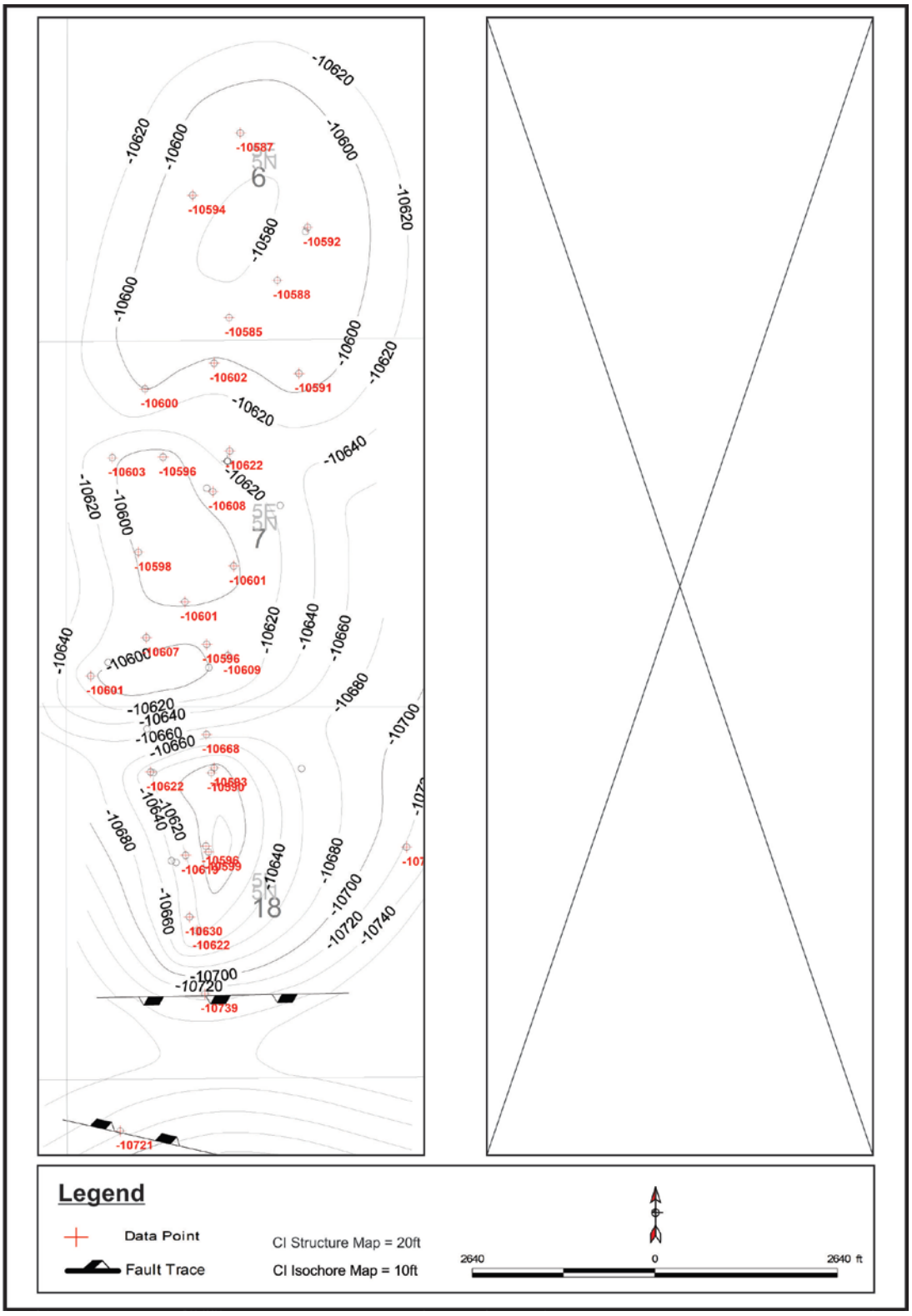

Figure 15. (Left): Top of Hosston Formation Structure Map. Depth in subsea. Depths in red correspond to data points. (Right): TST Isopach Map of Hosston Formation.

The principal dome within the Hosston structure contour map exhibits a gradient of 645 feet per mile at the southernmost edge of the high in section 18. This gradient is steeper than any of the other highs mapped in this formation.

Sligo Formation: The Sligo is also characterized by three north-south trending elongate paleohighs and a graben to the south. The Sligo is most structurally similar to the underlying Hosston Formation. The minimum Z value in the Sligo subsea dataset is -10506. The maximum Z value is -10317. The mean Z value is -10408. The three structural highs present in the Sligo Formation are also located in sections 18, 7, and 6 (Fig. 16). The principal dome within the Sligo structure contour map exhibits a gradient of 694 feet per mile at the southernmost edge of the high in section 18. This gradient is steeper than any of the other highs mapped in this formation and is also steeper than the gradient in the same position as calculated in the Hosston. This suggests re-initiation of halokinesis during deposition of the Sligo Formation. A west-east structural cross section over the crest of the paleotopographic high in section in section 6 (Fig. 17) shows slight thinning of the Sligo Formation in sections 6 and 7 as much as 16 feet over the shallowest paleohigh in section 6.

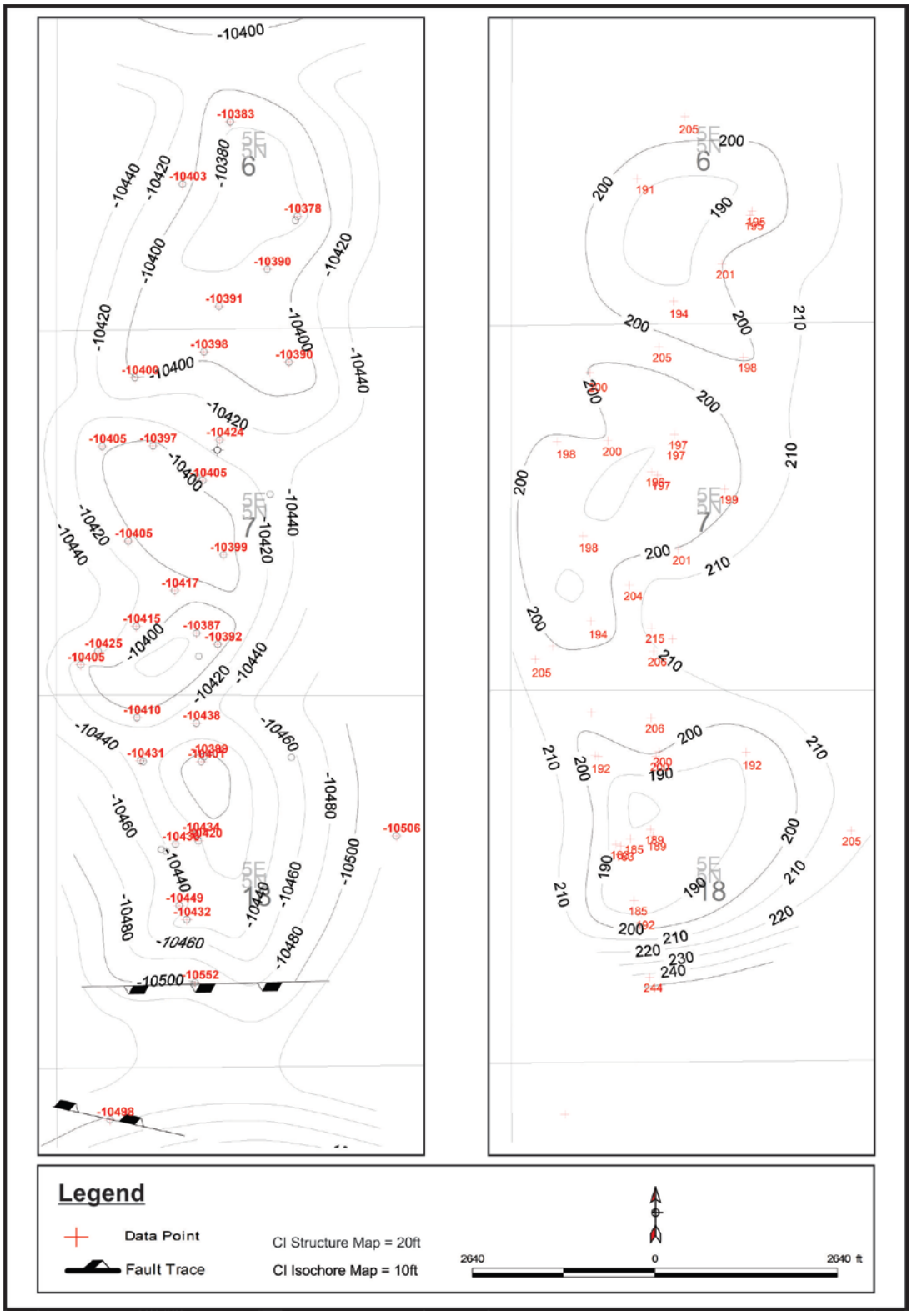

Figure 16. (Left): Top of Sligo Formation Structure Map. Depth in subsea. Depths in red correspond to data points. (Right): TST Isopach Map of Sligo Formation.

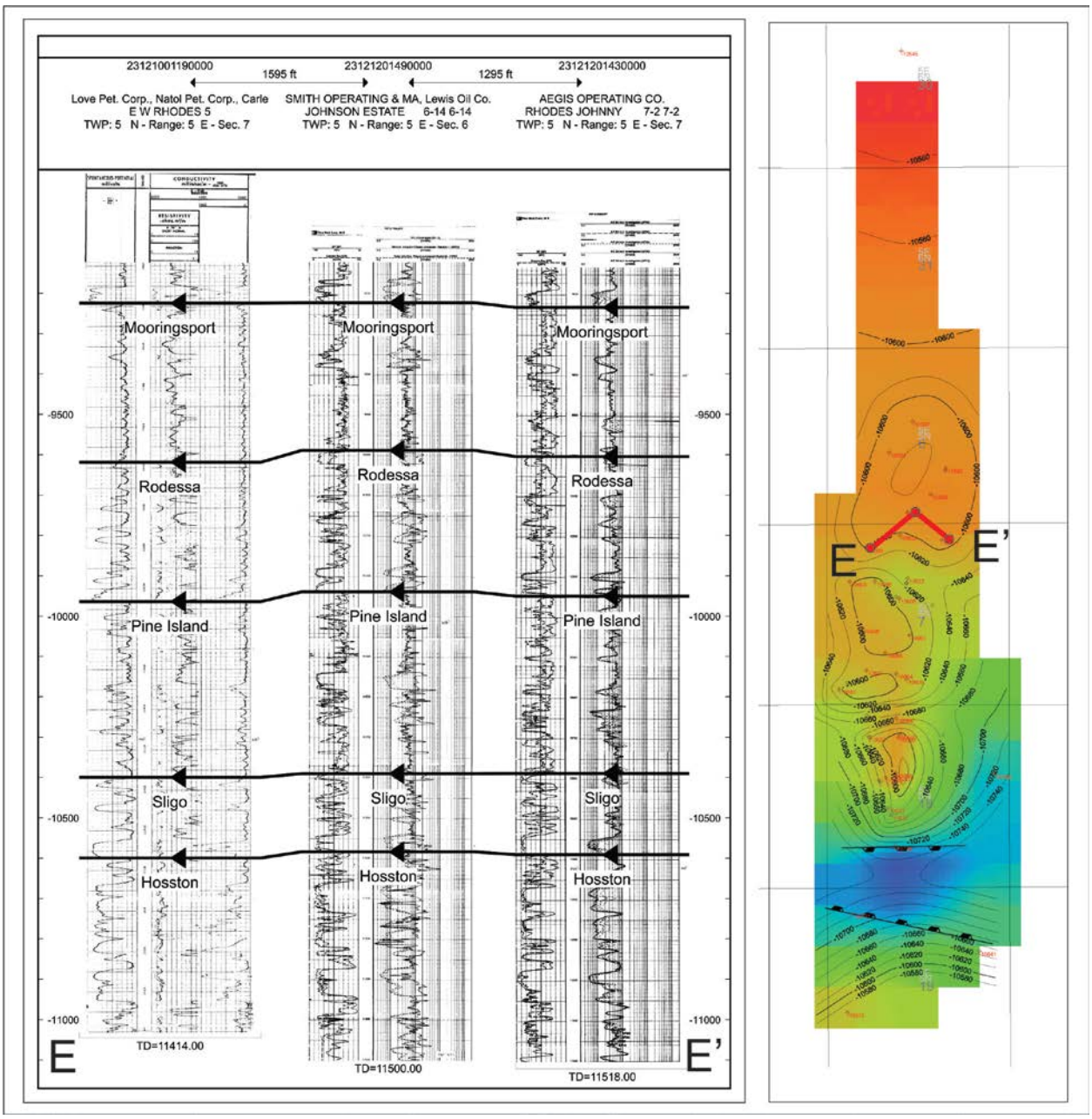

Figure 17. West to east structural cross section showing central uplift. Structure is more prominent to the south. Cross section is displayed over top of Hosston Formation structure map.

Pine Island Formation: The Pine Island is characterized by two north-south trending paleohighs, and a graben to the south. The minimum Z value in the Pine Island dataset is -10,131. The maximum Z value is -9,910. The mean Z value is -10,005. The paleotopographic low that existed between the highs in sections 18 and 7 is less prevalent in the subsea structure map of the Pine Island (Fig. 18). The paleotopographic low in this horizon can be contoured as one structural high rather than two. The most pronounced of these paleo highs is present in section 6 rather than section 18 in underlying formations. The gradient of the paleohigh in section 18 is 541 feet per mile, which is less steep than the underlying Sligo Formation. The Pine Island TST isopach shows thinning as much as 51 feet across structural crests of the underlying Sligo Formation. The Pine Island TST map also shows thinning on the western flank of the middle paleohigh in section 7.

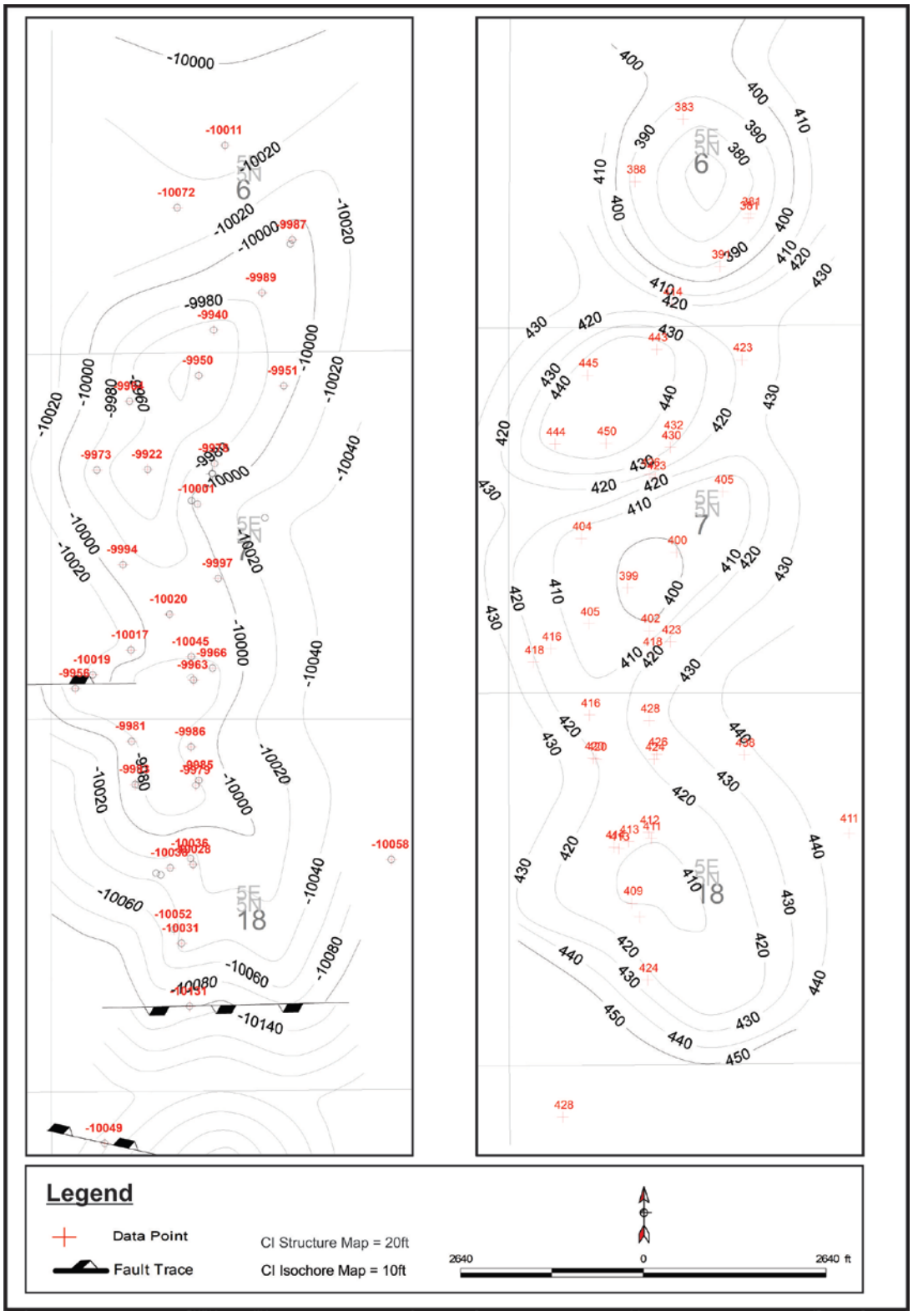

Figure 18. (Left): Top of Pine Island Formation Structure Map. Depth in subsea. Depths in red correspond to data points. (Right): TST Isopach Map of Pine Island Formation.

The Rodessa: The Rodessa is characterized by two north-south trending paleohighs with only one of the underlying faults present on the western flank of the southern paleohigh. Domal features in the Rodessa are less distinct than in underlying formations. The minimum Z value in the Rodessa dataset is -9,787. The maximum Z value is -9,540. The mean Z value is -9,668. The paleotopographic low between sections 18 and 7 is also less prevalent in the subsea structure contour map of the Rodessa (Figure 19).

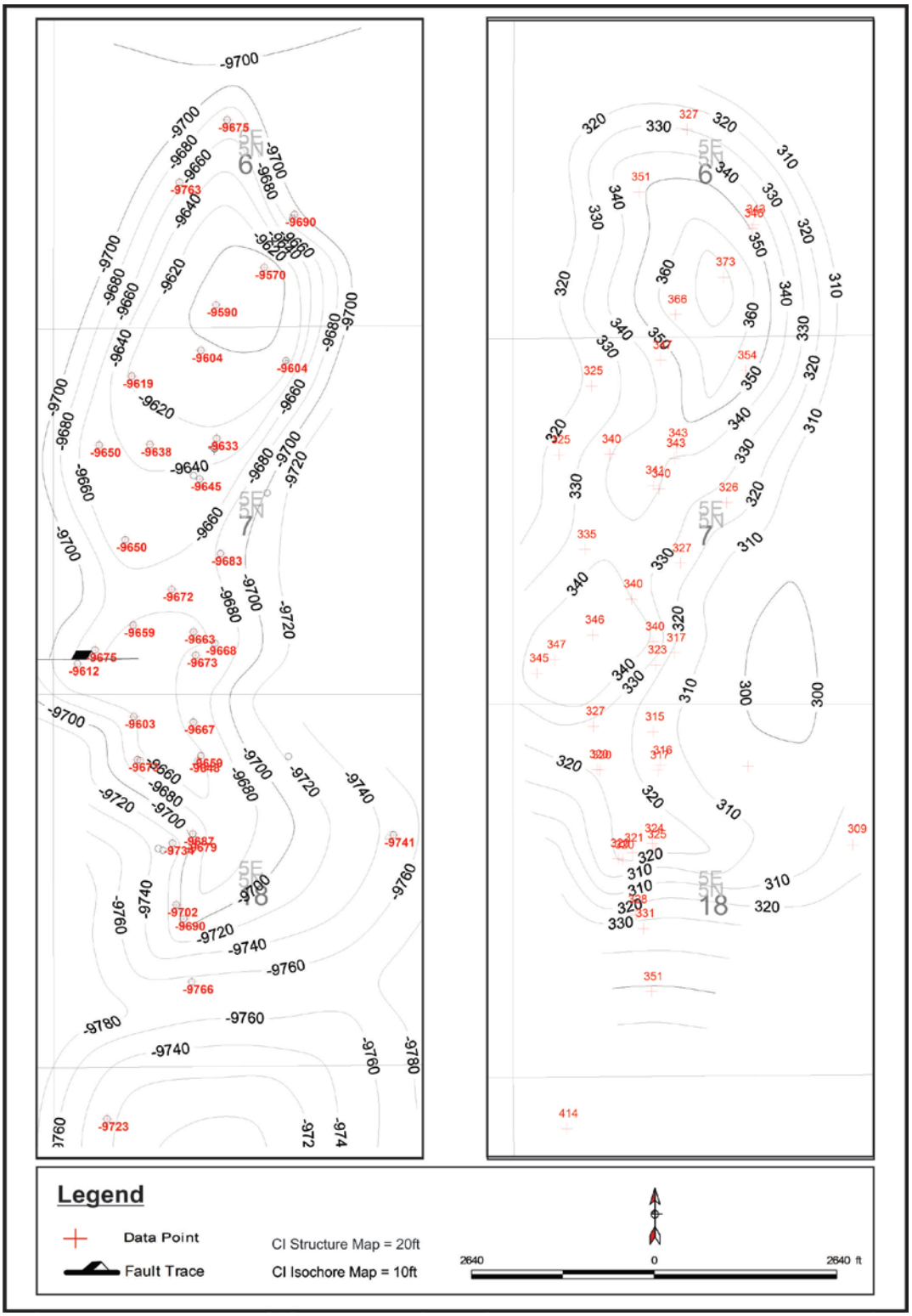

Figure 19. (Left): Top of Rodessa Formation Structure Map. Depth in subsea. Depths in red correspond to data points. (Right): TST Isopach Map of Rodessa Formation.

For this reason, one structural high is contoured rather than two in the southern half of section 7 and northern half of section 18. The most pronounced paleohigh is located in section 6, like the underlying Pine Island Formation. The gradient of the paleohigh in section 18 in the Rodessa Formation is 420 feet per mile, which is less steep than in the underlying Pine Island Formation. The Rodessa TST isopach shows thinning as much as 60 feet, but is not correlating with the underlying Pine Island Formation. Thickenning of the Rodessa is present in southeastern corner of section 6, the southwestern corner of section 7, and northeastern half of section 8. Thicker areas of the Rodessa Formation are bordered by thinner areas. The thickening and thinning pattern of the TST map records the presence of a channel in the base of the Rodessa Formation, which displays deflection around paleohighs present in the underlying Pine Island Formation (Fig. 20). The deeper Pine Island Formation top in the Davis #2 and the Sowell #1 correspond to what would be the depositional pattern characteristic of a channel thalweg on the outer perimeter of a meander. The Rodessa TST map shows higher stratigraphic thickness where the Pine Island shows lower stratigraphic thickness. The inner perimeter of the same meander records a rapid decrease in thickness. The rapid decrease on thickness would be representative of a shallow channel bank. The electric logs of the Davis#2 and Sowell #1 shown in the structural cross section in Figure 19 display offset in Pine Island and Rodessa top picks between the two inner

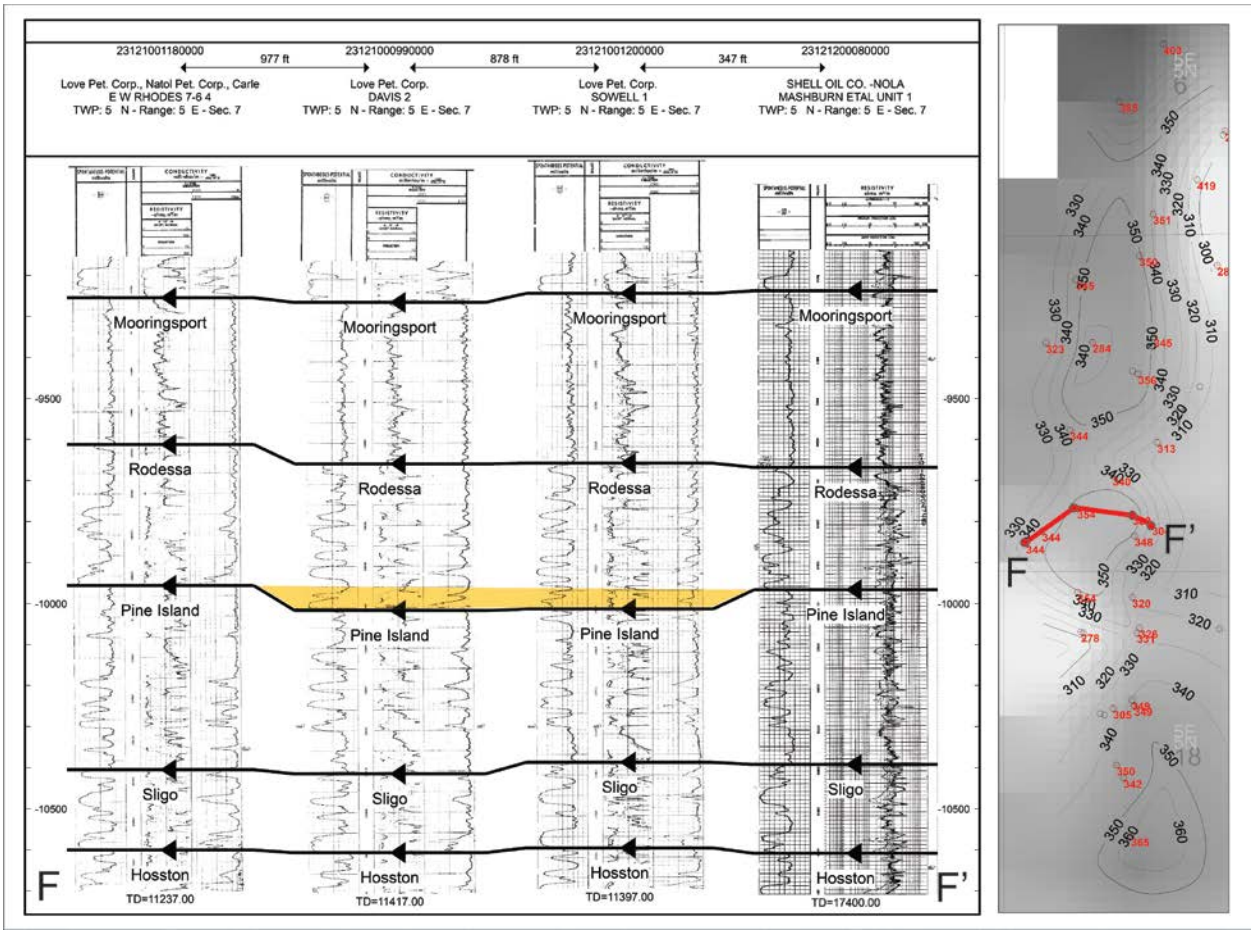

Figure 20. Structural cross section depicting possible channel in base of Rodessa in yellow shading. Isopach shows elongate thickening possibly attributed to erosion and channel infill.

wells, the Davis #2 and the Sowell #1, and the wells on the west and east, the E.W. Rhodes 7-6 #4 and the Mashburn et al. Unit 1. Close examination of the log signatures in the Davis #2, Sowell #1, E.W. Rhodes 7-6 #4, and the Mashburn et al. Unit 1 exposes a much thinner shale/siltstone interval within the upper Pine Island in the Davis #2 and Sowell #1 (Fig. 21).

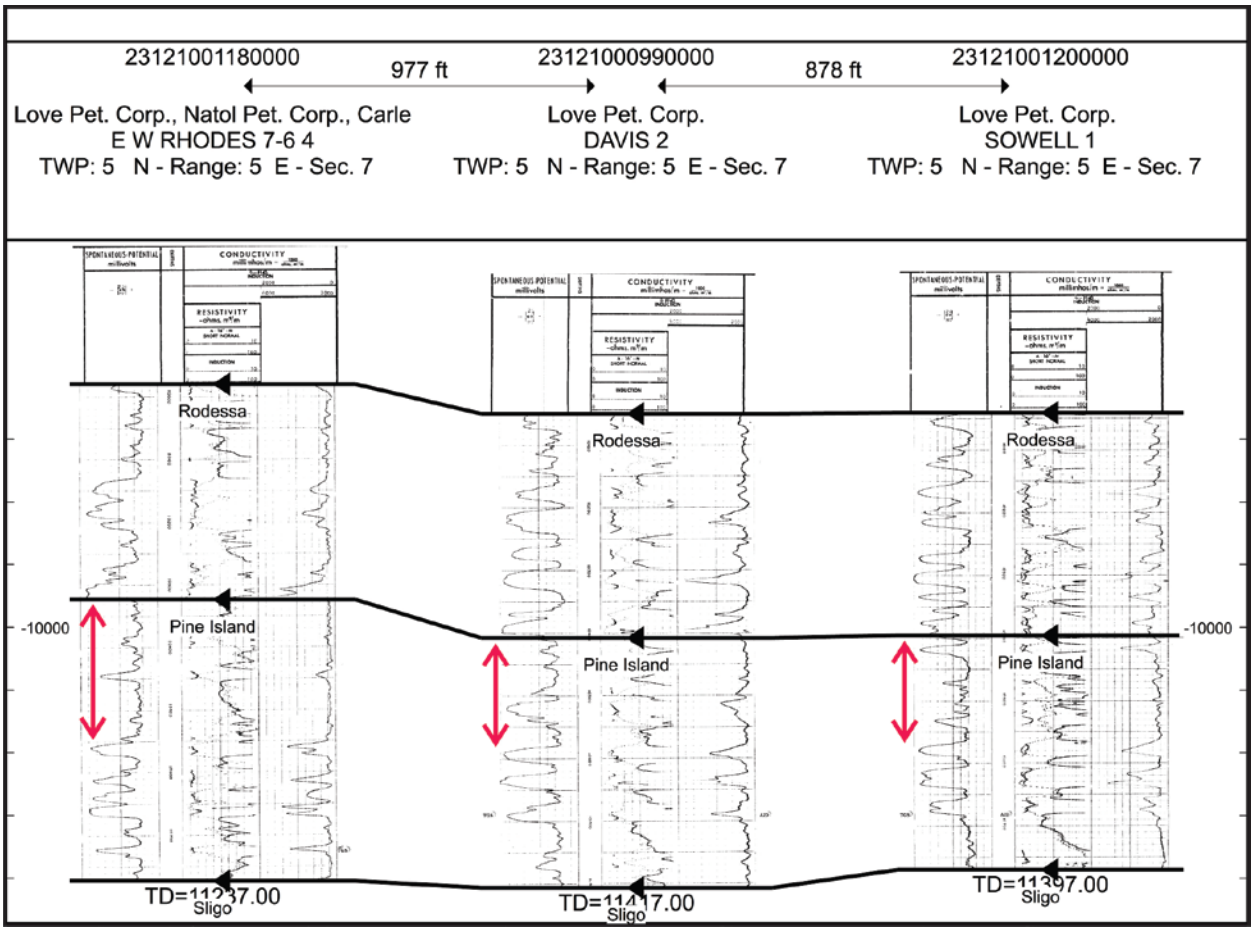

Figure 21. Structural cross section showing thinning of Pine Island upper shale interval.

Where the shale/siltstone interval is thinner, a basal sand is introduced that is not seen in the offset wells. This suggests that the underlying Pine Island shale/siltstone was eroded and infilled by the sands present at the base of the Rodessa. Furthermore, the Davis #2 and the Sowell #1 lie within the trend of thicker Rodessa deposits as shown in the Rodessa TST isopach. The trend of thicker deposits is similar to that of a meandering channel. If this trend was to continue, the channel would be expected to curve to the south-east across the north-eastern corner of section 18 towards the L.E. Knight well. This interpretation is solidified by similarities in the log signatures of the L.E. Knight to the Davis #2 and the Sowell #1. Although there is strong

evidence for this interpretation, it cannot be confirmed without a detailed lithologic analysis of at least one well within the channel trend or additional drilling or seismic data.

Mooringsport Formation: The Mooringsport is characterized by two paleohighs. The paleohighs, however, are the least distinct in the Mooringsport. There is a central low separating the northern and southern paleohighs and only one fault on the western flank of the southern paleohigh. The minimum Z value in the Mooringsport dataset is -9382. The maximum Z value is -9144. The mean Z value is -9276. Similar to the Rodessa Formation, the paleotopographic low between sections 18 and 7 is less prevalent in the subsea structure contour map of the Mooringsport (Fig. 22). One elongate structural high is present in the southern half of section 7 and northern half of section 18 rather than two. The most prominent paleohigh is located in section 6. The gradient of the paleohigh in section 18 in the Mooringsport Formation is 126 feet per mile. This gradient is over 3 times gentler than the same gradient in the underlying Rodessa Formation. This indicates sediment infill within the topographic lows of the Rodessa Formation. The Mooringsport TVT isochore shows thinning as much as 45 feet across the structural crests of the underlying Rodessa Formation. The thinning of formations across structural crests suggests that salt movement continued at various rates into the middle Albian.

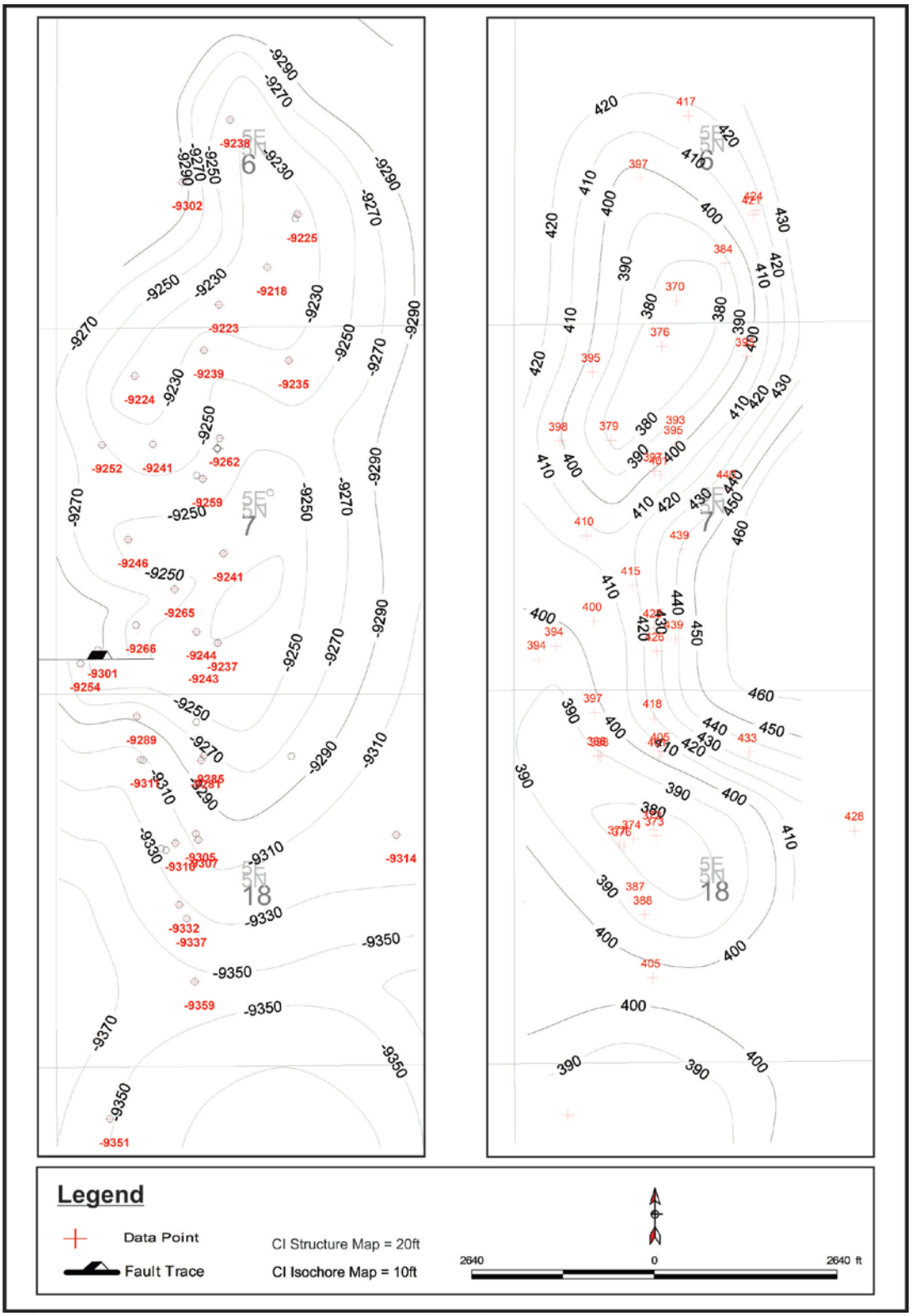

Figure 22. (Left): Top of Mooringsport Formation Structure Map. Depth in subsea. Depths in red correspond to data points. (Right): TST Isopach Map of Mooringsport Formation.

A 3D subsurface map of all preceding structure contour grids is shown in Figure 23, depicting well intersections with structure throughout the field. The contour surfaces

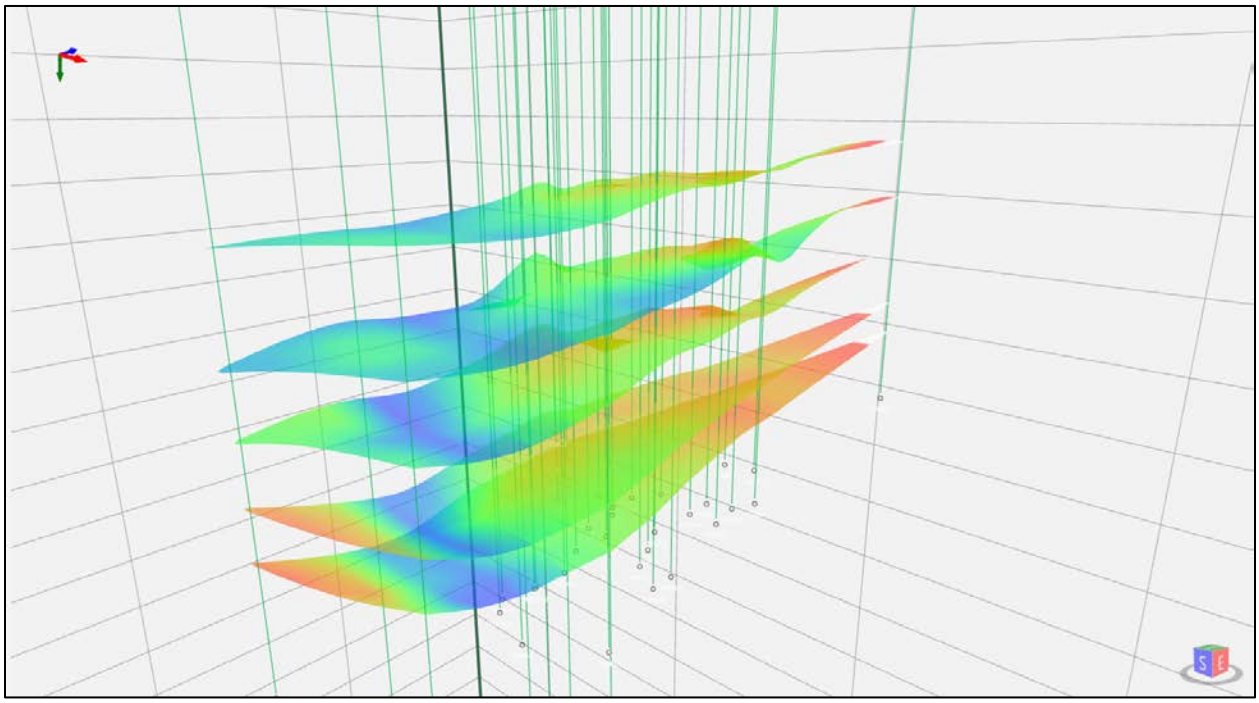

Figure 23. Subsurface view of Hosston, Sligo, Pine Island, Rodessa, and Mooringsport structure contour grids in 3D space. Wellbores are shown in green. TD of each well is labeled in white and posted at the bottom hole location. Vertical exaggeration equals 5.95. Horizontal grid lines represent 500 feet.

displayed in Figure 23 are the structure grids of the Hosston, overlain by the Sligo, overlain by the Pine Island, overlain by the Rodessa, overlain by the Mooringsport. In general, all of the horizons follow the same structural geometry, with less structural definition in younger horizons. An exception to this is found in the Sligo, where slightly steeper gradients are found on the flanks of the southern paleohigh quantified in the preceding paragraphs.

The structural closure seen in the Lower Cretaceous strata may act as an important trapping mechanism for the petroleum system. To qualitatively test this theory, production values assigned to producing formations by use of API gravities were superimposed onto a structure contour grid. Results from a preliminary investigation show that the formations within this study can be differentiated with confidence based on their produced oil API gravities. The one exception to this is between the Sligo Formation and the Hosston Formation. These two formations cannot be differentiated, which is consistent with their syndepositional nature in literature. Results from this preliminary investigation are recorded in (appendix c). The exercise allowed for a cumulative production bubble map with production in each horizon to be created (Fig. 24). The resulting bubble map overlaying the Rodessa Formation Top structure map

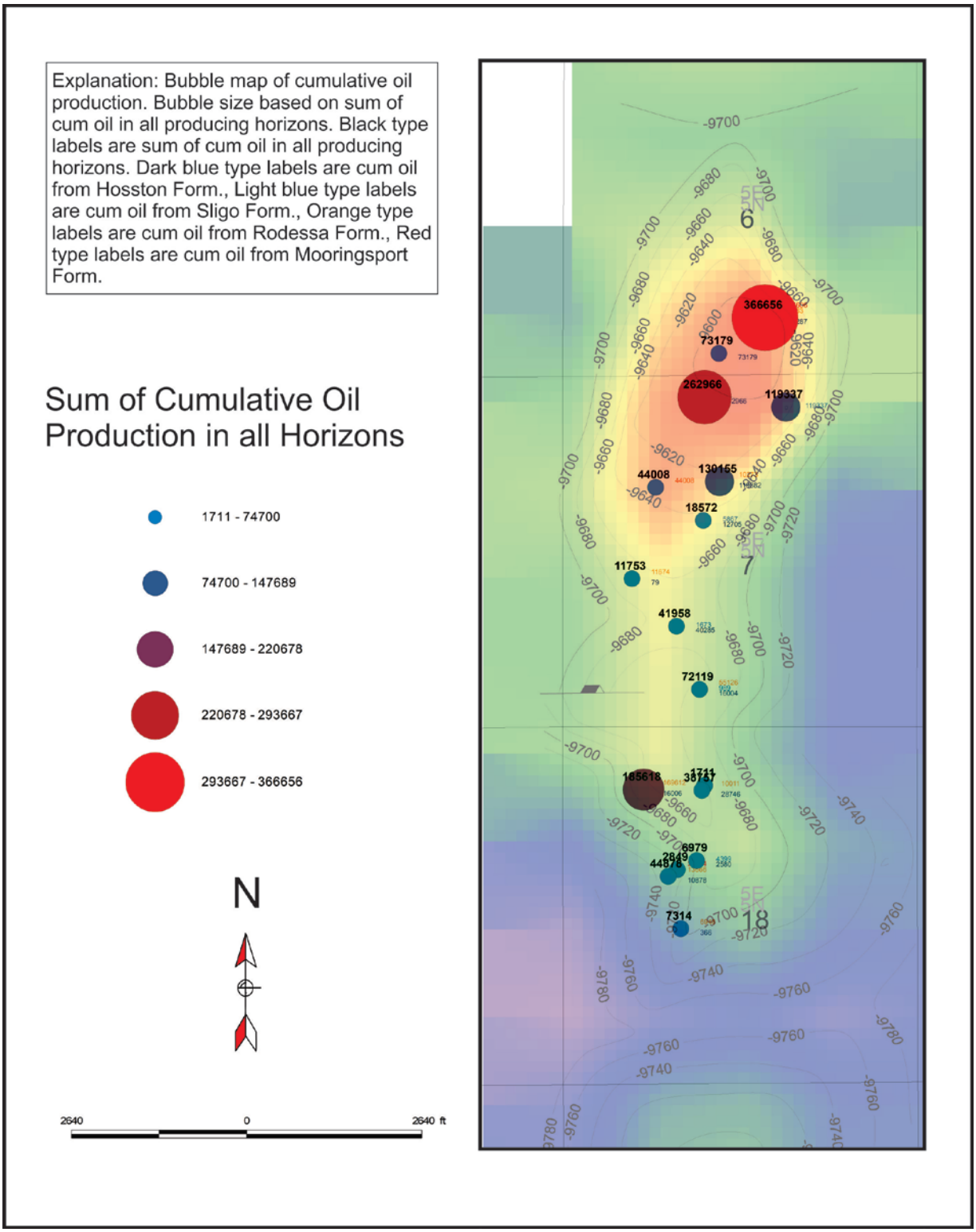

Figure 24. Cumulative oil production map overlaying Rodessa Formation structure top map.

confirms that closure is a hydrocarbon trapping mechanism. The Rodessa Formation structural grid was chosen for this map because the production dataset includes the most data values in this horizon. Bubble sizes represent the sum of cumulative oil produced in each formation perforated over the lifetime of the well. This map is not normalized in respect to days on production due to the lack of production data and should be used only qualitatively. This exercise shows that wells drilled within a paleohigh produce oil; those on the flanks of the structures are dry holes showing no production. There is also a positive correlation between higher cumulative oil and higher structural relief.

i. Environment(s) of Deposition

Results from the Loper #1 core analysis are recorded in (appendix d) and digitally rendered in Figure 25. This core covers 51 feet of the lower Mooringsport Formation, from -10,364 to -10,415. The core shift is 3 feet. The cored interval is primarily composed of red and maroon to slightly teal-gray clays

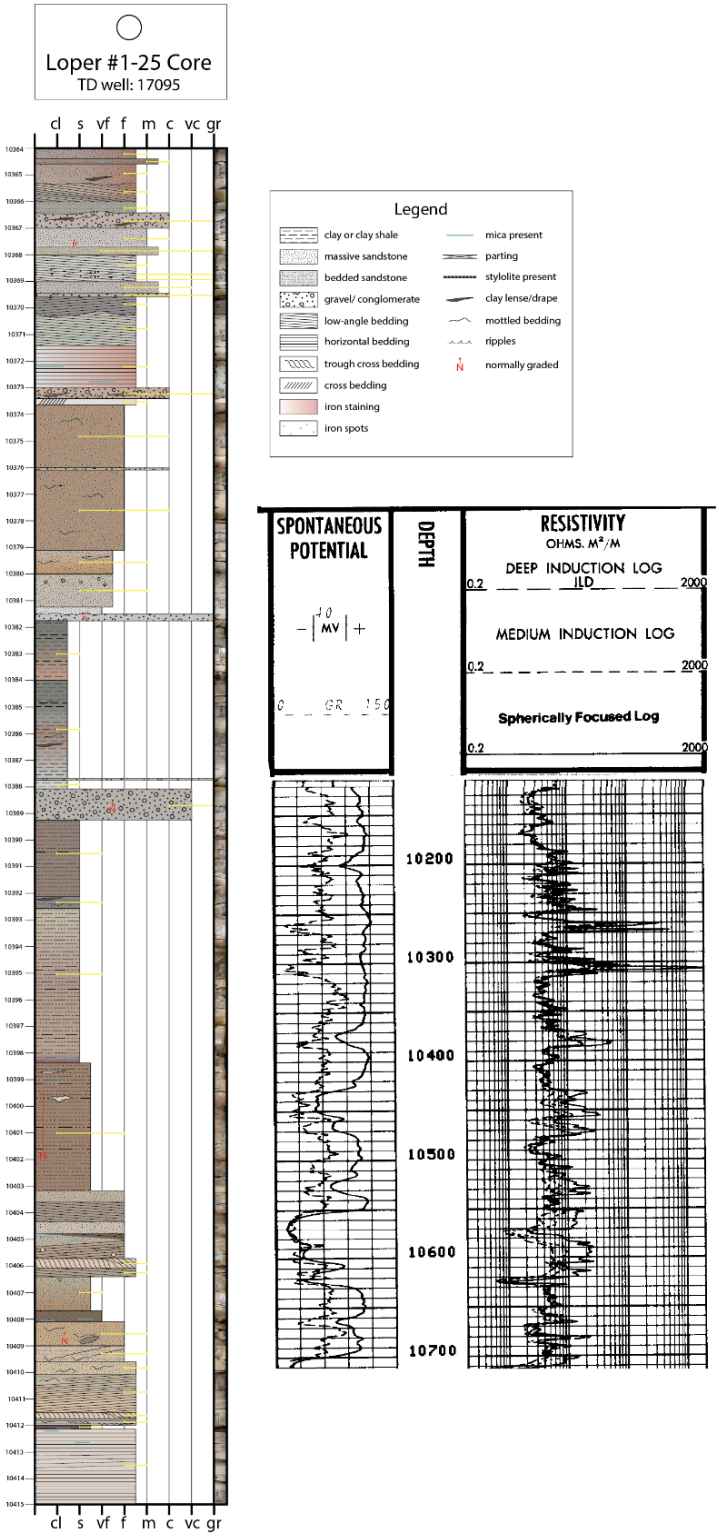

Figure 25. Core description of upper shoreface and coastal plain deposits in the Loper #1-25. API 23121201220000. Core shift of 3 ft.

and silts and pink-tan to gray very fine to medium grained calcareous sandstones. Sandstones are often massive, and often sub-rounded to sub-angular. Many normally graded very thin beds exist within the core. Seven coarse-grained to gravel sized conglomeritic beds are present within this section. The pebbles and gravel sized clasts are almost exclusively chert. These pebble interbeds are usually underlain by an erosional scour contact (Fig. 26).

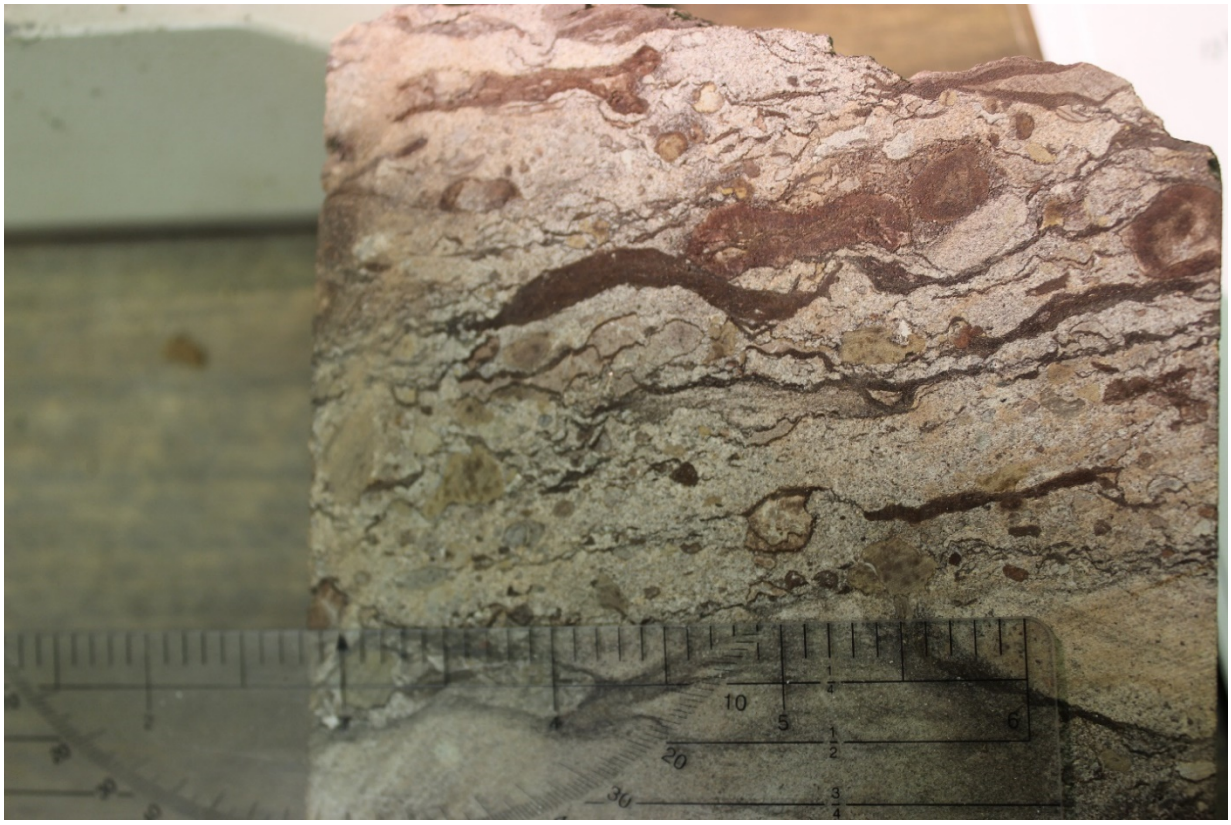

Figure 26. Pebble to gravel sized clasts in a mottled fine-medium grained sandstone matrix. Small tick marks are 1/10th of an inch. The basal contact is erosional and sharp. The unit is underlain by finer-grained sandstone. Clay draping and lenses are abundant and deformed. This interval represents a sediment-gravity-flow bed.

The pebble interbeds are commonly matrix supported in wavy, nonparallel calcareous silt and mud matrix. Upward from the scour surface, the beds typically grade into planar, low-angle lamination, and then into fine-grained, massive sandstones. These are interpreted to be high-energy flow events and storm deposits. Primary sedimentary structures include horizontal (Fig. 27), even, laminasets, planar, low-angle laminasets (Fig. 28), ripple cross-lamination (Fig. 29), curved, planar, laminasets, wavy, nonparallel lamination (Fig. 30), flaser bedding, clay draping, variegated bedding, pebble lag, and parting. Bioturbation is minimal in the cored section (Fig. 31).

Figure 27. Fine-grained sandstone light pink to grey in color showing repetitive horizontal, planar, lamination. Interpreted as tidal rythmites.

Figure 28. Low-angle planar lamination in a predominantly fine-medium-grained sandstone.

Pebble beds present. Middle section shows coarse lag at the base of a fining-upward sequence.

Figure 29. Ripple cross-lamination in a fine-medium grained sandstone. Lower core shows clay lenses and rip up clasts.

Figure 30. Bioturbated, nonparallel cross lamination.

Figure 31. Iron-rich mud and siltsone showing burrows infilled with coarser grains.

Most bedding contacts are planar, but five erosional contacts exist. In one case, the erosional surface exists at the top of a sandstone exhibiting low-angle, planar cross lamination. Two instances of dip reversals within planar, low-angle lamination are present in intervals 6 and 7, which are in the middle 1/3 of the cored interval. The base of the cored interval is more calcareous than the upper intervals. The basal intervals are classified as wackestones. Many of the beds are iron stained. One instance of cross-cutting iron stains is encountered in interval 9. The increasing abundance of iron in the top of the cored interval suggests shallowing of water and an increasingly oxidizing environment. Many clay lenses and drapes are present throughout the core. This core is indicative of an upper shoreface to coastal plain environment with fluvial influence.

The M.D. Ragsdale cuttings are much less complete as a dataset than the Loper #1 core. The cuttings are more similar to residual fragments of quarter core than to drill cuttings. Although this does

not allow for a detailed analysis of bedding, some primary and secondary sedimentary structures are visible. The descriptions of the M.D Ragsdale cuttings are less complete, but are more pertinent to this field than the Loper, #1 core, which lies about 14 miles to southwest of Pelahatchie Field and therefore reflects a more basinward paleodepositional environment. The M.D. Ragsdale cuttings are grouped into two depth intervals and described in (appendix e). Interval 1 covers 57 feet of the Rodessa Formation. Interval 2 covers just 24 feet of the top of the Hosston Formation. The Hosston descriptions will be excluded in this discussion. Cuttings from the Rodessa interval are composed primarily carbonate clastics composed of dark red, red, and grey calcareous sandstones. Primary bedding features are commonly horizontal, planar lamina. Sandstones in this well contain 10-20% calcareous matrix, making them much more calcium-rich than the Rodessa in the Loper #1 core in general. Light grey, dark grey, and white calcareous sandstones are also common. Clasts in this interval are mainly calcareous, but plagioclase feldspar and potassium feldspar wackes are also present, indicating an influx of terrigenous matrix material. One white to grey quartz wacke interval exhibits little to no porosity, possibly providing a hydrocarbon seal. Horizontal, planar, rhythmic, dark and light grey laminae are present in the lower portion of depth interval 2 of the Rodessa. Rhythmic sequences of multiple lighter layers deposited above, and bounded by darker layers of finer-grained sediment are characteristic of tidal rhythmites. Presence of tidal rhythmites suggests deposition in a tide-dominated environment. The lower depth interval contains small amounts of fibrous selenite and anhydrite towards the base, suggesting a low-energy, restricted environment. This sample interval is representative of the underdeveloped Ferry Lake Anhydrite in central Rankin County. Brown-red mud to very-fine sandstone is present in the upper portion of the interval. Plagioclase feldspar wacke and potassium feldspar wacke are noted in the core descriptions of depth interval 5 of interval 1 in the M.D. Ragsdale cuttings. Extraformational feldspathic clasts agree with the interpretation of fluvial channels within the Rodessa Formation. The M.D. Ragsdale is indicative of an upper shoreface, to restricted lagoonal or tidal environment. Interpretations of the core indicate a highly interactive paleoenvironment with tidal and fluvial influences representative of a transgressive coastal environment.

Lithologic identification based on the one available lithodensity log in the Clifton Rhodes 6-15 #1shows that the Glen Rose Subgroup in Pelahatchie Field is composed mainly of interbedded shales, siltstones, and sandstones, with thinly bedded limestones and dolomitic shales (Figure 32).

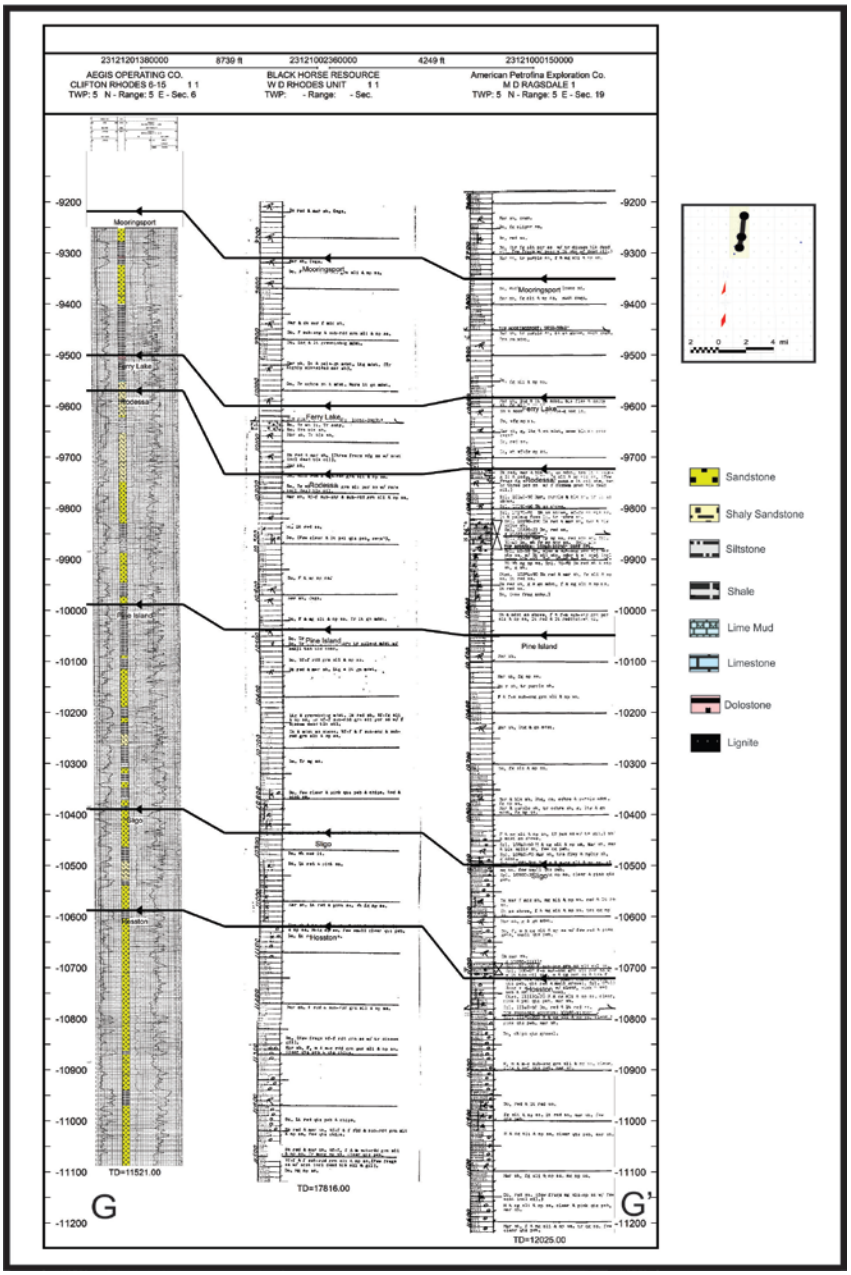

Figure 32. Structural cross section showing synthetic lithologic log based on Clifton Rhodes #6-15 PE-density porosity-neutron porosity log responses, showing strong correlation to sample logs and confirming dolomitic nature of Ferry Lake Anhydrite in central Rankin County.

The following paragraphs will discuss each formation in depth.

The base of the Mooringsport Formation is a calcium cemented sandstone that grades upward into a siltstone. Overlying this sandstone is a ten foot thick dolostone interval. This dolostone represents the Ferry lake Anhydrite equivalent in this area, indicating that the field was above the up-dip limit of Ferry Lake anhydrite deposition. However, mudlogging records indicate trace amounts of anhydrite over this interval in nearby wells, indicating that the area may have experienced a brief period of deposition within a shallow water, restricted circulation, hot and arid, environment. This dolostone is topped by a thick shale unit followed by a massive sandstone. Above this sandstone is a thin shale unit, and a very thin dolomitic limestone. The top of the PeF log reading in the Mooringsport is a massive sandstone.

The Rodessa Formation is composed interbedded sandstones and shales. A thin basal sandstone. Overlying this is a thin shale, and a very thin dolomitic shale, topped by a thick interval of sandstone interbedded with shale. Overlying this unit is a normally graded, calcium cemented siltstone to shale bed. This is overlain by a thick sandstone, which is overlain by a shaley sandstone. This is followed by a shale which is capped by a very thin dolostone layer. Mudloggers record the presence of lignite in the upper Rodessa Formation in the Earl Huffman.

The Pine Island Formation is composed of a thin basal shale, overlain by a normally graded sandstone to siltstone to shale bed. This is overlain by a sandy limestone. The low Pe value in this interval may also be indicative of cherty dolomite, in which case, the effect of silica is confounded by the effect of dolomite. This will cause the neutron and density porosities to falsely overlay. This is overlain by a dolomitic shale, and a thin limestone unit, followed by another dolomitic shale. Overlaying this shale is a sand unit composed of three fining-upward sequences, the lowest of which includes a sandy dolomitic sandstone. This is followed by a thin shale interval, capped by a well-cemented calcareous sandstone. This is followed by a thick shale interval, with one very thin, tight limestone interbed.

CONCLUSIONS

Results from this study indicate that the environment of deposition in the Glen Rose Subgroup from the Loper #1 area in southern Rankin County, transitions from upper shoreface deposits south of the study area, to estuarine tidal flats in a more restrictive environment within Pelahatchie Field in north, central Rankin County. The Glen Rose Subgroup in central Rankin County includes two major fining-upward successions as seen on SP and GR log signatures. The base of each of the fining-upward successions represent a parasequence boundary and record an overall transgression of sea-level, with smaller regressive episodes marked by a rapid increase of sediment influx following maximum flooding surfaces. This is confirmed by paleodeposits depicting sediment flows with erosional bases overlying mudstones within each core. This is also substantiated by log signatures showing an abrupt change in facies immediately overlying the maximum flooding surfaces associated with fining upward sequences. Extraformational plagioclase and potassium feldspar clasts within M.D. Ragsdale cuttings confirm updip igneous sediment sources. Indications of a mappable channel near the base of the Rodessa Formation supports the interpretation of deposition within a tidal flat environment. The presence of channels provide an explanation for the method of transport of extraformational clasts and can be important to the petroleum system if proven to be of reservoir quality. Structure in the field is controlled by an underlying salt dome, creating slight structural closure and faulting within study area. Salt movement was syndepositional with the lower and middle Glen Rose Subgroup, but halted before Mooringsport deposition based on stratigraphic relationships within the field.

Understanding the environments of deposition and structural controls on production are important to the continued oil and gas exploration of salt dome plays in the Mississippi Interior Salt Basin and the recovery of hydrocarbons. Identifying migration pathways and trapping mechanisms related to faulting, closure, and stratigraphy of paleoenvironments within the MISB will contribute to future salt feature play development.

LIST OF REFERENCES

ADAMS, G.S., 1985, Depositional history and diagenesis of the middle Glen Rose reef complex (Lower Cretaceous), east Texas and Louisiana: Master's Thesis, Louisiana University, 200 p.

ANDERSEN, M.A., 2011, Introduction to Wireline Logging *in* The Defining Series: Schlumberger Oilfield Review, v.23, no. 1, p.58-59.

ASQUITH, G., KRYGOWSKI, D., 2004, Basic Well Log Analysis *in* AAPG Methods in Exploration Series 16: American Association of Petroleum Geologists, Tulsa, p. 39-42.

BADON, C.L., 1975, Stratigraphy and Petrology of Jurassic Norphlet Formation, Clarke County, Mississippi: American Association of Petroleum Geologists Bulletin, v. 59, no. 1, p. 377-392.

BECKMAN, M.W., AND BLOOMER, P.A., 1953, Athens Field, Claiborne Paris, Louisiana: Shreveport Geological Society; Reference Report on Certain Oil and Gas Fields of North Louisiana, South Arkansas, Mississippi and Alabama, v. 3, no. 2, p.41-53.

BLOUNT, S.B., SARTIN, A.A., AND LEDGER, E.B., 1986, Depositional and diagenetic history of the Hosston Formation (Travis Peak), Neuvo Leon Group, Trawick Field, Nacogdoches County, Texas: GCAGS Transactions, v. 36, p. 19-29.

BOYLES, J.M., SCOTT, AND A.J., RINE, J.M., 1986, A logging form for graphic descriptions of core and outcrop *in* Exploration and Production Research: Cities Service Oil and Gas Corporation, p. 567-568.

BUFFLER, R.T., 1991, Early evolution of the Gulf of Mexico basin, *in* D. Goldthwaite, ed., An Introduction to Central Gulf Coast Geology, New Orleans: New Orleans Geological Society, p. 1-15.

CONSOLIDATED ODYSSEY EXPLORATION INC. AND U.S. OIL AND GAS RESOURCES INC.: Progress

Report on Puckett Field, 2005, https://www.thefreelibrary.com/Consolidated Odyssey Exploration Inc. and U.S. Oil and Gas Resources...-a0133401276. Checked December, 20, 2017.

CULLOM, T., GRANATA, W., GAYER, S., HEFFNER, R., PIKE, S., HERMANN, L., MEYERTON, C., AND SIGLER, G., 1962, The basin frontiers and limits for exploration in the Cretaceous System of central Louisiana: GCAGS Transactions, v. 12, p. 97-115.

DAVIES, D.K., WILLIAMS, B.P., VESSEL, R.K., 1991, Reservoir models for meandering and straight fluvial channels; examples from the Travis Peak Formation: GCAGS Transactions, v. 41, p. 152-174.

DAVIS, D.C., LAMBERT, E.H., JR., 1963, Mesozoic-Paleozoic producing areas of Mississippi and Alabama: Mississippi Geologic Society, v. 2, p.11-136.

Devery, D.M., 1981, Hosston and Sligo Formations in South Mississippi *in* Mississippi Geology: The Department of Natural Resources, v. 1, no. 4, p. 1-3.

DOCKERY, D.T., MARBLE, J.C., HENDERSON, J., 1997, The Jackson Volcano: The Department of Environmental Quality, v. 18, no. 3, p. 33-45.

DOLL, H.G., 1949, The S.P. Log: Theoretical Analysis and Principles of Interpretation. Society of Petroleum Engineers.

DRILLINGINFO: A database delivering data and energy analytics to oil and gas industries, 1999, http://www.drillinginfo.com. Checked January 2018.

DUTTON, S.P., CLIFT, S.J., HAMILTON, D.S., HAMLIN, H.S., HENTZ, T.F., 1993, Major low permeability sandstone gas reservoirs in the continental United States: Bureau of Economic Geology, University of Texas/GRI Report of Investigations no. 211, p. 221.

DUTTON, S.P., FINLEY, R.J., 1988, Controls on reservoir quality in tight sandstones of the Travis

Peak Formation, east Texas: SPE Paper #15220.

DUTTON, S.P., LAUBACH, S.E., TYE, R.S., BAUMGARDNER, R.W., HARRINGTON, K.L., 1990, Geology of the Lower Cretaceous Travis Peak Formation, East Texas-depositional history, diagenesis, structure, and reservoir engineering implications: Bureau of Economic Geology, University of Texas/GRI Topical Report 90/0090, p. 170.

DYMAN, T.S., CONDON, S.M., 2006, Assessment of undiscovered conventional oil and gas resources – Lower Cretaceous Travis Peak and Hosston Formations, Jurassic Smackover Interior Salt Basins total petroleum system, in the East Texas Basin and Louisiana – Mississippi Salt basin provinces: U.S. Geological Survey Digital Data Series DDS-69-E, Chapter 5, p. 2-39.

FAILS, T.G., 1990, The Northern Gulf Coast Basin: a classic petroleum province: The Geologic Society special publication, v. 50.1, p. 221-248.

FORGOTSON, J.M., 1957, Stratigraphy of the Comanchean Cretaceous Trinity Group: AAPG Bulletin, v. 41, p. 2328 – 2363.

FORGOTSON, J.M., AND FORGOTSON, J.M., JR., 1975, "Porosity pod": concept for successful stratigraphic exploration of fine-grained sandstones: AAPG Bulletin, v. 59, p. 1113-1125.

GARNER, N., FRANKS, C., LIVINGSTON, J., 1987, Cotton Plant Field – Hosston, T13N-R2E, Caldwell Parish Louisiana: Shreveport Geological Society: Report on Selected Oil and Gas Fields, v. 7, p. 62-65.

GORROD, H.M., 1980, Clear Branch Field – Hosston, T-14 & T-15N, R-1 & 2 W, Jackson Parish, Louisiana: Shreveport Geological Society: Report on Selected Oil and Gas Fields, v. 6, p. 58-62.

GRANATA, W.H., 1963, Cretaceous stratigraphy and structural development of Sabine Uplift Area, Texas and Louisiana: Reference Report of the Shreveport Geological Society, v. 5, p. 50-96.

HARTMAN, J. A., 1968, The Norphlet sandstone, Pelahatchie Field, Rankin County, Mississippi: Gulf Coast Association of Geological Societies Transactions, v. 18, p. 2-11.

HERMANN, L.A., 1976, James Limestone in Winn and Nacogdoches parishes, Louisiana: AAPG Bulletin, v. 60, p. 1611.

KARGES, H., 1968, Pelahatchie Field- Mississippi Giant?: Gulf Coast Association of Geological Societies Transactions, v. 18, p. 264-274.

KLITGORD, K.D., POPENCE, P., SCHOUTEN, H., 1984, Florida: a Jurassic transform plate boundary: Jour. Geophysical Res., v.89, p. 7753-7772.

KUPFER, D.A., CROWE, C.T., AND HESSENBRUCH, J.M., 1976, North Louisiana Basin and salt movements (halokinetics): GCAGS Transactions, v. 26, p. 94-110.

LOBAO, J.J., AND PILGER, R.H., 1985, Early evolution of salt structures in the North Louisiana Salt Basin; GCAGS Transactions, v. 35, p. 189-198.

MANCINI, E.A, AHARON, P., GODDARD, D.A., HORN, M., BARNABY, R., 2012, Basin analysis and petroleum system characterization and modeling, interior salt basins, central and eastern Gulf of Mexico: Part 1: North Louisiana Salt Basin: AAPG Bulletin: Search and Discovery Article #10396.

MANCINI, E.A., MINK, R.M., BEARDEN, B.L., and WILKERSON, R.P., 1985, Norphlet Formation (Upper Jurassic) of southwestern and offshore Alabama; Environments of deposition and petroleum geology: American Association of Petroleum Geologists Bulletin, v. 69, no. 6, p. 881-898.

MANCINI, E.A., PENG, L., GODDARD, D.A., and ZIMMERMAN, R.K., 2005, Petroleum Source Rocks of the Onshore Interior Salt Basins, North Central and Northeastern Gulf of Mexico: Gulf Coast Association of Geological Societies Transactions, v. 55, p. 486-504.

MARZANO, M.S., PENSE, G.M., and ANDRONACO, P., 1988, A comparison of the Jurassic Norphlet Formation in Mary Ann Field, Mobile Bay, Alabama to onshore regional Norphlet trends: Gulf Coast Association of Geological Societies Transactions, v. 38, p. 85-100.

MCBRIDE, E.F., 1981, Diagenetic history of Norphlet Formation (Upper Jurassic), Rankin County, Mississippi: Gulf Coast Association of Geological Societies Transactions, v. 31, p. 347-351.

MCFARLAN, E. and MENES, S.L., 1991, Lower Cretaceous, *in* The Geology of North America, The Gulf of Mexico Basin: The Geological Society of America, U.S.A., p. 181-204.

MILLER, J.A., 1982, Structural control of Jurassic sedimentation in Alabama and Florida: AAPG Bulletin, v. 66, p.1289-1301.

MISSISSIPPI OIL AND GAS BOARD: A database documenting well and regulatory information in the state of Mississippi, 2002, updated October 20, 2017, http://www.ogb.state.ms.us/. Checked August 2018.

MONTGOMERY, S. L., AND ERICKSEN, R.L., 1997, Dry Creek Salt Dome, Mississippi Interior salt Basin: AAPG Bulletin, v. 81, p.351-366.

MONTGOMERY, S.L, PETTY, A.J., POST, P.J., 2002, James Limestone, northeastern Gulf of Mexico: Refound opportunity in a Lower Cretaceous trend: AAPG Bulletin, v. 86, p. 381-398.

NUNN, J.A., 1984, Subsidence histories for the Jurassic sediments of the northern Gulf Coast; thermal-mechanical model: Third Annual Research Conf., Gulf Coast Section, SEPM Foundation, p. 309-322.

PEPPER, F., 1982, Depositional environments of the Norphlet Formation (Jurassic) for Southwestern Alabama: Gulf Coast Association of Geological Societies Transactions, v. 32, p. 17-22.

PETTY, A.J., 1995, Ferry Lake, Rodessa, and Punta Gorda Anhydrite bed correlation, Lower Cretaceous, offshore eastern Gulf of Mexico: GCAGS Transactions, v. 45, p. 487-493.

PILGER, R.H., Jr., 1981, The opening of the Gulf of Mexico: implications for the tectonic evolution of the northern Gulf Coast: GCAGS Transactions, v. 31, p. 377-381.

PINDELL, J. L., 1985, Alleghenian reconstruction and subsequent evolution of the Gulf of Mexico, Bahamas, and Proto-Caribbean: Tectonics, v.4 p.1-39.

RICE, D.D., SCHENK, C.J., SCHMOKER, J.W., FOX, J.E., CLAYTON, J.L., DYMAN, T.S., HIGLEY, D.K., KEIGHIN, C.W., LAW, B.E., and POLLASTRO, R.M., 1997, Deep natural gas resources *in* Deep Natural Gas Resources in Eastern Gulf of Mexico: U.S. Geological Survey Bulletin, Washington, p. 219-229.

SALVADOR, A., 1991, Triassic-Jurassic, *in* The Geology of North America, The Gulf of Mexico Basin: The Geological Society of America, U.S.A., p. 131-180.

SALVADOR, A., 1987, Late Triassic-Jurassic paleography and origin of the Gulf of Mexico Basin: AAPG Bulletin, v. 71, p. 419-451.

SAUCIER, A.E., FINLEY, R.J., DUTTON, S.P., 1985, The Travis Peak (Hosston) Formation of east Texas and north Louisiana: SPE/DOE Paper #13850, Conference on Low Permeability Gas Reservoirs, Denver, Colorado, p. 15.

SAWYER, D.S., BUFFLER, R.T., AND PILGER, R.H., JR., 1991, The crust under the Gulf of Mexico, *in* A. Salvadore, ed., The Gulf of Mexico Basin:Decade of North American Geology, Boulder, GSA, p.53-72.

STUDLICK, J.R.J., SHEW, R.D., BASYE, G.L., RAY, J.R., 1990, A Giant Carbon Dioxide Accumulation in the Norphlet Formation, Pisgah Anticline, Mississippi, *in* Barwis, J.H., McPherson, J.G., Studlick, J.R.J., eds., Sandstone Petroleum Reservoirs: Casebooks in Earth Sciences: Springer, New York, p. 181-182.

TEARPOCK, D.J., BISCHKE, R.E., 2002, Applied Subsurface Geological Mapping with Structural Methods, v. 2.

VAN SICLEN, D.C., 1984, Early opening of initially-closed Gulf of Mexico and central North Atlantic Ocean: GCAGS Transactions, v. 34, p. 265-275.

VARHAUG, M., 2016, Basic Well Log Interpretation *in* The Defining Series: Schlumberger Oilfield Review.

WEEKS, W.B., 1938, South Arkansas stratigraphy with emphasis on the older coastal plain beds: AAPG Bulletin, v. 22, p. 953-983.

WINKER, C.D., AND BUFFLER, R.T., 1988, Paleogeographic evolution of early deep-water Gulf of Mexico and margins, Jurassic to Middle Cretaceous (Comanchean): AAPG Bulletin, v. 72, p. 318-346.

YUREWICZ, D.A., MARLER, T.B., MEYERHOLTZ, K.A., SIROKY, F.X., 1993, Early Cretaceous carbonate platform, north rim of the Gulf of Mexico, Mississippi and Louisiana, *in* J.A. Toni Simo, R.W. Scott, and J.P. Masse, eds., Cretaceous carbonate platforms: AAPG Memoir 56, p. 81-96.

ZHOU, Q., and WICAKSONO, A., 2005, Proper Interpretation of Cased-Hole Resistivity Logs.

Society of Petrophysicists and Well-Log Analysts.

APPENDICES

Appendix A: Helmerick & Payne Loper #1 Core Analysis

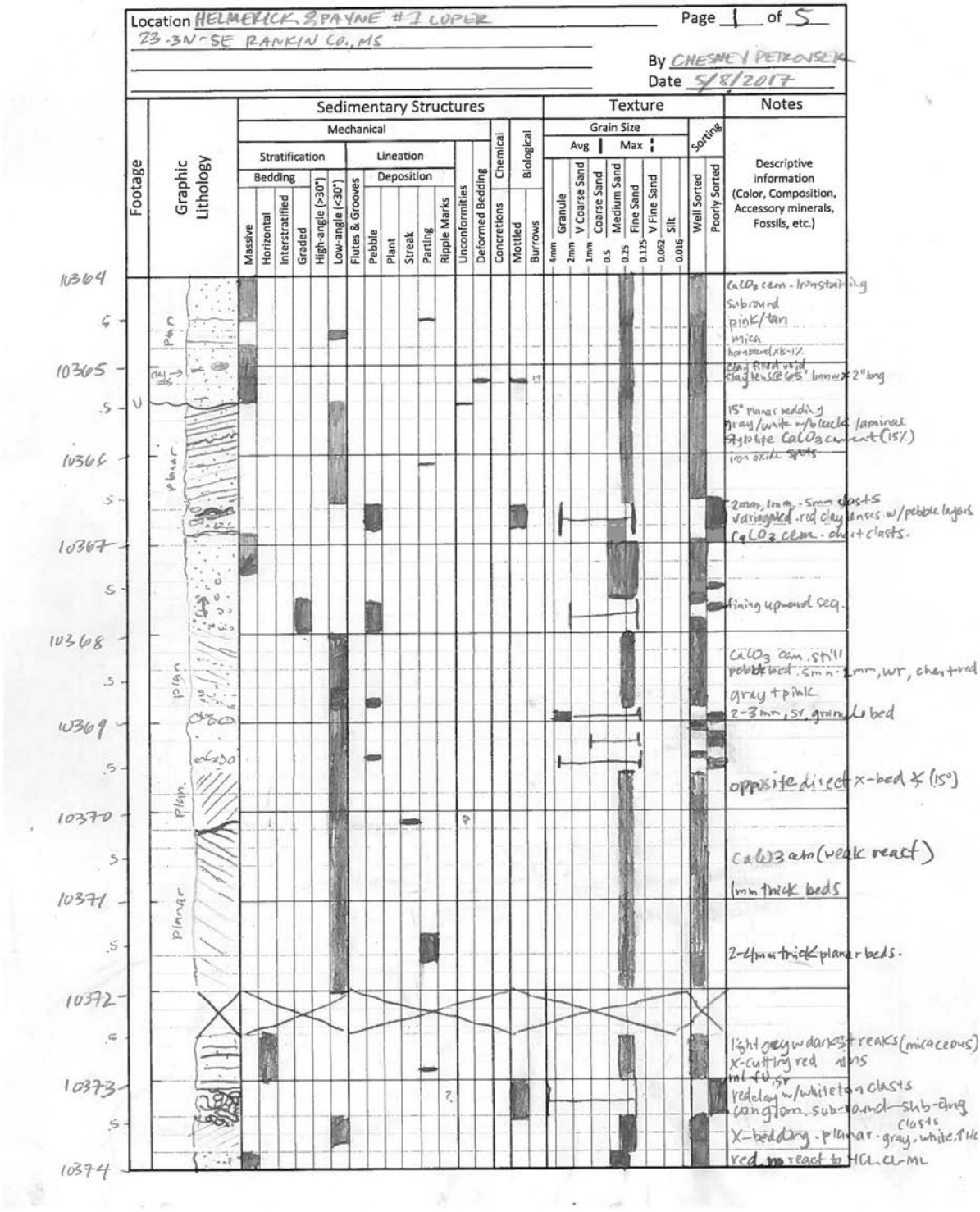

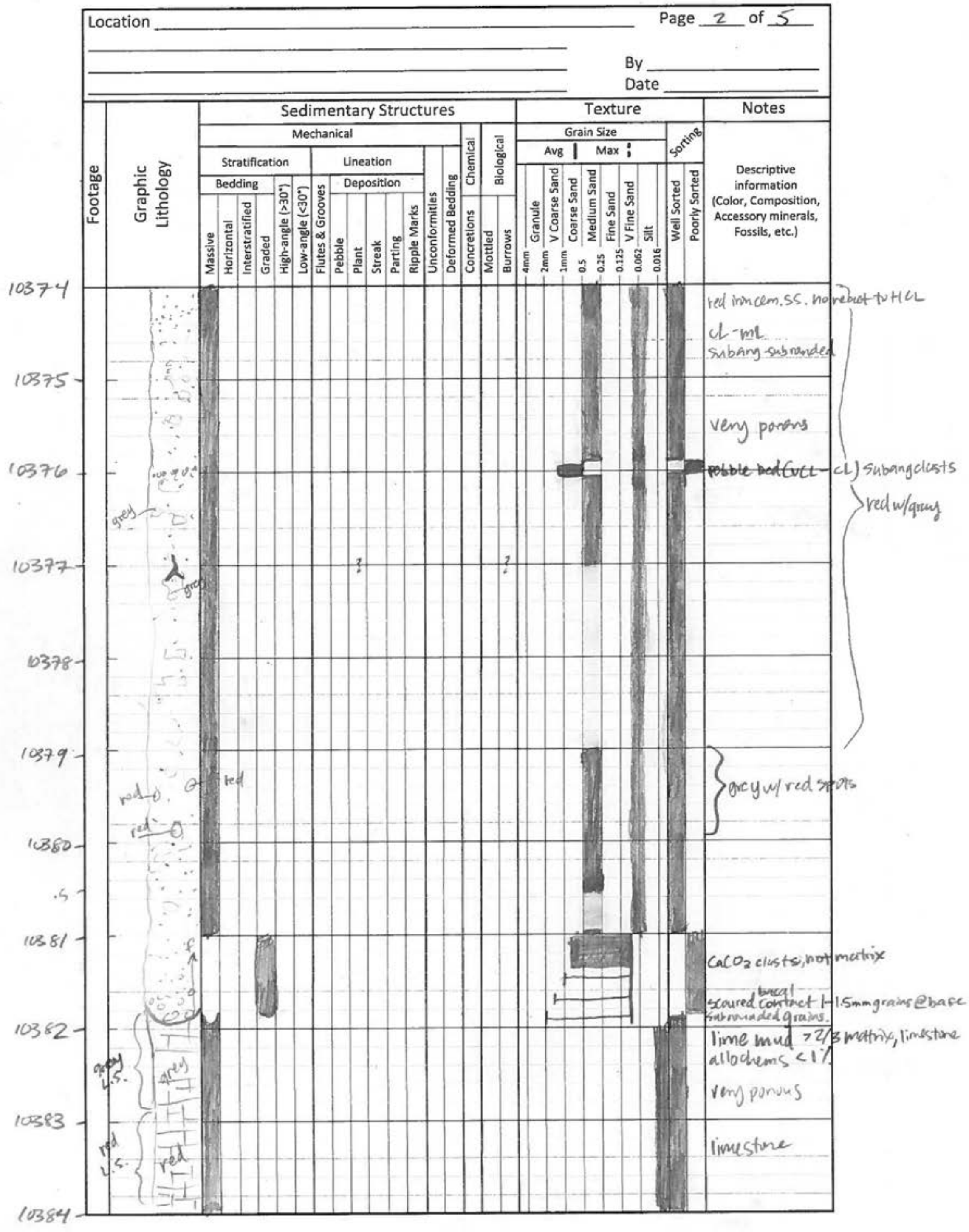

Location
Page 2 of 5
By
Date
Sedimentary Structures
Mechanical
Stratification
Bedding
Massive
Horizontal
Interstratified
Graded
High-angle (>30°)
Low-angle (<30°)
Lineation
Deposition
Flutes & Grooves
Pebble
Plant
Streak
Parting
Ripple Marks
Unconformities
Deformed Bedding
Chemical
Concretions
Biological
Mottled
Burrows
Footage
Graphic Lithology
Texture
Grain Size
Avg
Max
Granule
V Coarse Sand
Coarse Sand
Medium Sand
Fine Sand
V Fine Sand
Silt
4mm
2mm
1mm
0.5
0.25
0.125
0.062
0.016
Sorting
Well Sorted
Poorly Sorted
Notes
Descriptive information (Color, Composition, Accessory minerals, Fossils, etc.)
10374
10375
10376
10377
10378
10379
10380
.5
10381
10382
10383
10384
grey
red
red
red
grey L.S.
grey
red L.S.
red
red iron cem. SS. no rebut to HCL
cL-mL
subang-subrounded
very porous
pebble bed (vcL-cL) subang clasts
red w/ grey
grey w/ red spots
CaCO₃ clasts, not matrix
scoured basal contact 1-1.5mm grains @ base
subrounded grains.
lime mud >2/3 matrix, limestone
allochems <1%
very porous
limestone

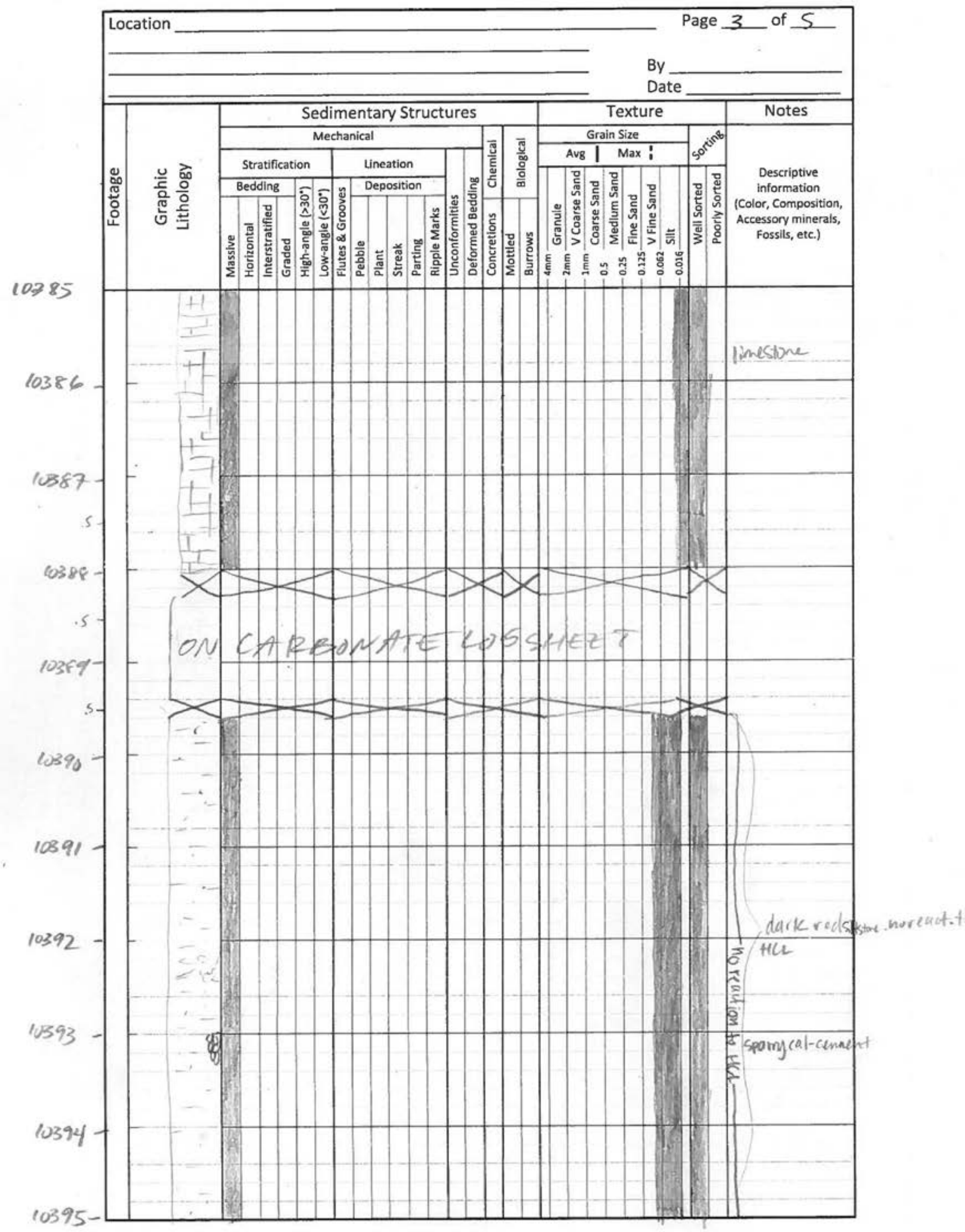
Location
Page 3 of 5
By
Date
Footage
Graphic Lithology
Sedimentary Structures
Mechanical
Stratification
Bedding
Massive
Horizontal
Interstratified
Graded
High-angle (>30°)
Low-angle (<30°)
Lineation
Deposition
Flutes & Grooves
Pebble
Plant
Streak
Parting
Ripple Marks
Unconformities
Deformed Bedding
Chemical
Concretions
Biological
Mottled
Burrows
Texture
Grain Size
Avg
Max
4mm
Granule
2mm
V Coarse Sand
1mm
Coarse Sand
0.5
Medium Sand
0.25
Fine Sand
0.125
V Fine Sand
0.062
Silt
0.016
Sorting
Well Sorted
Poorly Sorted
Notes
Descriptive information (Color, Composition, Accessory minerals, Fossils, etc.)
10385
10386
10387
.5
10388
.5
10389
.5
10390
10391
10392
10393
10394
10395
limestone
ON CARBONATE LOSSHEET
dark red siltstone. no react. to HCL
No reaction to HCL
spongy cal-cement

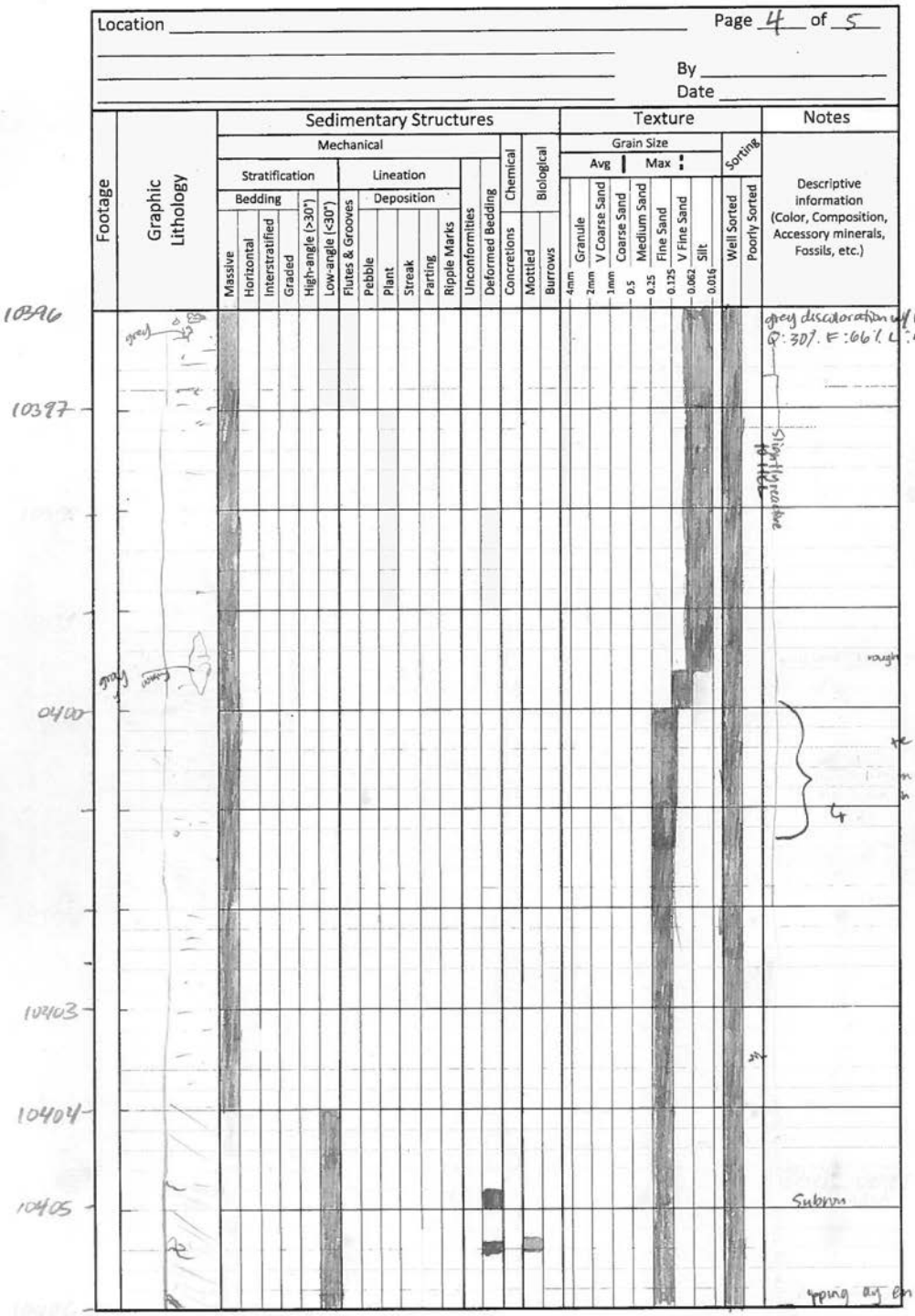
Location
Page 4 of 5
By
Date
Sedimentary Structures
Mechanical
Stratification
Bedding
Massive
Horizontal
Interstratified
Graded
High-angle (>30°)
Low-angle (<30°)
Lineation
Deposition
Flutes & Grooves
Pebble
Plant
Streak
Parting
Ripple Marks
Unconformities
Deformed Bedding
Chemical
Concretions
Biological
Mottled
Burrows
Texture
Grain Size
Avg
Max
4mm
Granule
2mm
V Coarse Sand
1mm
Coarse Sand
0.5
Medium Sand
0.25
Fine Sand
0.125
V Fine Sand
0.062
Silt
0.016
Sorting
Well Sorted
Poorly Sorted
Notes
Descriptive information (Color, Composition, Accessory minerals, Fossils, etc.)
Footage
Graphic Lithology
10396
10397
10400
10403
10404
10405
grey discoloration w/ no Δ in grainsize.
Q: 30%. F: 66%. L: 4%.
Subarn

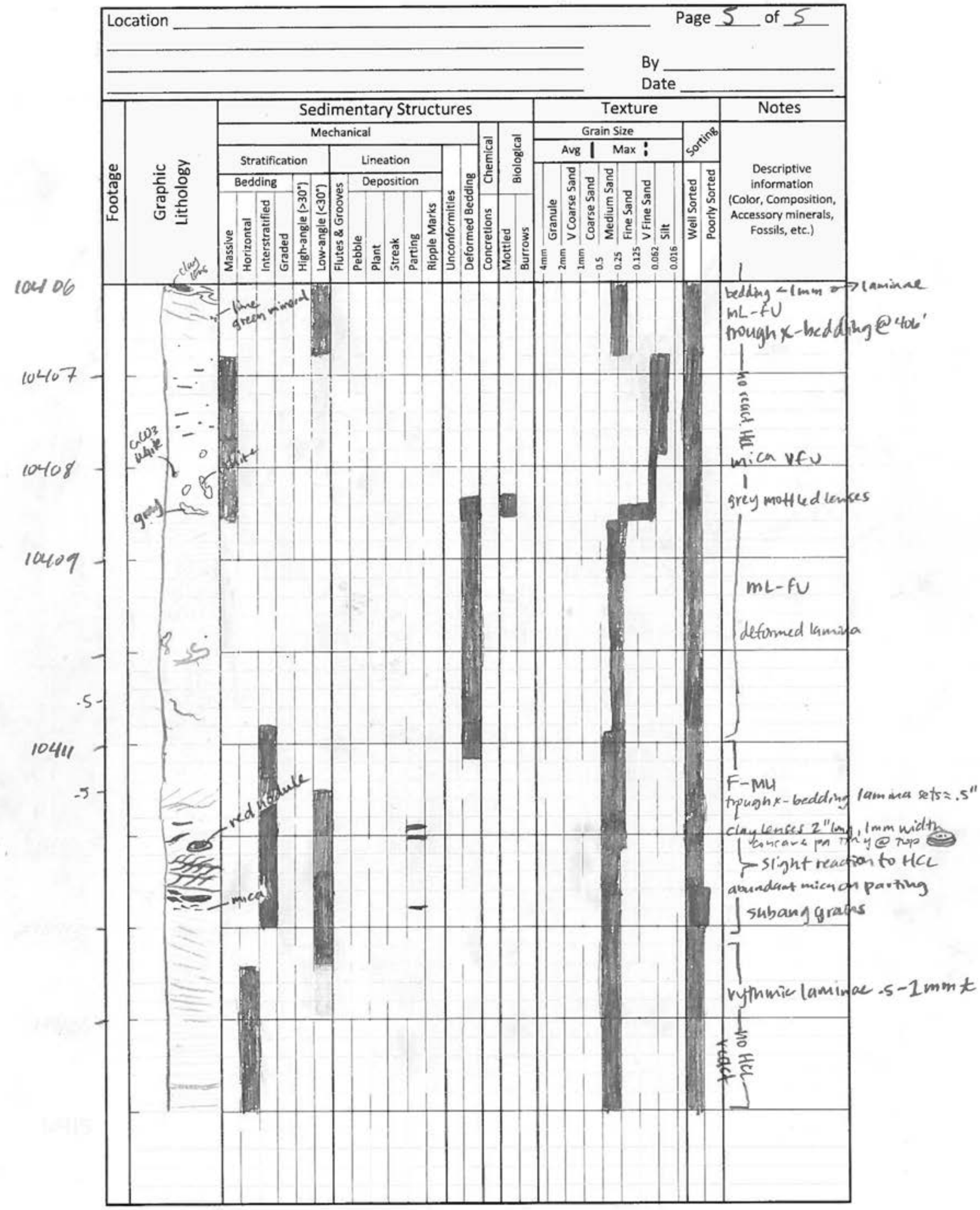
Location
Page 5 of 5
By
Date
Sedimentary Structures
Mechanical
Stratification
Bedding
Lineation
Deposition
Chemical
Biological
Massive
Horizontal
Interstratified
Graded
High-angle (>30°)
Low-angle (<30°)
Flutes & Grooves
Pebble
Plant
Streak
Parting
Ripple Marks
Unconformities
Deformed Bedding
Concretions
Mottled
Burrows
Texture
Grain Size
Avg
Max
Sorting
Granule
V Coarse Sand
Coarse Sand
Medium Sand
Fine Sand
V Fine Sand
Silt
Well Sorted
Poorly Sorted
Notes
Descriptive information (Color, Composition, Accessory minerals, Fossils, etc.)
Footage
Graphic Lithology
10406
10407
10408
10409
.5
10411
.5
clay
lime green mineral
CaCO3 white
white
grey
red nodule
mica
bedding <1mm → laminae
mL-fU
trough x-bedding @ 406'
no react HCL
mica vfU
grey mottled lenses
mL-fU
deformed lamina
F-MU
trough x-bedding lamina sets ≈ .5"
clay lenses 2" long, 1mm width
slight reaction to HCL
abundant mica on parting
subang grains
rythmic laminae .5-1mm ±
no HCL react

MEASURED SECTION / WELL: HELMERICK # PAYNE #1 LOPER (MD) LOCATION: 25-3N-5E RANKIN CO., MS

STRATIGRAPHIC INTERVAL: 10364- LOGGED BY: CHESNEY PETERSEN DATE: 5/9/17

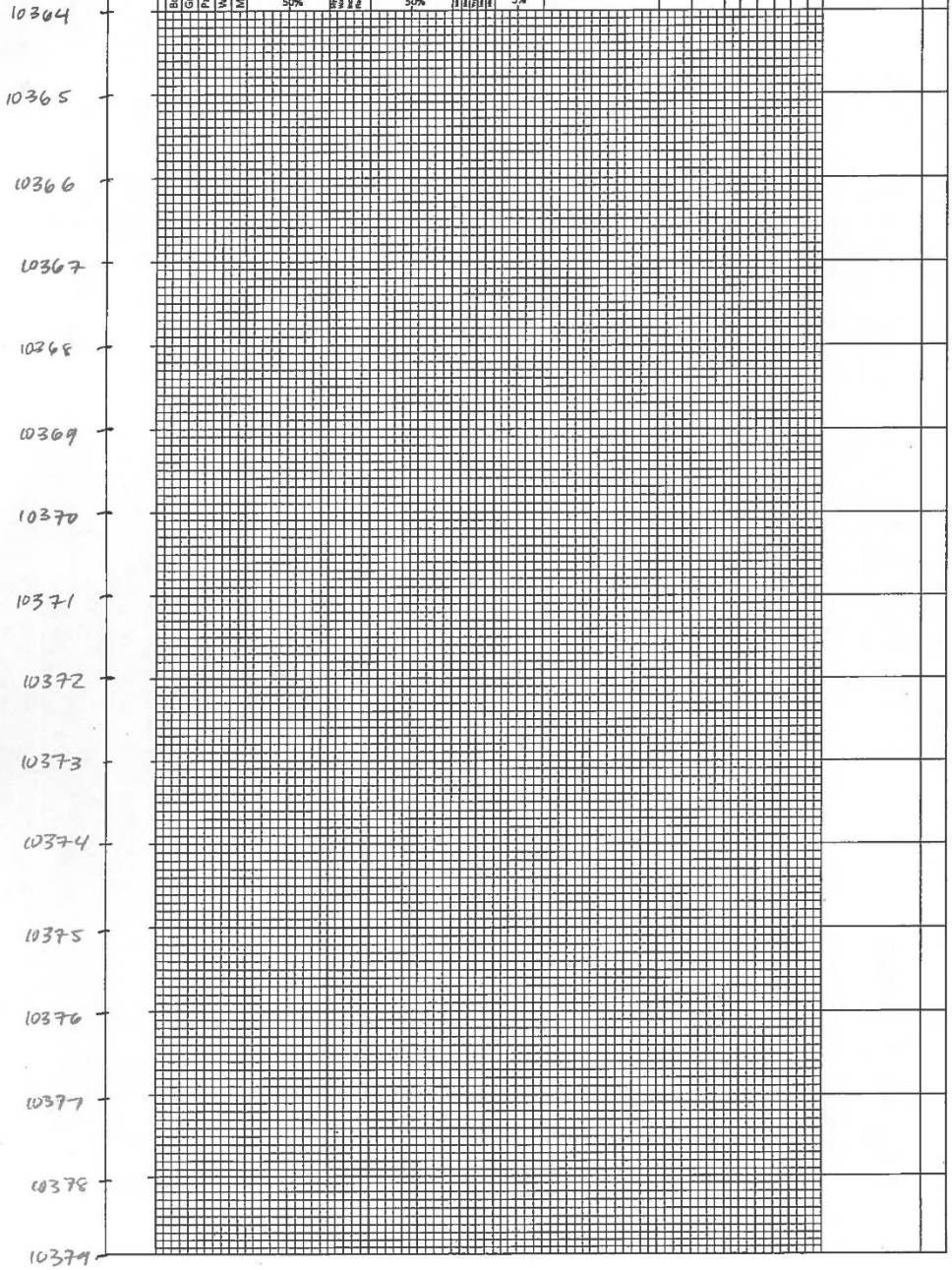

MEASURED SECTION / WELL: _____ LOCATION: _____

STRATIGRAPHIC INTERVAL: _____ LOGGED BY: _____ DATE: _____

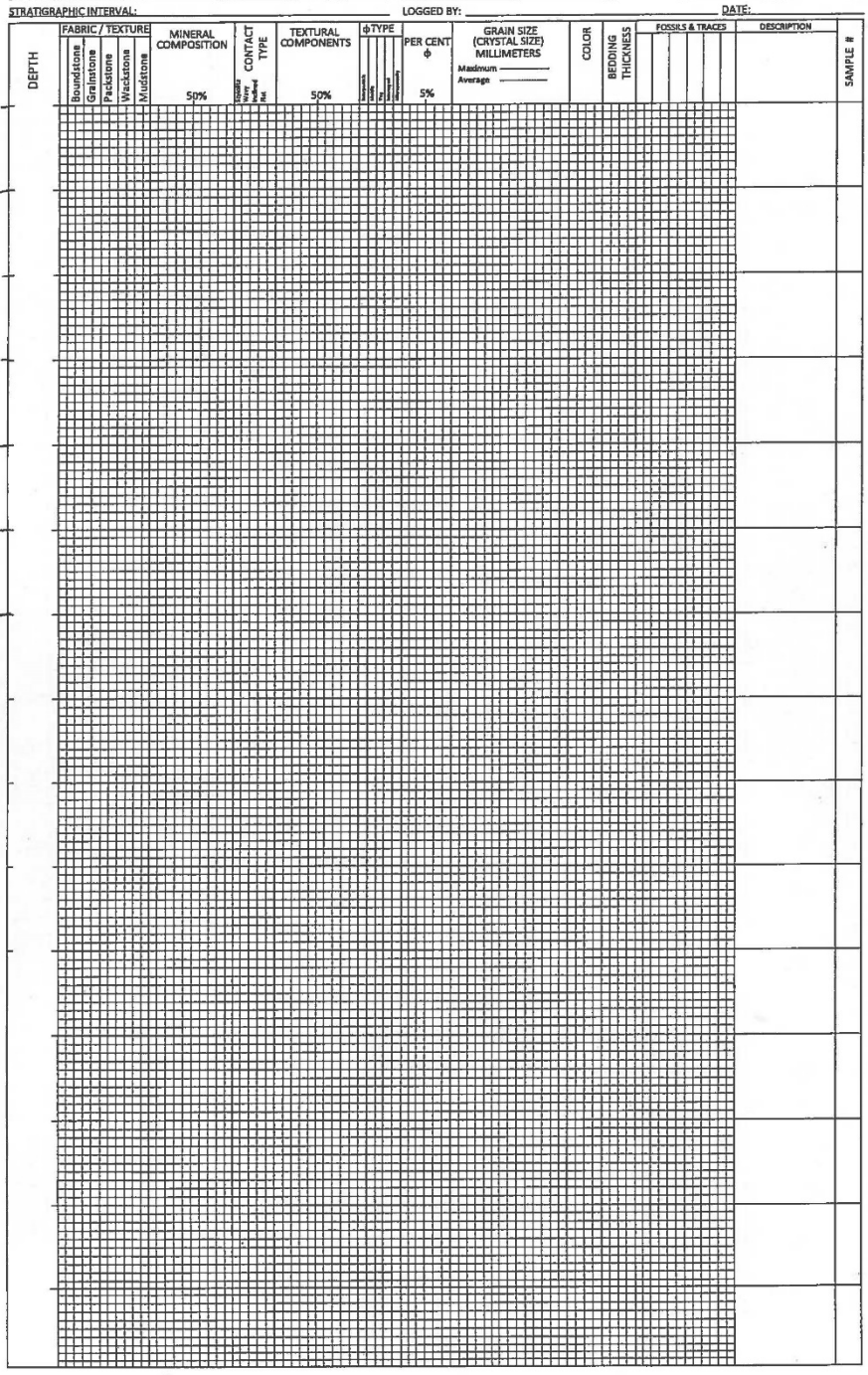

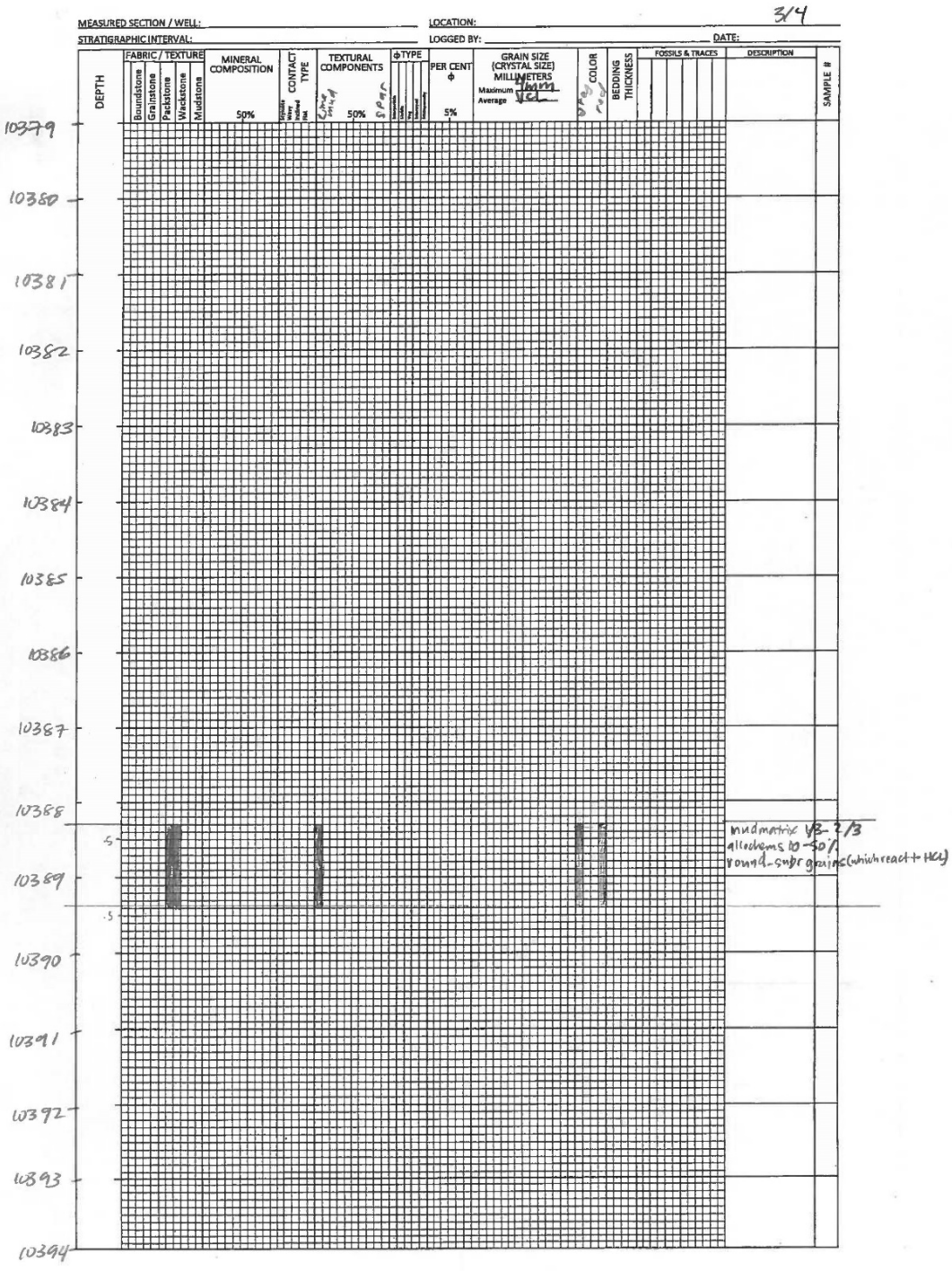
MEASURED SECTION / WELL:
LOCATION:
3/4
STRATIGRAPHIC INTERVAL:
LOGGED BY:
DATE:
DEPTH
FABRIC / TEXTURE
Boundstone
Grainstone
Packstone
Wackestone
Mudstone
MINERAL COMPOSITION
50%
CONTACT TYPE
TEXTURAL COMPONENTS
50%
Lime mud
Spar
ΦTYPE
PER CENT Φ
5%
GRAIN SIZE (CRYSTAL SIZE) MILLIMETERS
Maximum
Average
COLOR
BEDDING THICKNESS
FOSSILS & TRACES
DESCRIPTION
SAMPLE #
10379
10380
10381
10382
10383
10384
10385
10386
10387
10388
10389
10390
10391
10392
10393
10394
mudmatrix VF-F 2/3
allochems 10-50%
round-subr grains(which react+ HCl)

MEASURED SECTION / WELL: LOCATION:

STRATIGRAPHIC INTERVAL: LOGGED BY: DATE:

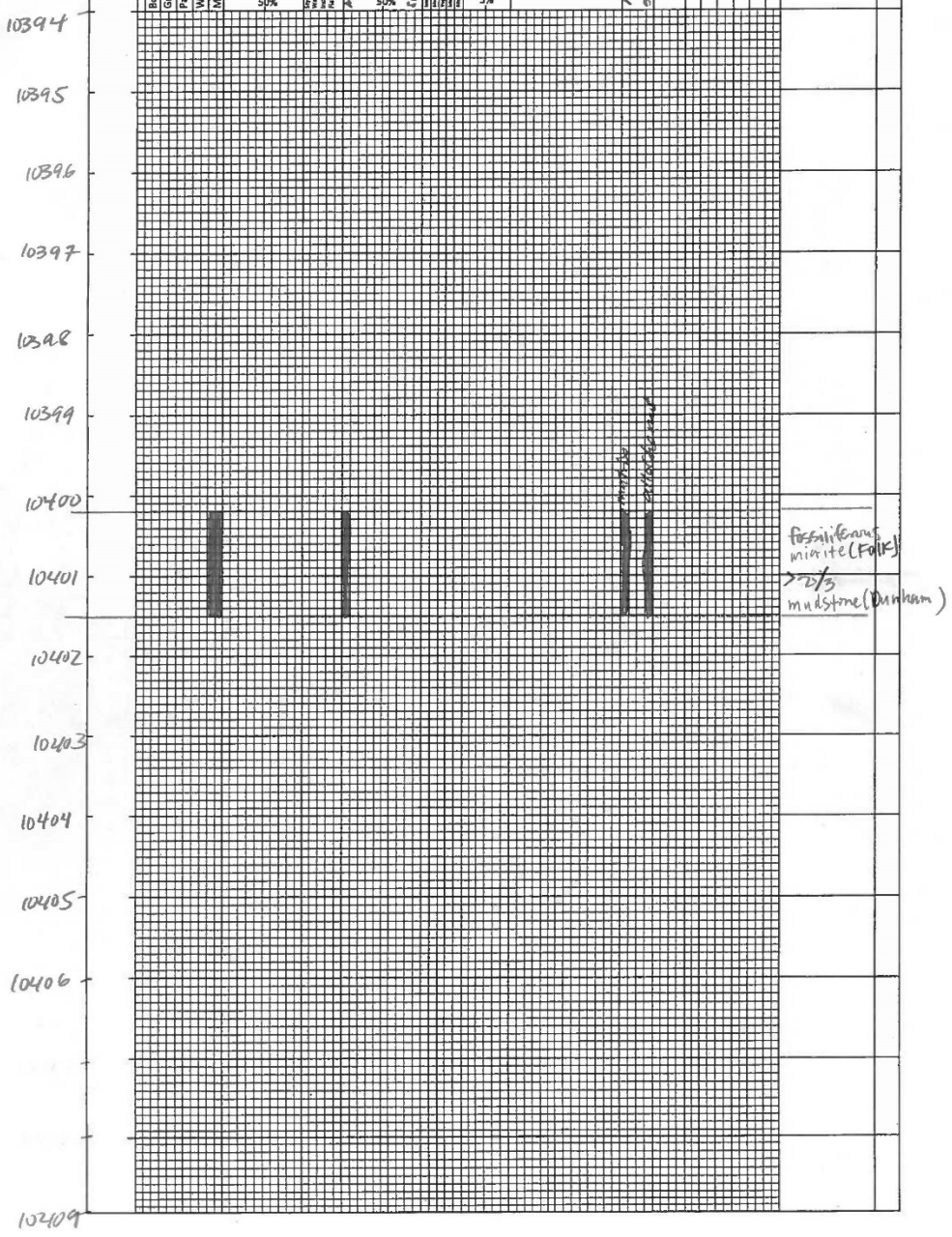

Appendix B: American Petrofina M.D. Ragsdale #1 Core Analysis

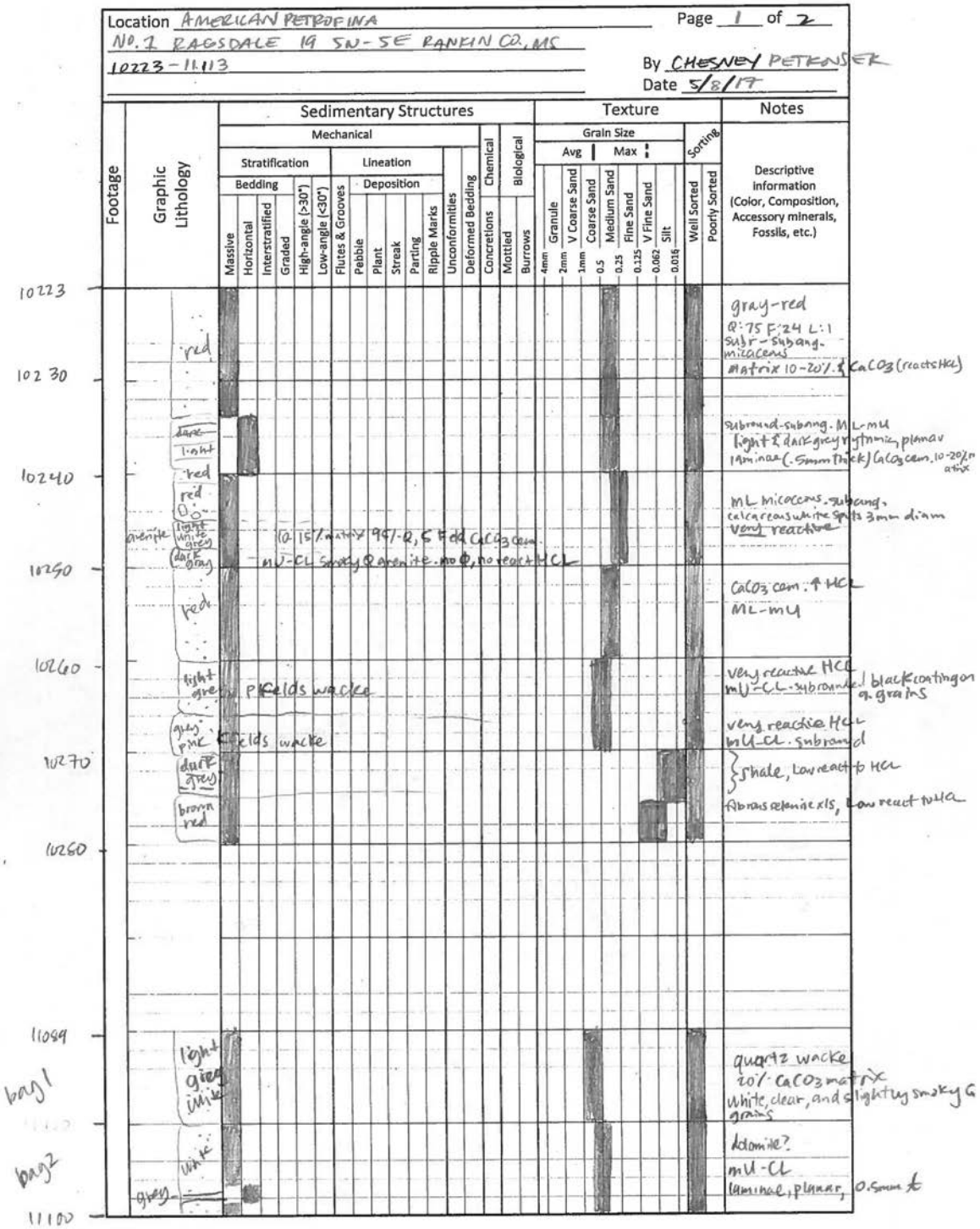

Location ______________________________ Page 2 of 2

By ____________
Date ____________

Footage	Graphic Lithology	Sedimentary Structures — Mechanical — Stratification — Bedding: Massive, Horizontal, Interstratified, Graded, High-angle (>30°), Low-angle (<30°); Lineation — Deposition: Flutes & Grooves, Pebble, Plant, Streak, Parting, Ripple Marks; Unconformities; Deformed Bedding; Chemical: Concretions; Biological: Mottled, Burrows	Texture — Grain Size (Avg ▌ Max ┇): 4mm Granule, 2mm V Coarse Sand, 1mm Coarse Sand, 0.5 Medium Sand, 0.25 Fine Sand, 0.125 V Fine Sand, 0.062 Silt, 0.016	Sorting: Well Sorted, Poorly Sorted	Notes — Descriptive information (Color, Composition, Accessory minerals, Fossils, etc.)
11100	light gray white				low porosity slow- no react to HCL
11107	write				Q:90% F:9% L:1% -wacke 20% cement CaCO3 Very porous. CU sub ∡, xl ine
11113	white				no φ cL-mU orange XLS

vug!

Appendix C: Box and whisker plot of produced oil gravities with accompanying ANOVA table. p<.0001.

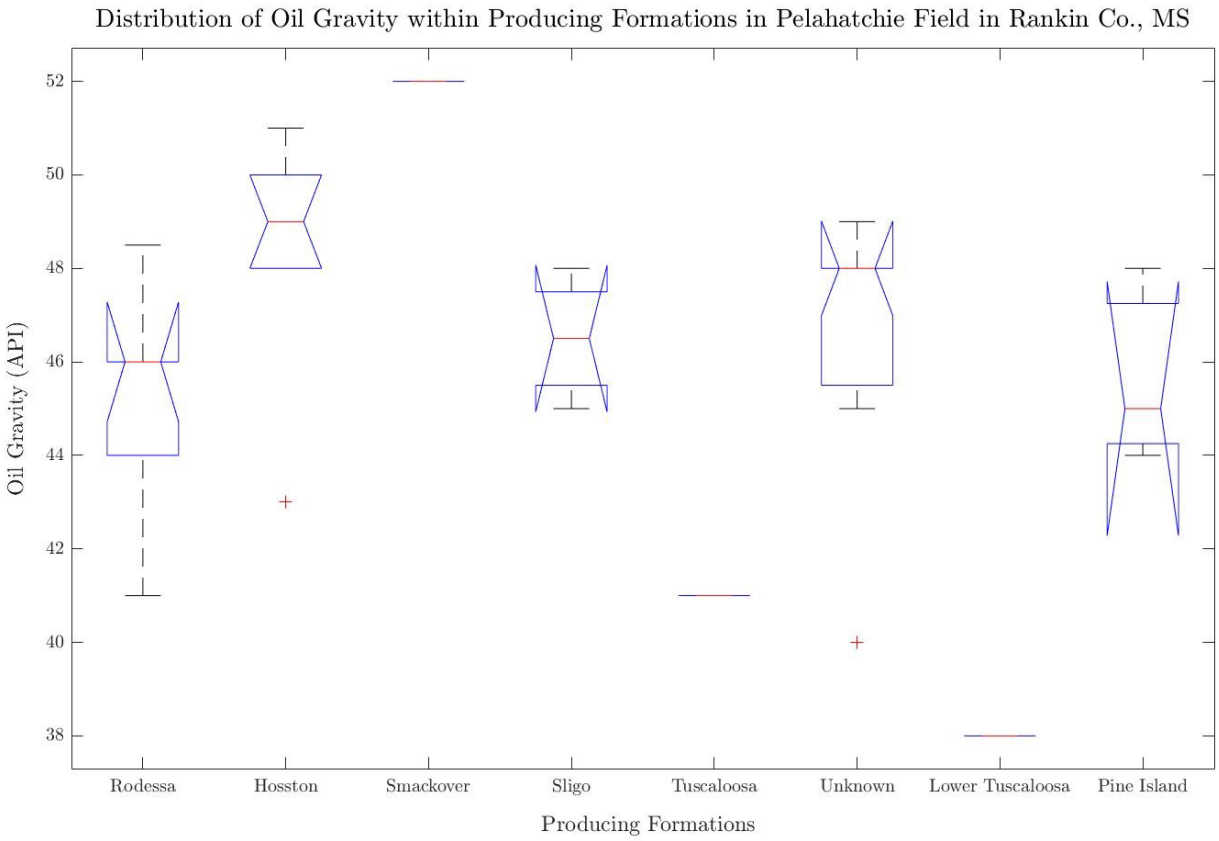

ANOVA Table

Source	SS	df	MS	F	Prob>F
Groups	189.149	7	27.0213	5.28	0.0004
Error	168.875	33	5.1174		
Total	358.024	40			

Appendix D: Helmerick & Payne Loper #1 Core Desciptions

Depth Interval 1: 10,364-10365 ft.— Color pink to tan; grain size fine-medium; subrounded; well sorted; massive; low-angle stratification present in middle; parting present in middle; calcareous cement; iron staining; mica present; hornblende present (<1%).

Depth Interval 2: 10,365-10,366 ft.— Color light pink to light grey; grain size fine-medium; well sorted; massive in upper section; low-angle stratification (15° planar bedding) in lower section; deformed bedding and mottles in middle section, underlain by unconformity; clay-filled void in upper section (1mm wide, 2 inches long); low-angle stratification is gray-white with dark gray-black laminae; stylolite present; calcareous cement (15% occurrence); iron oxide spots present.

Depth Interval 3: 10,366-10,367 ft.— Color light grey to light grey tan; grain size fine-medium and well sorted in upper 5"; grain size fine to granule and poorly sorted in lower 7"; planar, low-angle, laminated bedding in upper 5"; deformed, variegated bedding in lower 7" with red clay lenses and very thin pebble layers present; chert clasts present in lower 7"; calcareous matrix.

Depth Interval 4: 10,367-10,368 ft.— Color light grey; grain size fine-coarse; well-sorted with thin intervals of poorly sorted; massive; normally graded bedding sequence present at base with grain size very fine- granule; matrix supported pebble layers present.

Depth Interval 5: 10,368-10,369 ft.— Color light grey to light pink grey; grain size fine-medium with thin fine- granule intervals interbedded; well-poorly sorted; low-angle, planar stratification; granule and pebble interbeds present consist of well-rounded, red chert clasts; calcareous matrix.

Depth Interval 6: 10,369-10,370 ft.— Color light grey; grain size fine-very coarse in uppermost section, underlain by a thin fine-granule bed, underlain by a fine-medium lower section; well-poorly sorted; low-angle (15°), planar stratification; bedding dips in opposite direction of overlying bedding.

Depth Interval 7: 10,370-10,371 ft.— Color light grey tan; grain size fine-medium; well sorted; planar, low-angle stratification; average bedding thickness = 1mm; parting present in upper section; dip direction change at part, possible unconformity; calcareous matrix (weak reaction).

Depth Interval 8: 10,371-10,372 ft.— Color light grey tan; grain size fine-medium; well sorted; planar, low-angle stratification; average bedding thickness = 2-4mm; parting in lower section.

Depth Interval 9: 10,372-10,373 ft.— Upper section unrecovered; lower section color light grey with dark, micaceous laminations; grain size fine-medium, well sorted; .5-1mm thick horizontal laminations; parting present in lower section; cross-cutting red stains present in lower section.

Depth Interval 10: 10,373-10,374 ft.— Color pink tan and light grey; upper section grain size fine->4mm, conglomerate, red clay with white-tan, sub-round to sub-angular clasts; poorly sorted; possible ripple marks; planar cross-bedding present in middle section; middle section is fine-medium in grain size; well sorted; cross beds are grey and white in color and have strong reaction to diluted hydrochloric acid; lower section is medium in grain size; well sorted; massive; red in color with no reaction to diluted hydrochloric acid.

Depth Interval 11: 10,374-10,375 ft.— Color pink to tan to grey; grain size medium lower-coarse lower and silt - very fine; well sorted; massive; surrounded to subangular; red cement spots; no reaction to hydrochloric acid.

Depth Interval 12: 10,375-10,376 ft.— Color pink to tan to grey (grey is in clots within pink color); grain size medium lower- coarse lower and silt - very fine; well sorted; massive; very porous; very coarse lower - coarse lower pebble bed or sub angular clasts at base.

Depth Interval 13: 10,376-10,377 ft.— Color pink to tan to grey (grey is in clots within pink color); grain size medium lower-coarse lower and silt -very fine; well sorted; massive.

Depth Interval 14: 10,377-10,378 ft.— Color pink to tan to grey (grey is in mottled? clots within pink color); grain size silt- very fine; well sorted; massive.

Depth Interval 15: 10,378-10,379 ft.— Color pink to tan to grey; grain size silt-very fine; well sorted; massive.

Depth Interval 16: 10,379-10,380 ft.— Color grey and red; grain size medium and silt - very fine; well sorted; massive; red spots within grey sands.

Depth Interval 17: 10,380-10,381 ft.— Color light grey with red clasts; grain size medium and silt - very fine; well sorted; massive; lower section silt- very fine in grain size.

Depth Interval 18: 10,381-10,382 ft.— Color light grey; grain size very fine in upper section, granule in lower section, normally graded bedding; poorly sorted; scoured basal contact with 1-1.5mm clasts at base of scour; subrounded; well sorted at base; clasts react to HCL; matrix does not react to HCL.

Depth Interval 19: 10,382-10,383 ft.— Color light grey to grey, red tan at base; grain size mud to silt; well sorted; massive; >2/3 matrix, <1% allochems; very porous.

Depth Interval 20: 10,383-10,384 ft.— Color red grey; grain size mud to silt; well sorted; massive.

Appendix E: Qualitative Descriptions of American Petrofina's M.D. Ragsdale #1 Cutting Samples

Begin Interval 1 (Rodessa)– cuttings

Depth Interval 1: 10,223-10,230 ft.— Color red grey; grain size medium; subrounded-subangular; well sorted; massive; micaceous; matrix = 10-20% and calcareous.

Depth Interval 2: 10,230-10,240 ft.— Color red with darker grey and light grey laminae; grain size medium lower-medium upper; subrounded-subangular; well sorted; massive in upper portion of section, horizontal, rhythmic, planar bedding in lower portion (dark grey and light grey laminae, each = 0.5mm in thickness); matrix = 10-20% and calcareous.

Depth Interval 3: 10,240-10,250 ft.— Color red interval overlying a light, white grey interval, overlying a dark grey basal interval; grain size fine-medium in upper portion of section, medium upper-coarse lower in dark grey basal section; well sorted; massive; upper section is micaceous and subangular with white, $CaCO_3$ rich clasts at base; the underlying white grey interval has 10-15% matrix, 95% Q, 5% feldspar, with $CaCO_3$ cement (cement is very reactive to HCL), is classified as a quartz wacke; the underlying basal interval has 10-15% matrix, very low to no porosity, and no reaction to HCL.

Depth Interval 4: 10,250-10,260 ft.— Color red; grain size medium lower-medium upper; well sorted; massive; $CaCO_3$ cement (very reactive to HCL).

Depth Interval 5: 10,260-10,270 ft.— Color light grey in upper portion of section, overlying a grey pink lower portion of section; grain size medium upper-coarse lower; subrounded; well sorted; massive; upper section is very reactive to HCL and some grains have black coating; classified as a plagioclase feldspar wacke; lower section is very reactive to HCL and classified as a potassium feldspar wacke.

Depth Interval 6: 10,270-10,280 ft.— Color dark grey in upper portion of section, brown red in lower portion of section; grain size mud-very fine in upper portion of section, silt-fine in lower portion of section; well sorted; massive; upper portion classified as a silty shale and has low reaction to HCL; lower portion contains fibrous selenite/ anhydrite? xls and has a low reaction to HCL.

Begin Interval 2 (Hosston) – fragmented ¼ core in small envelopes

Depth Interval 1: 11,089-11,100ft.— Envelope 1: Color light grey, white; grain size coarse; well sorted; massive; grains are white, clear, and slightly smokey in color; matrix = 20% and reacts to HCL; classified as a quartz wacke. Envelope 2: Color white with interbed of grey color; grain size medium upper-coarse lower; well sorted; massive with horizontal, grey interbed = 0.5 mm in thickness; slow reaction to HCL.

Depth Interval 2: 11,100-11,107ft.— Color light grey white; grain size medium; well sorted; massive; slow to no reaction to HCL; low porosity.

Depth Interval 3: 11,107-11,113ft.— Envelope 1: Color white; grain size coarse upper; subangular; well sorted; massive; 90% Q, 9% F, 1% L; matrix = 20% and is calcareous; very porous interval; classified as a wacke; crystalline clasts present. Envelope 2: Color white; grain size medium upper-coarse lower; well sorted; massive; orange xls present; no porosity.

VITA

Education: Bachelor of Science in Geology, May 2016
University of Mississippi, University, MS 38655

Work Experience: Geologist, 2017 – present
Callon Petroleum Company
Houston, TX

Publications: "Synergistic Effects of Halogen Bond and pi-pi Interactions in Thiophene-based Building Blocks," RSC Advances (2015)

Memberships and Awards:

American Association of Petroleum Geologists, Dallas Young Professionals in Energy, Dallas Geological Society, Houston Geological Society, West Texas Geological Society. Chancellors Honor Roll, Sigma Aloha Lambda honors organization, Gamma Beta Phi honor organization, Geologist in Training

Grants: IHS University Grant for Kingdom PAKaged Suite, Academic Add-on, and IHS Petra- awarded in 2016